Geographic Information System (GIS) Integration of geological, geochemical and geophysical data from the Aggeneys base metal province, South Africa.

Isayvani Naicker

Thesis submitted to the Faculty of Science, University of Cape Town, South Africa, in fulfilment of the requirements for the degree of Master of Science.

Department of Geological Sciences
Cape Town, 1993

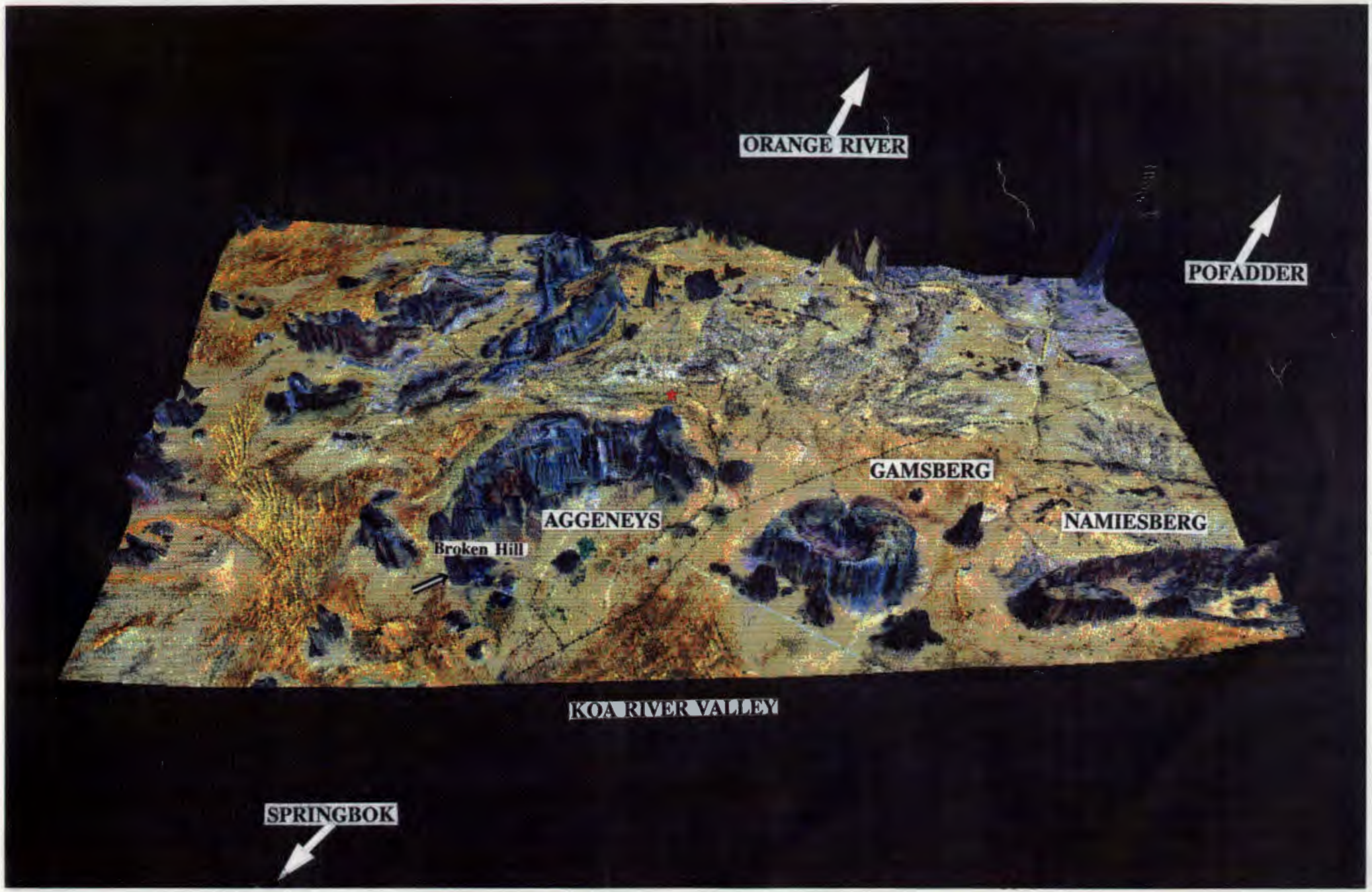
ORANGE RIVER
POFADDER
GAMSBERG
AGGENEYS
NAMIESBERG
Broken Hill
KOA RIVER VALLEY
SPRINGBOK

FRONTISPIECE

Colour reproduction of digitally enhanced Landsat TM image covering the central Bushmanland Subprovince at Aggeneys in the North Western Cape. Generalised high-pass filtered contrast stretched enhancements of bands 7, 4 and 1 were used to produce the colour composite highlighting geological contrast in the area. The image described above is draped over a Digital Elevation Model created from elevation data contoured over this area. The perspective view is created with the observer positioned 220 km away, at azimuth 45° and 1.5 m above a viewing target marked with a red star. The mean relief in the area is 975 m above sea level. The topography undulates gently and local highs coincide with outcropping inselbergs of supracrustal rocks in the study area.

Magenta to purple depicts inselbergs of the Proterozoic supracrustal rocks. Cyan highlights scree slopes associated with these inselbergs. The yellow colour reflects the Cambrian Nama and Mid-Palaeozoic Karoo cover sequences. The solid patch of green, in the south-west delineates the Aggeneys mining town, an oasis of cultivated greenness in this arid region. The black broken line running from the south to north-east corner is the N2 national road which connects the town of Aggeneys with the towns of Springbok in the south and Pofadder in the East. The network of streams visible in the north-east, drain into the Orange River to the north. Other minor streams drain off the inselbergs to the south, as seen on the northern exit of the rounded basin structure (Gamsberg); these are perennial streams which terminate in small alluvial fans. Linear seif dunes (yellow-yellow-brown) are visible to the south and south east, occurring around the Koa Valley depression which extends further south, off this image.

dedicated to the memory of my beloved mother

Abstract

Geographic Information System (GIS) technology aids in storage, manipulation, processing, analysis and presentation of spatial data sets. GIS can effectively interrogate large multidisciplinary exploration data sets in the search for new mineral exploitation targets. A spatial database, the **AGG**eneys **E**xploration **D**atabase (AGGED), has been created, comprising exploration data gathered during two decades of exploration for base-metals in the Aggeneys area, Bushmanland, South Africa. AGGED includes data extracted from analog maps, as well as digital remotely sensed sources, stored in vector and raster data structures, respectively. Vector data includes field based observations such as the extent of outcropping geological units, litho- and chrono-stratigraphic data; structural data; laboratory data based on regional geochemical stream sediment and traverse sampling; cadastral data and known mineral occurrences. Raster data includes Landsat satellite TM imagery and airborne magnetic data.

Spatial variation within single data maps are examined. Spatial correlation between three different data maps are facilitated using colour analysis of hue, saturation and value components in a perceptual colour model. Simultaneously combining lead and zinc data with Landsat TM and geophysical magnetic data spatially delineates four new "geoscience" anomalies in the area under investigation. Two distinctive anomalies occur on the farms Aroams and Aggeneys. The Aroams anomaly (GSA1) has not been previously recognised, whereas the Aggeneys anomaly (GSA2) has been located before. The two other "geoscience" anomalies, on the farm Haramoep (GSA3 and GSA4), are slightly less distinct. Overlaying fold axial trace patterns and anomalies on the farm Haramoep, indicate that F2 and F3 fold structures are closely associated with these two anomalies.

The location of the Aroams anomaly occurs along the same east-west trend of the four known major ore-deposits viz. Big Syncline, Broken Hill, Black Mountain and Gamsberg. Extrapolating F2 and F3 fold patterns using magnetic data locates this Aroams anomaly along the F3 axial trace extending from Big Syncline through to Gamsberg. The elevated Pb-Zn geochemical anomaly and structural data associated

with the Aroams anomaly makes it a promising future exploitation target.

The AGGED database can be expanded both in geographic extent to include surrounding areas, and to allow for inclusion of future surveys. Analytical processing of data in AGGED can also be continued and expanded. GIS is a burgeoning field and developments in GIS technology will impact on the explorationist. Developments in object-oriented and knowledge-based database technologies, visualisation techniques and artificial intelligence, incorporated in future GIS need to be closely monitored and evaluated by geoscience explorationists.

Table of Contents

Abstract i

Table of Contents iii

Acknowledgements viii

List of abbreviations ix

List of Tables x

List of Figures xii

Chapter 1

Introduction 1-1

1.1. Location of the Study Area 1-2

1.2. Regional Setting 1-2

1.3. Climate, Geomorphology and Vegetation 1-3

1.4. Status of Previous Exploration and Research 1-3

1.5. Objectives of Present Investigation 1-4

Chapter 2

Regional Geological Framework 2-1

2.1. The Namaqualand Metamorphic Complex 2-1

2.1.1. Regional Tectonic Framework 2-1

2.1.2. Bushmanland Tectono-Stratigraphy 2-4

2.1.2.1. Basement 2-4

2.1.2.2. Supracrustal Sequence 2-4

2.1.3. Structure 2-7

2.1.4. Metamorphism 2-11

2.1.5. Geochronology 2-11

2.2. Mineral Deposit Geology and Mineralization 2-12
2.2.1. Geology of Aggeneys Area 2-13
2.2.2. Broken Hill 2-14
2.2.3. Big Syncline 2-14
2.2.4. Black Mountain 2-15
2.2.5. Gamsberg 2-15
2.3. Stratigraphic Correlations 2-16
2.4. Discussion 2-17

Chapter 3
Origin of Namaqualand Proterozoic Sediment hosted Base Metal Mineralization 3-1
3.1. Introduction 3-1
3.2. Metallogenesis 3-4
3.2.1. Petrographic Aspects 3-4
3.2.2. Tectonic Aspects 3-6

Chapter 4
Geographic Information Systems (GIS): an overview 4-1
4.1. Introduction 4-1
4.2. Conceptual Geographic (Spatial) Database Design 4-2
4.2.1. Geographical features 4-2
4.2.2. Geographic (Spatial) Data Models 4-4
4.2.2.1. Vector Spatial Data Model 4-5
4.2.2.2. Raster Spatial Data Model 4-7
4.2.3. Relational Attribute Data Model 4-7
4.2.4. Combined Geo-relational Model 4-8
4.3. Software and Hardware Description 4-8
4.4. Data Analysis and GIS 4-9
4.5. Using GIS as an application system for predictive Mineral Exploration 4-11
4.6. GIS and Remote Sensing 4-13
4.7. Discussion 4-13

Chapter 5

Construction of the AGGeneys Exploration Database (AGGED) 5-1

5.1. Introduction 5-1

5.2. Data Sources 5-2

5.3. The AGGED Database Structure 5-3

5.3.1. Geological Layer 5-3

5.3.1.1. Spatial Data 5-5

5.3.1.2. Attribute Data 5-7

5.3.2. Geochemical Layer 5-8

5.3.2.1. Spatial Data 5-9

5.3.2.2. Attribute data 5-9

5.3.3. Geophysical Layer 5-9

5.3.3.1 Spatial Data 5-10

5.3.4. Topographic and Cadastral Layer 5-11

5.3.4.1. Spatial Data 5-11

5.3.4.2. Attribute Data 5-11

5.4. Sources of error in AGGED 5-11

5.5. Discussion 5-12

Chapter 6

Methodology of Data Processing and Analysis within AGGED 6-1

6.1. Introduction 6-1

6.2. Geological Data Sets 6-1

6.2.1. Classification 6-1

6.3. Geochemical Data Sets 6-2

6.3.1. Interpolation 6-2

6.3.2. Classification 6-3

6.3.2.1. Colour Display 6-4

6.3.2.2. Data Values 6-4

6.3.2.3. Data using Colour 6-5

6.3.3. Contouring of interpolated surfaces 6-6

6.4. Geophysical Data Sets 6-6

6.4.1. Classification 6-7

6.5. Topographic data 6-7
6.5.1. Digital Elevation Model 6-7
6.5.2. Slope and Aspect of elevation data 6-8
6.7. Integrating Grids using the Hue-Saturation-Value (HSV) Colour Model 6-8
6.8. Summary 6-9

Chapter 7
Integration and Analysis in AGGED - Results 7-1
7.1. Introduction 7-1
7.2. Regional Analysis 7-1
7.2.1. Geochemical Patterning 7-1
7.2.2. The relationship between Lithology and Geochemistry ... 7-3
7.2.3. Three Component Colour Mapping 7-3
7.2.3.1. Integrating Pb, Zn and Cu data 7-3
7.2.3.2. Integrating Geochemical and Magnetic data 7-5
7.2.3.3. Integrating Geochemical and Geological data 7-6
7.2.3.4 Integrating Geochemistry, Magnetics and Geology 7-7
7.3. Local Analysis 7-7
7.3.1. Integrating Geology, Geophysics and Geochemistry 7-7
7.4. Discussion and Conclusions 7-8

Chapter 8
Summary and Conclusions 8-1
8.1. Digital Integration 8-1
8.2. Newly Identified Target Areas 8-2
8.3. Concluding Remarks 8-3
8.3.1. Fractal Analysis in the further study of the distribution of ore Deposits in Bushmanland 8-3
8.3.2. Limiting factors of GIS and proposed future developments 8-4

References 9-1

Appendix 1
The Functionality of GIS A-1

Appendix 2 ..... A-9
Co-ordinate systems and Map projections

Appendix 3
Geochemical Data Listing A-13

Appendix 4
Registration problems with the aeromagnetic data A-14

Appendix 5
Explanation for not using the Digital Elevation Model produced by the Regional Department of Surveys and Mapping A-15

Appendix 6
Principles of Interpolation using Kriging A-16

Appendix 7
Colour display of raster data using spectral remapping on the computer graphics screen A-20

Appendix 8
Remapping of data values in the Hue-Saturation-Value Colour Model A-21

Acknowledgements

I thank Maarten de Wit for his resourcefulness in securing a project that helped me combine my interest in both computing and geology. His comments and advice during the project and drafting of this thesis was extremely helpful. The finances, data and brief for this project came from Gold Fields of South Africa, making this project possible. My thanks go to Dave Mourant, who was my contact person at Gold Fields. The interest shown in this project by Richard Viljoen, Rael Lipson, Cecil Begley, Fred Stevenson, Piet Smith and others at Goldfields, is appreciated. The GFSA workers at the Aggeneys mining offices, Springbok exploration offices, and Remote Sensing unit were very helpful in compiling the data for this project.

Shirley Butcher, head of the GIS centre, at the Information and Technology department, UCT was very patient and helpful in assisting me to grapple with and learn to use this powerful new technological tool. The knowledge gained from and shared with Shirley Butcher added to my skill in using GIS.

Sue Bindell, Prof. Hines Rutter, Henti Waker and others in the Department of Surveying, UCT, offered their assistance, support and pleasant companionship during the long hours spent working on this project.

The assistance of Greg Forsythe and Dave Mc Kelly at Forestek, in printing all the color maps, and Erminia Vitali who printed the Gondwana GIS maps, is acknowledged. The support from fellow students and staff in the Department of Geological Sciences, notably my fellow Masters students, as well as Ian Ransome, John McStay, Kevin Faure, Richard Armstrong, Gavin Doyle, Neville Buchanan, Patrick Sieas, Charlie Basson, Nazla Adonis is greatly appreciated.

I want to thank my friends and family whose support, patience and love motivated me to complete this project through trying times.

List of abbreviations used in this study

AGGED - AGGeneys Exploration Database

BSP- Bushmanaland Sub-Province

BMM - Black Mountain Mining

CAD - Computer Aided Design

ESRI - Environmental Systems Research Institute

EROS - Earth Resource Observation Site

GIS - Geographical Information Systems

GFSA - Gold Fields of South Africa

GSA - GeoScience Anomaly

GO-GEOID - GOndwana GEOscientific Indexing Database

GEOSIS - GEOscience Spatial Information System

GRID - subsystem for cell-based modelling within ARC/INFO

KBS - Knowledge Based Systems

NP - Namaqua Province

NMC - Namaqualand Metamorphic Complex

NNMB - Namaqua Natal Mobile Belt

RSP - Richtersveld Sub-Province

RISC - Reduced Instruction Set Chips

RAM - Random Access Memory

SAGS - South African Geological Survey

SD - Standard Deviation

SCCB - Southern Cape Conductive Belt

TIN - Triangulated Irregular Network modelling tool integrated within ARC/INFO

TVL - Tantalite Valley Line

T_{CHUR} - Chur model age

UOFS - University of Orange Free State

UC - Upward Continuation

ARCEDIT - ARC/INFO graphics and attribute editing program

ARCPLOT - graphics display and query system for ARC/INFO

ARCVIEW - viewing subsystem within ARC/INFO

List of Tables

Number refers to page on which table is placed

Table 2.1 - Lithostratigraphy of the Bushmanland and Okiep Groups in a generalized structural succession adapted from SACS (1980) 2-5

Table 2.2 - A summary of deformation events in the Bushmanland Area and the characteristic structure developed. 2-10

Table 2.3 - Correlation of different fold phases(F) interpreted by workers in the study area. ... 2-10

Table 2.4 - Ore Reserve and Grades of the Aggeneys-Gamsberg Deposits. 2-13

Table 2.5 - Variations in metal grade in the Aggeneys-Gamsberg orebodies. 2-17

Table 2.6 - Metal ratios of the Aggeneys-Gamsberg ore-bodies. 2-17

Table 3.1 - List of Sediment hosted Pb-Zn massive sulphide deposits, adapted from Sawkins (1990) with references cited. 3-2

Table 3.2 - Summary of important characteristics and relations that are known or suspected to be associated with Bushmanland stratiform base metal deposits (summarised from various authors mentioned in the text). 3-3

Table 3.3 - Synopsis of the Aggeneys-Gamsberg orebodies and the possible physical\chemical characteristics for their formation; modified from Lipson (1990). 3-7

Table 4.1 - Four generic geographical features classified according to euclidian dimensionality, adapted from Maguire and Dangermond (1991). 4-3

Table 4.2 - Basic classification of attribute data using level of measurement according to Stevens (1946) 4-3

Table 4.3 - Classification of basic types geographical data used in GIS within a two dimensional table linking dimensionality and levels of measurement, adapted from Robinson et al. 1984, and Unwin, 1981. 4-4

Table 4.4 - Summary of differences between the vector and raster data models. 4-5

Table 4.5 - Classification of some generic GIS analysis functions, adapted from Marble and Peauquet, 1983; and ESRI's ARC/VIEW Manual, 1992. Examples of usage in this study are added. 4-10

Table 5.1 - Phases of exploration activity in the Aggeneys area. 5-1

Table 5.2 - AGGED file storage layers (columns) in the different data models (rows). 5-4

Table 5.3 - Description of raster data files in the five sub layers of AGGED. 5-4

Table 5.4 - Description of vector data files in the five sub-layers of AGGED. 5-5

Table 5.5 - Characteristics of TM spectral bands 1, 4 and 7 in the visible and infrared wavelength region of the electromagnetic spectrum (adapted from Sabins, 1978). 5-7

Table 5.6 - Geochemical elements examined in this study. 5-8

Table 5.7 - Time taken to create, analyse and present data from AGGED. 5-13

Table 6.1 - Descriptive statistics of traverse sampled data (S), surface data interpolated through kriging (I). 6-5

Table 7.1 - Mean, minimum and maximum concentrations (in ppm) of elements Pb, Zn, Cu, Mn and Ni in zones defined by lithological units defined in Figure 2.3. 7-4
Table 8.1 - Key spatial analytical research topics that should be incorporated in future GIS after Openshaw (1990a). 8-7
Table 8.2 - Basic generic spatial analysis procedures after Openshaw (1990b). 8-7
Table A 3.1 - Partial listing of geochemical data stored in the AGGED database A-13

List of Figures

Number refers to page introducing the figure

Figure 2.1 - (A) Location of the study area within the tectono-stratigraphic framework of Namaqualand, modified after Hartnady et al., 1985. Location of the study area within the geographical framework of (B) Southern Africa and (C) Western Cape Province, South Africa. 1-2

Figure 2.1 - A - Tectonic subdivisions of Southern Africa, showing the location of the study area. B - Distribution of the Proto-Proterozoic to Meso-Proterozoic (Eburnian) and Neo-Proterozoic (Kibaran) Orogens 2-1

Figure 2.2 - Stratigraphic units of the Aggeneys area, Bushmanland, compiled from mapping done in the Aggeneysberge by Lipson (1978); the Gamsberg, Rozendaal (1975); Namiesberge area, Moore (1977); and the Haramoep and Hotson area (Thorpe, 1986) 2-6

Figure 2.3 - Lithological summary of Figure 2.2 into 11 units 2-7

Figure 2.4 - Interpolated image of the second vertical derivative aeromagnetic contour map with reduction to the pole; overlain with (1) axial traces of major F1, F2 and F3 synformal (dark grey) and antiformal folds, (2) interpreted thrust zones and (3) magnetic lineaments ... 2-9

Figure 2.5 - Regional metamorphic zonation within the western and central Namaqualand 2-11

Figure 3.1 - Distribution of Proterozoic Pb-Zn deposits within Gondwanaland 3-4

Figure 3.2 - Figure illustrating the sequence of events during collision 3-8

Figure 4.1 - Functional characteristics of a GIS toolkit, progressing from data capture (A) to data presentation (J) 4-1

Figure 4.2 - Schematic representation of the (A) Vector and (B) Raster data model used to define topological relations in spatial data 4-5

Figure 4.3 - Illustration of a query in the Gondwana GIS, linking spatial and attribute data 4-7

Figure 4.4 - Geo-Relational and Relational linkages used to reclassify the Litho-Stratigraphic map to a Lithological map 4-8

Figure 5.1 - Streams network overlain on TM image which highlights local geology Five separate contour maps of Pb, Zn, Cu, Mn and Ni analysed from stream sediment samples are overlain on this image 5-9

Figure 5.2 - Geophysical survey data collected in the Aggeneys area 5-10

Figure 5.3 - Contoured relief data used to create a Digital Elevation model 5-11

Figure 6.1 (A-B) - Interpolated Pb data displayed before and after linear colour coding was applied to the data 6-4

Figures 6.2 (A-E) - Graphed frequency distribution of 1374 traverse soil sample data points for Pb, Zn, Cu, Ni and Mn, all in ppm, collected over the study area and analysed 6-4

Figures 6.3 (A-E) - Logarithmic transformation of 1374 traverse soil sample data points, for elements Pb, Zn, Cu, Ni, and Mn 6-4

Figure 6.4 (A-B) - Comparison of interpolated surface data for Pb displayed with linear colour coding before and after logarithmic normalisation of the data, (A) and (B) respectively 6-5

Figure 6.5 (A-E) - Displays interpolated data grids (in ppm), logarithmically transformed and linear-colour-coded, for Zn, Pb, Cu, Mn and Ni in Figures A-E, respectively 6-6
Figure 6.6 - Digital Elevation Model of Bushmanland surface at Aggeneys, with relief shaded from south-east 6-8
Figure 6.7 - Hue-Saturation-Value (HSV) colour model used in three component colour mapping 6-9
Figure 7.1 - Three component colour map integrating Pb, Zn and Cu data using the HSV model . 7-4
Figure 7.2 - Three component colour map integrating Magnetics (1st derivative) and Pb, Zn data 7-5
Figure 7.3 - Three colour component map combining Landsat TM image composite (bands 7 4 1) and Pb, Zn data 7-6
Figure 7.4 - Three colour component map combining Landsat image, Magnetics and combined Pb/Zn data 7-7
Figure 7.5 - Three colour component map combining Lithology, Magnetics and combined Pb/Zn data, focused on the Aggeneys, Aroams and Gams farms 7-7
Figure 8.1 - Example of the hierarchical data structure for rock classification in GEOSIS (modified from Curry and Ady, 1989) 8-8
Figure A 2.1 - The geographic and planar co-ordinate system representations A-9
Figure A 4.1 - Geology vector map overlain on Government aeromagnetic image A-14
Figure A 6.1 (A-B) - Comparison of Pb point data interpolated using Kriging (A) and Inverse Distance Weighting (IDW; B) function A-16
Figure A 6.2 - Semivariograms modelling Lead (Pb), Zinc (Zn), Copper (Cu), Manganese (Mn) and Nickel (Ni) traverse geochemical data A-17
Figure A 6.3 (A-B) - Comparison of PB data interpolated surface (A), and semivariance associated with the interpolated surface (B) A-18
Figure A 8.1 - Conical representation of the Hue-Saturation-Value (HSV) model A-21

Chapter 1

Introduction

Applications of Geographic Information System (GIS) technology has seen a rapid proliferation in the areas of land use management, urban planning, and more recently mineral exploration. GIS is a computer software tool in which diverse data types are managed in a spatially referenced database. Analytical tools, an integral part of GIS, allow for analytical manipulation, integration and modelling of spatial features, summarised from earth data. In exploring for minerals, an understanding of information that describes the earth and earth processes is sought. Towards this end, geological, geochemical and geophysical data is collected during the various phases of a mineral exploration programme and can be efficiently managed and analysed in a GIS system.

In many countries, including South Africa, the mining industry has recognised GIS as a powerful technological tool that can support the exploration process. The ability of GIS to manipulate, integrate and analyse large volumes of data generated during mineral exploration programmes may lead to improved efficiency in the delineation of target areas.

Misconceptions, however, on the definition and capabilities of GIS do abound, resulting in GIS being either over- or under- estimated as a useful technology by geoscience explorationists. The former results in expensive failures where the system does not deliver expected analysis, management and output capabilities. The latter could deny the explorationist, involved in an information intensive discipline, access to a powerful technological tool.

The geological division of Gold Fields of South Africa (GFSA), a mineral exploration and mineral development company, recognised the emergence of GIS in exploration, and wanted to investigate the capabilities of GIS using a test study. This project was commissioned by Gold Fields of South Africa and the brief was to:

(i) select subsets of exploration geological, geochemical and geophysical data from the Aggeneys base metal province, South Africa.

(ii) design a spatial database incorporating the selected data sets.

(iii) analyse, interrogate and integrate these data sets using the GIS analytical toolkit.

A similar project was contracted to an independent consultant by GFSA in the Okiep Copper district, which lies to the north-west of the study area.

1.1. Location of the Study Area

The study area is located within the north-western Cape Province, in the Republic of South Africa (Figure 1.1 B and C). More specifically the study focuses on an area within the regional framework of Bushmanland, north-western Cape Province; centred around the Aggeneys farm and extending from Wortel Hill in the east, to Aggeneysberge to Gamsberg in the west (Figure 2.2). The extent of the study area is approximately 60 km by 30 km, and is within the longitudes 18°30' to 19°15'E and latitudes 29°00' to 29°19'S (Figure 1.1 A).

The Aggeneys farm itself is situated approximately 100 km north-east of Springbok and 60 km to the west of Pofadder, in the Namaqualand District of the north-western Cape Province (Figure 1.1 C). Aggeneys is a mining town, situated on the Aggeneys farm, that presently services the Pb-Zn mine at Broken Hill and will service any further development in the Aggeneys area. A national road, the N2, runs through the southern part of the study area (broken black line in Frontispiece). The road connects Springbok (magisterial seat in the Okiep copper district), with the mining town at Aggeneys, and continues eastward through Pofadder to Kakamas.

1.2. Regional Setting

A short statement on the regional geology and setting of the study area, within the framework of the Namaqualand District, follows. This is expanded in chapter 2.

The lithologies of the study area constitute part of the Namaqua Province of the Proterozoic Namaqualand Metamorphic Complex (NMC; Kroner and Blignault, 1976). The Bushmanland Subprovince forms the southern part of the Namaqualand Metamorphic Complex, and comprises a sequence of Mid-Proterozoic metasedimentary, metavolcanic and intrusive rocks (Tankard et al., 1982). The rocks of the Bushmanland Subgroup were formed around 1.6-2.0 Ga ago, and metamorphosed around 1.0-1.3 Ga.

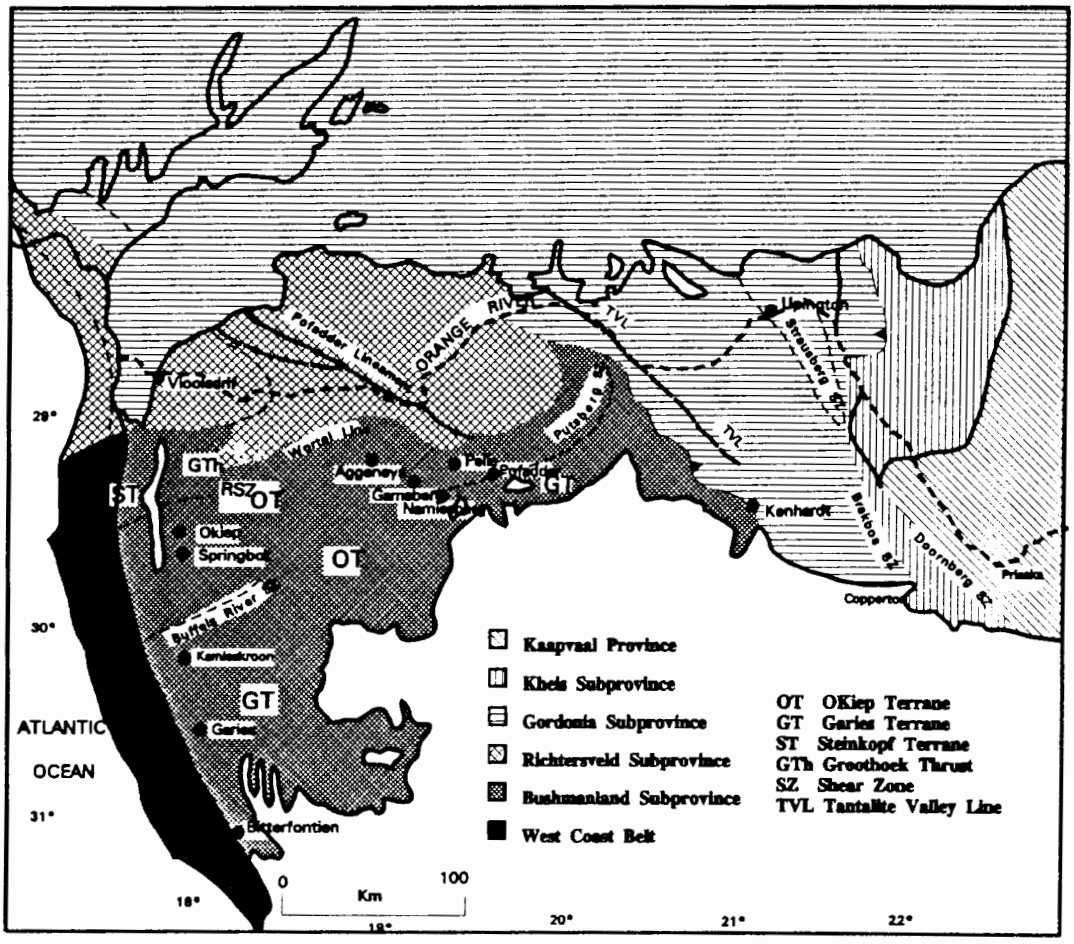

(A)

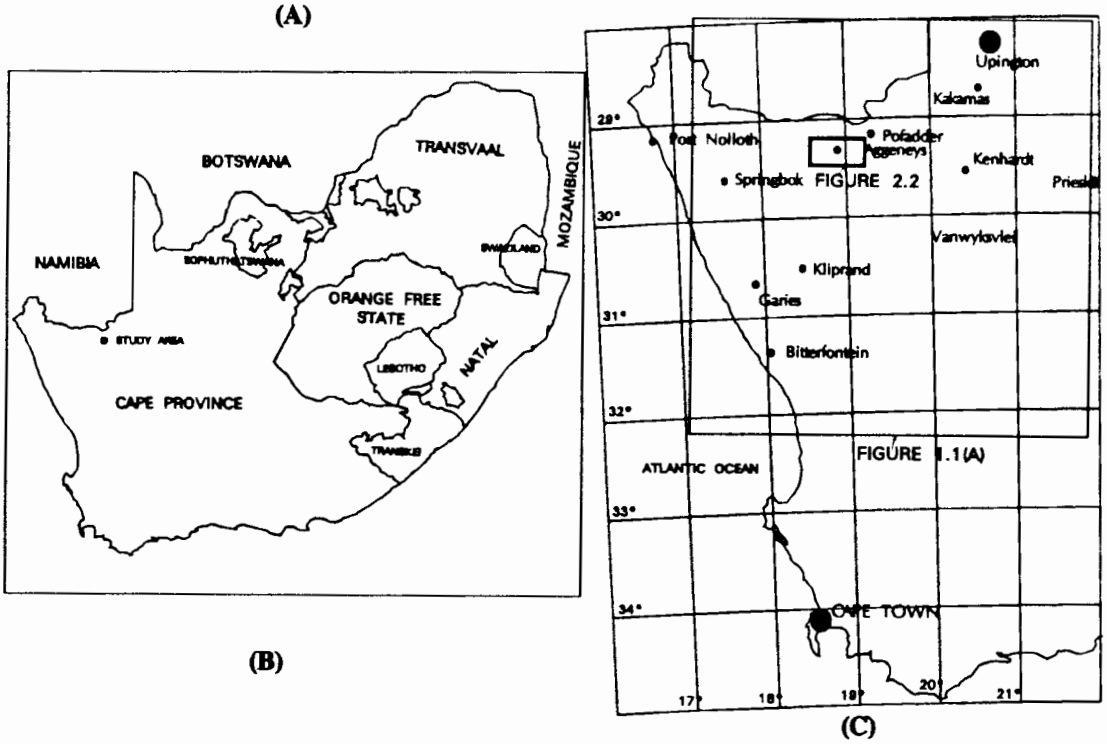

(B)

(C)

Figure 1.1 - (A) Location of study area within the the tectonostratigraphic framework of Namaqualand (modified after Hartnady et al., 1985).
Location of the study area within the geographical framework of (B) Southern Africa and (C) Western Cape Province, South Africa.

The Aggeneys Subgroup, a sequence of supracrustal rocks in the Bushmanland Subprovince of the NMC, contains four world class stratabound, massive-sulphide, Zn-Pb-Cu deposits, with estimated reserves of 10^7 - 10^8 million tonnes. Three deposits are located on the Aggeneys farm (Black Mountain, Broken Hill, Big Syncline ore bodies) and one at Gamsberg (Gamsberg Ore Formation). Host rocks and ores in the NMC have been subjected to regional metamorphism (amphibolite to granulite grade; Waters, 1986) related to four different phases of deformation (Joubert, 1974b).

1.3. Climate, Geomorphology and Vegetation

Climatic conditions in the study area are semi-arid, with average summer temperatures above 30 °C. Rainfall in the area is restricted to the summer months, tending to be concentrated in a few sporadic downpours, causing rainfall figures to be highly variable. The area forms part of the sand-rock desert of the North-Western Cape Province. Vegetation in the area is sparse, consisting mainly of xerophytic plants and bushes, and kokerbome scattered over the high ground. This can be seen on the Landsat image as palegreen areas (Frontispiece).

In the Aggeneys area, the Bushmanland surface falls away gently in the south into the dry, westward draining Koa river valley, which constitutes a regional paleo-drainage system. Highlands in the northern sector of the microsystem site are drained by ephemeral streams which terminate in small alluvial fans on the surrounding floodplain (Frontispiece). These streams converge in a northerly direction and drain into the Orange river.

1.4. Status of Previous Exploration and Research

The Aggeneys area has recorded a long and interesting history of exploration. The Aggeneys farm dates back to the 1908, and the area was investigated for mineral potential from as early as 1928. During this initial phase of exploration a shaft approximately 20 m deep was sunk at Black Mountain, in the northern extremities of the orebody, where mineralized intersections were poor, discouraging further exploration (Black Mountain Mining (BMM) company reports, 1983).

In 1971, on the advice of Dr P.Ryan exploration manager for Phelps Dodge, option

to the Aggeneys area was obtained for the above company when the structure of Cu-Pb-Zn-Ag mineralization was delineated at Aggeneys. Ryan recognised for the first time the structure of the outcrop and the localization of mineralization in a synformal fold plunging ENE (BMM company reports, 1983).

Following this discovery, gossans were recognised at Broken Hill (then known as Noeniepoort se Kop), Big Syncline and Gamsberg, lying generally south-east of Black Mountain, respectively (Lipson, 1990). The quick succession of base metal mineralization discovery at Aggeneys (Pb, Zn) in 1971, Gamsberg (Zn-Pb) in 1972, and Putsberg (Cu-Ag-Co) in 1973; resulted in a base metal exploration boom in the Namaqualand area (Wheatley, 1978). Multi-national corporations (Phelps Dodge, Gold Fields, Anglo American) commenced an intensive programme of base metal exploration in the north-western Cape Province.

The typical exploration strategy for Pb-Zn deposits in the Aggeneys area commenced with geological mapping, followed by stream sediment and whole rock geochemical surveys and ground and airborne geophysical surveys. The time span separating these phases in exploration ran into years. The multidisciplinary data collected during such research and exploration activities were often "filed and forgotten". An inventory of the data is difficult because the storage media used and location of the data are variable. Data is stored on paper maps and magnetic media; located mainly at exploration offices, Universities, head offices of companies or government surveying departments, and synthesis of such data is difficult.

1.5. Objectives of Present Investigation

The objectives of this study are to utilise GIS tools to examine the spatial relationships that exist between known occurrences of Pb-Zn deposits in the Aggeneys area, Bushmanland, and various geologic variables.

The project sequence is to:

i) Compile a spatial database comprising a subset of geological, geochemical and geophysical exploration data, over an area that includes the four known Pb-Zn deposits in the Aggeneys area.

ii) Manipulate, analyse and integrate these exploration datasets using the GIS.

iii) Examine correlations between geological, geochemical and geophysical data.

iii) Target potential mineralised areas for continued research and exploration.

vi) Evaluate GIS technology for mineral exploration.

Chapter 2

Regional Geological Framework

2.1. The Namaqualand Metamorphic Complex

This summary draws on reviews of the Namaqualand Metamorphic Complex and environs by Joubert (1971, 1986a,b), Tankard et al. (1982), a collection of papers in Botha (1983), Albat (1984), Stowe (1984), Hartnady et al. (1985), Watkeys (1986), Moore (1989), Lipson (1990), Mc Stay (1992), and Harris (1992).

2.1.1. Regional Tectonic Framework

The Namaqua Province forms the western part of a continuous tectono-metamorphic zone, extending as far as Natal in the east, termed the Namaqua-Natal mobile belt (NNMB; Tankard et al., 1982; Figure 2.1). The southern boundary of the NNMB has been delineated as the Southern Cape Conductive Belt (SCCB) by aeromagnetics surveys (De Beer and Meyer, 1983). The SCCB has been interpreted as a paleo-subduction zone which spatially corresponds to the Beattie Magnetic Anomaly (De Beer and Meyer, 1983); or as a cross-cutting Pan African suture to the south of the Beattie anomaly (Thomas et al. 1992). Comparable isotopic ages and kinematic histories also defines this broadly contiguous Namaqua-Natal belt (Jacobs et al., 1993). Thick Phanerozoic Karoo cover separates the Namaqualand outcrops from those in Natal.

Most of the Namaqua province is represented by rocks in the Central Zone (Tankard, 1982), collectively termed the Namaqualand Metamorphic Complex. The Meso-Proterozoic Namaqualand Metamorphic Complex (NMC), consists of polyphase deformed and metamorphic rocks of sedimentary, volcanic and intrusive origin. The Namaqua Province (NP) borders the western and southern boundaries of the Kaapvaal Craton (Figure 2.1). Along its western margin, the NP is bounded by the late Precambrian Gariep Province.

The Kheis and Richtersveld Subprovinces (Figure 2.1), formed during the 2.0 Ga Eburnian orogenic event in the eastern and western Namaqualand (Thomas et al., 1993). The Kheis Subprovince occupies a transitional zone between the gneissic

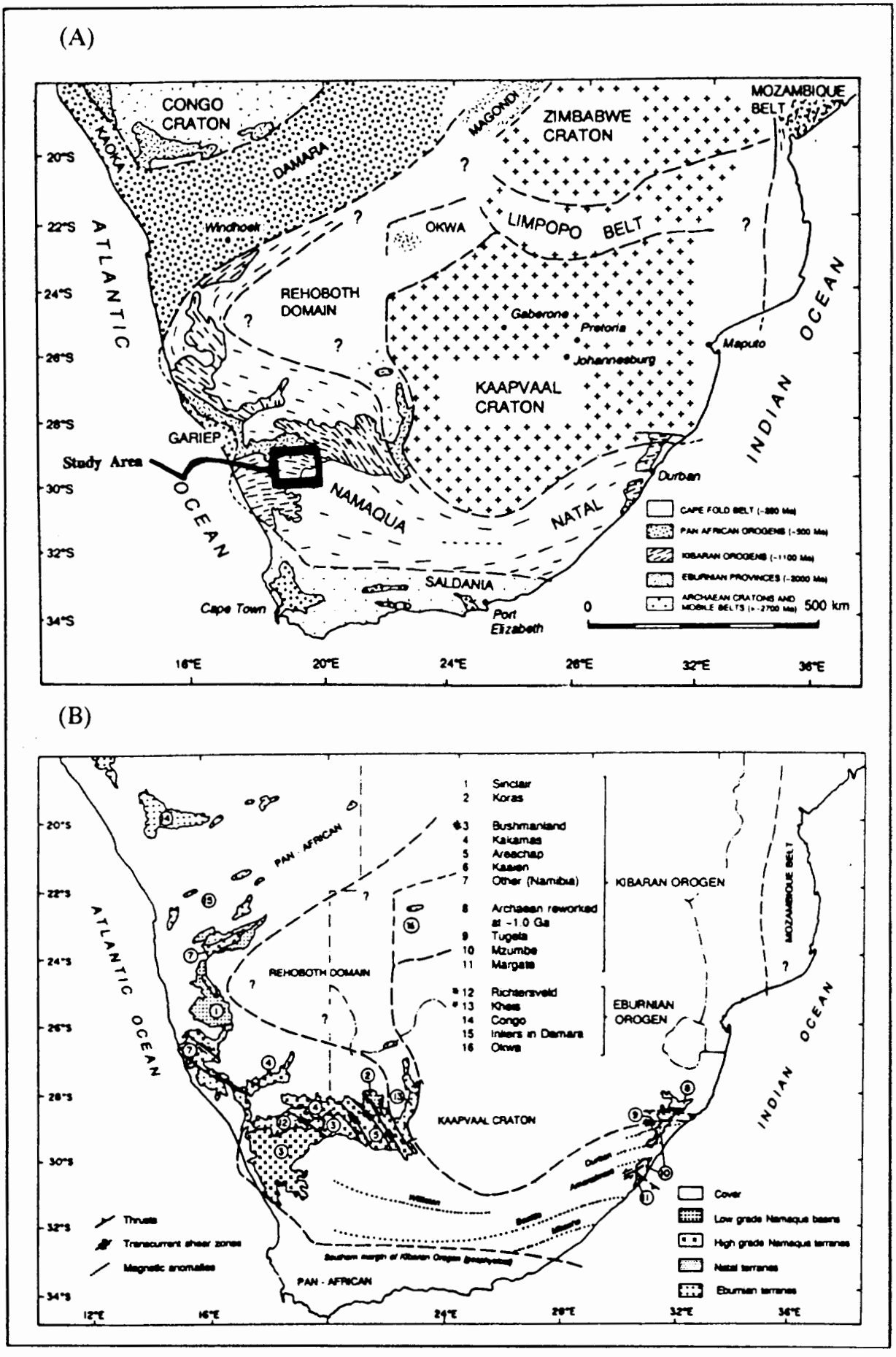

Figure 2.1 A - Tectonic subdivision of Southern Africa, showing the location of study area. B - Distribution of the Proto to Meso-Proterozoic (Eburnian) and Neo-Proterozoic (Kibaran) Orogens. Orogens marked with an asterix * are referred to in the text. Modified after Hartnady et al., 1985; Thomas et al., 1993).

terranes of the Namaqua Province in the west and basement and cratonic sequences of Kaapvaal Craton in the east (Tankard et al., 1982). The structurally distinct Kheis Subprovince extending north along the western margin of the Kaapvaal Craton (Hartnady et al., 1985; Figure 2.1), is a fold and thrust belt developed in a 2.0 Ga old quartzite, phyllite and amphibolite sequence (Stowe, 1984).

The Richtersveld Province (RSP) (Figure 2.1) contains the 2.0 Ga Orange River Group supracrustal sequence intruded by the Vioolsdrif, Richtersveld and Goodhouse Intrusive Suites (Reid and Barton, 1983). The rocks of the Richtersveld Subprovince probably represent the remnants of an island-arc assemblage in a convergent continental margin setting (Reid and Barton, 1983). The Gordonia Subprovince (Figure 2.1), incorporates a line of volcano-plutonic ampbibolite complexes (Stowe, 1984) and is segmented by bifurcating shear zones with north and west trends (Watkeys, 1986). The northern margin of the Gordonia Subprovince is obscured under cover of Late Pre-Cambrian Nama Group; the western margin is deformed and juxtaposed against the Kheis Subprovince.

The Groothoek Thrust, a northward dipping shear zone, marks a paleo-suture between the 2.0 Ga to 1.7 Ga Richtersveld Subprovince (Reid, 1982) and the 1.6 to 1.3 Ga Bushmanland Subprovince to the south (Blignault et al., 1983; Moore, 1989). The Wortel Line, lying along the Groothoek Thrust, comprises a series of amphibolitised mafic and ultramafic bodies (Joubert, 1974a).

The volcano-sedimentary Bushmanland Subprovince (BSP) forms the southern part of the Namaqualand Metamorphic Complex. The supracrustal gneisses of the BSP, deposited between 1.6-1.3 Ga, host the vast stratiform exhalative base-metal sulphide deposits of Big Syncline, Broken Hill, Black Mountain and Gamsberg (Moore, 1989; Moore et al., 1990). Figures 2.2 and 2.3 outline the extent of the study area showing location of these four deposits and outcrop of major paragneiss belts in the area. The BSP comprises largely granitic rocks of Kibaran age (1400 - 1100 Ma; Clifford et al., 1975, 1981; Tankard et al., 1982). These are intrusive, and infolded into thin but extensive E-W-trending belts of supracrustal rocks (Joubert, 1974b, 1986a).

The Tantalite Valley Line (TVL, Figure 1.1. a) marks a suture along which the RSP and BSP micro-continent was accreted to the Gordonia Subprovince in the north (Joubert, 1986b). The Bushmanland Subprovince is divided into the northern Okiep terrane and southern Garies terrane, separated by the Buffels River and Putsberg Shear Zones (Hartnady et al., 1985). Colliston and Praekelt (1988) subdivided the Bushmanland into the Aggeneys, Steinkopf and Okiep terranes; they do not recognise Hartnady's Garies terrane, but rather delineate a Pofadder terrane in the Richtersveld.

In the supracrustal rocks of Namaqua Province there is a marked change in structural grain from mainly E-W fabric in Bushmanland to north-west trending in the Gordonia Subprovince. This structural criteria was used by Hartnady et al. (1985) and Joubert (1986b) to delineate a tectonic boundary separating a Kakamas terrane (Gordonia Subprovince) from a Garies terrane (Bushmanland Subprovince). This division is disputed by Harris (1990). Recognising differences in structural geometry across the two subprovinces, Harris (1990) has shown that the interacting factors of shared D1-D4 deformation events led to a distinct change in structural pattern across the Bushmanland-Gordonia boundary zone. Therefore, the Kakamas and Garies terrane may form part of the same tectonic zone, contradicting proposed terrane models in the eastern Namaqua Province (Harris, 1990).

Mantle differentiation at approximately 2000 Ma and 1200 Ma ago, produced continental crust during the Orange River and Namaqua tecto-genetic events, respectively (Barton , 1983). Supracrustal rocks are associated with the early phase of the Orange River orogeny; whereas the main effect of the Namaqua orogeny was the generation of granitoids (Blignault et al., 1983). A continental collision model is presently proposed to explain the nature of the supracrustal sequences observed in the western NMC (Moore, 1989). The Bushmanland and Richtersveld are interpreted as part of a an exotic 2.0-1.6 Ga micro-continent that accreted with the Gordonia Subprovince at around 1.7 Ga (Joubert, 1986b, Hartnady et al. 1985). At 1.3 Ga the above assemblage in the southwest converged with Kaapvaal Craton to the north-east (Joubert, 1986b). The Southern Cape Conductive belt probably marks the cordilleran type subduction zone along which the Namaqua Province formed (De Beer and Meyer, 1983).

Gondwana reconstruction (Groenewald et al., 1991) place the 1.0 Ga metamorphic belt of western Dronning Maud Land, East Antarctica, and the Namaqua-Natal metamorphic belt in Southern Africa adjacent to each other. This suggests, according to Jacobs et al. (1993), that the Namaqua-Natal belt in Southern Africa and the Heimefrontjella (East Antarctica) orogens constitute fragments of an originally continuous, Kibaran (Grenvillian) orogenic belt. This orogen was accreted onto the southern margin of the Kaapvaal Craton (Jacobs et al., 1993).

2.1.2. Bushmanland Tectono-Stratigraphy

2.1.2.1. Basement

There is as yet no confirmed recognition of a basement to the supracrustal rocks in Bushmanland, although certain candidates have been proposed (eg. Watkeys, 1986 and Moore, 1977). In the Aggeneys area, the basal units of the sequence comprise porphyroblastic and banded biotite gneisses (Watkeys, 1986). The basal units include the Achab Gneiss, which is proposed as a possible basement complex to the supracrustal rocks in the Aggeneys area (Moore, 1977; Watkeys ,1986; Armstrong et al., 1988). For example, Moore (1977) argues that because the Achab Gneiss displays more phases of deformation than the overlying units, it might represent a basement sequence.

2.1.2.2. Supracrustal Sequence

The Bushmanland is characterised by an extensive, approximately 1000 meter thick sequence of supracrustal rocks. Litho-stratigraphic subdivisions in the Bushmanland sequence are listed in Table 1.1. Two sub-groupings are defined; the Okiep Group in the west, and the Bushmanland Group in the east (Table 1.1). The Bushmanland Group comprises various mica-sillimanite schist and quartzite associations (Pella and Aggeneys Subgroups), biotite/hornblende schists and gneisses (Guadom Subgroup) and leucogneisses with interbanded metasediments (Hom Subgroup) (Moore, 1989).

Metasedimentary rocks of the Aggeneys Subgroup, Bushmanland, host the four known base metal deposits in the Aggeneys area. In the study area, the supracrustal succession is exposed as flat topped inselbergs generally capped by resistant quartzite and surrounded by a flat, sand covered peneplain; the TM image Frontispiece displays

this vividly. The Aggeneys Subgroup comprises a lithological package of schists, quartzites, banded iron formation and amphibolites, with intrusive gneisses. The original sedimentary nature of the Bushmanland Group rocks is apparent from the gross lithological layering into formations of regional extent; as well as the occurrence of sedimentary structures such as cross-bedding and heavy-mineral-layers in the quartzites, the fine-scale interlayering of different lithologies; and the presence of intraformational conglomerates (Moore, 1989; Barr, 1988).

Table 2.1 - Lithostratigraphy of the Bushmanland and Okiep Groups in a generalized structural succession adapted from SACS (1980)

BUSHMANLAND GROUP		OKIEP GROUP	
Subgroup	Lithology	Subgroup	Lithology
Pella	Quartz muscovite schist and conglomerate unit Iron Formation Unit Metaquartzite Unit Schist Unit	Een Riet	Metasediments north of Steinkopf
		Khurisberg	Metaquartzites and schists of the Copper District and environs
Guadom	Mafic gneiss with intercalated metasediments		
		Aardvark	Metaquartzites and schists on the coastal plain east of Port Nolloth
Hom	Leucocratic pale grey gneisses with intercalated metasediments		
		Garies	All the undifferentiated grey gneisses of Namaqualand
Aggeneys*	Quartz muscovite schist and conglomerate units Iron Formation (Gams Formation) Metaquartzite unit Namies Schist Formation	Bitterfontein	Metaquartzites and schists of southern Namaqualand

* host to base metal deposits

The regional map of the Bushmanland area divides the supracrustal sequence into quartzites, schists and gneisses with amphibolites and minor calc-silicates. During

subsequent, more detailed lithostratigraphic mapping at Aggeneys by Lipson (1978) and Ryan et al., (1986); at Gamsberg by Rozendaal (1986), and in the Namiesberg Moore (1977) there has been little agreement on the details of the stratigraphic sequence.

A litho-stratigraphic compilation of the above workers mapping in the study area was prepared and is presented in Figure 2.2. The legend of Figure 2.2 summarises the metamorphic lithologies contained in the Aggeneys area in chrono-stratigraphic order. The Aroams Gneiss represents a syn-tectonic post-Bushmanland intrusive lithology (Armstrong et al., 1988), whilst the pink gneiss may represent a basement lithology in the area (Watkeys et al., 1988). Moore (1977), describes the pink gneiss as a widespread lithology in the Aggeneys area and suggests that the schist-quartzite succession (Aggeneys Subgroup) of the Bushmanland Group represents reworked detritus from the same volcanic event that created the pink gneisses. The Pink gneiss remains an enigmatic lithology in the Bushmanland area.

The Bushmanland cover sequences, above the pink gneisses, appear to have accumulated in shallow water (Tankard et al., 1982). The original pelitic bulk composition of the aluminous Namies Schist suggests that it was derived from a terrigenous provenance. Along with basement lithologies, terrigenous sediments from the Orange River Group, have been proposed as source material for the cover sequences in Bushmanland (Reid and Barton, 1983; Moore, 1989). A sequence of white quartz-arenites (Namies Quartzite) overly the pelitic rocks. The Bushmanland Sequence contains stratabound deposits of Zn-Pb-Cu in the south and sillimanite concentration in the north (Figure 2.2). The Zn-Pb-Cu deposits are hosted in predominantly siliceous, clastic sediments, interpreted to have been deposited in low energy restricted basins, capped by calcareous sediments with precipitates of Fe, Mn and Ba (Rozendaal, 1986; Ryan et al., 1986).

The combined ore succession is termed the Gams Iron Formation, comprising a package of massive sulphide and banded iron formations hosted by pelitic schists (metapelites), associated with massive quartzite (Figure 2.2). The top of the sequence in Bushmanland consists a variable sequence of layered gneisses of granitoid or basic

Litho-Stratigraphic Map Legend

LITHOLOGY	INTERPRETED STRATIGRAPHY
Upper Amphibolite Unit(2)	Nosees Mafic Gneiss
Quartzite	Gams Iron Formation
Quartzose Layered Schist	
Calc Silicate Unit	
Magnetite Amphibolite	
Quartz Muscovite Rock	Fly Schist
Dark Quartzite	Pella Quartzite
Schistose Quartzite	
White Massive Quartzite	
Interlayered Quartzite	
Schist (with massive sillimanite)	Namies Schist
White Quartzite	
Quartz Sillimanite Rock	
Schist	
Lower Conglomerate Amphibolite	Hotsan Gossan Unit
Quartz Biotite Schist	
Layered Quartzite	
Schist	
White Quartzite	Haramoep Antiform Unit
Schist	
Layered Feldspathic Quartzite	
Layered Quartzite Schist	
Purple Quartzite & schist	
Pink Gneiss	Hoogoor Suite
Grey Gneiss	Hom and Guadom Subgroup
Aroams Gneiss	Klein Namaqualand Suite
Undifferentiated Quartzite	
Undifferentiated Schist	
Undifferentiated Gneiss	

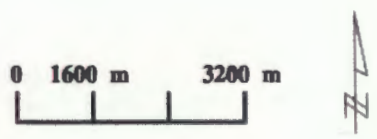

farm boundaries

geological contact

Sillimanite Mine

Black Mountain

Big Syncline

Broken Hill

Gamsberg

Figure 2.2 - Stratigraphic units of the Aggeneys area, Bushmanland, compiled from mapping done in the Aggeneysberge by Lipson (1978); the Gamsberg area, Rozendaal (1975); Namiesberg area, Moore (1977); and Haramoep and Hotson area (Thorpe, 1986). The units are placed in interpreted stratigraphic order from the Haramoep Antiform Unit upwards, with younger units placed above. The units below the Haramoep Antiform Unit represent units with uncertain stratigraphic status. The Aroams Gneiss is an intrusive lithology. Both the Pink and Grey Gneiss probably represent basement lithologies in the area, but their exact stratigraphic positions are unknown. Interpreted basement lithologies have not been mapped in outcrop over this area. Farm boundaries and names are overlain on the stratigraphic map. The extent of the study area averages 60 by 32 Km. For reference purposes, this map also shows the names of the farms and the locations of the four major deposits; these are omitted from subsequent maps.

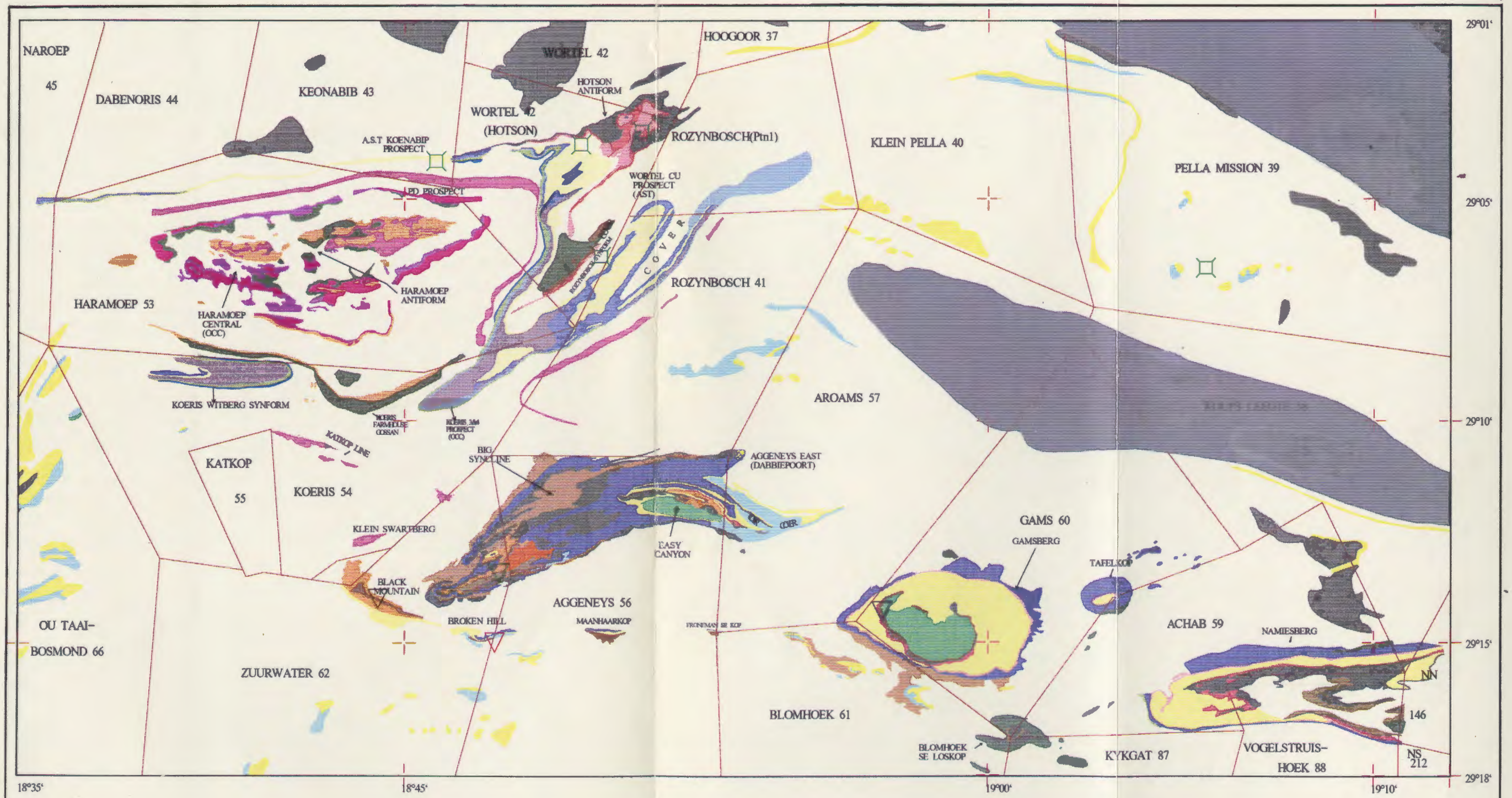

Litho-Stratigraphic Map, of the study area, centered on the Aggeneys farm, Bushmanland, NW Cape, South Africa (overlain with farm boundaries (brown line) and farm names)

composition, amphibolites and conglomerate (Nousees Mafic Gneiss). The stratigraphic position of the grey gneisses, comprising the Hom and Guadom Subgroup, is not clear since the gneisses are not in contact with the cover sequences. They might represent intrusive lithologies (Tankard et al., 1982).

Researchers from the University of Orange Free State (UOFS, viz. Praekaelt et al., 1983; Van Aswegan et al., 1987; and Colliston et al., 1989) completed a regional sequence mapping programme in the Bushmanland in 1983. UOFS researchers proposed the existence of a series of major thrust faults (Figure 2.4, overlay 2) to account for stratigraphic complexity in the area. They mapped a complex stratigraphic succession in the study area that include the several formation not included in Figure 2.2. Moore et al. (1990) believe that many of the formations recognised by the UOFS workers can in fact be correlated, and that thickness variations between formations are a result of lateral facies change and not thrusting. The proposed stratigraphic sub-divisions in Bushmanland therefore remain contentious to date. These subdivisions are therefore not incorporated into the litho-stratigraphic map (Figure 2.2).

At present the lithostratigraphic subdivision of the Namaqualand Metamorphic Complex (eg. Table 1.1 and Figure 2.2), is according to geographical regions between which correlation is only tentative given the present state of knowledge (Moore, 1989). Contributing to this are the absence of good marker horizons within the sequence and the inability to follow rock layers in the area between the inselbergs. There is also a distinct lack of precise geochronology in the area.

In this study, a more simplified map based purely on lithological subdivisions has been constructed (Figure 2.3). Figure 2.3 effectively reclassifies 32 subdivisions of the stratigraphic map (Figure 2.2), into eleven lithologic groupings. The aim of this new map is to simplify factual lithological data into a format that can be more easily handled for quantitative GIS analysis (see Chapter 6).

2.1.3. Structure

The Namaqualand Metamorphic Complex was subjected to a complex, polyphase, deformation history. Four major phases of deformation, D1 to D4, are identified in

Simplified Lithological Map, of the Aggeneys farm, and surroundings, Bushmanland, NW Cape, South Africa

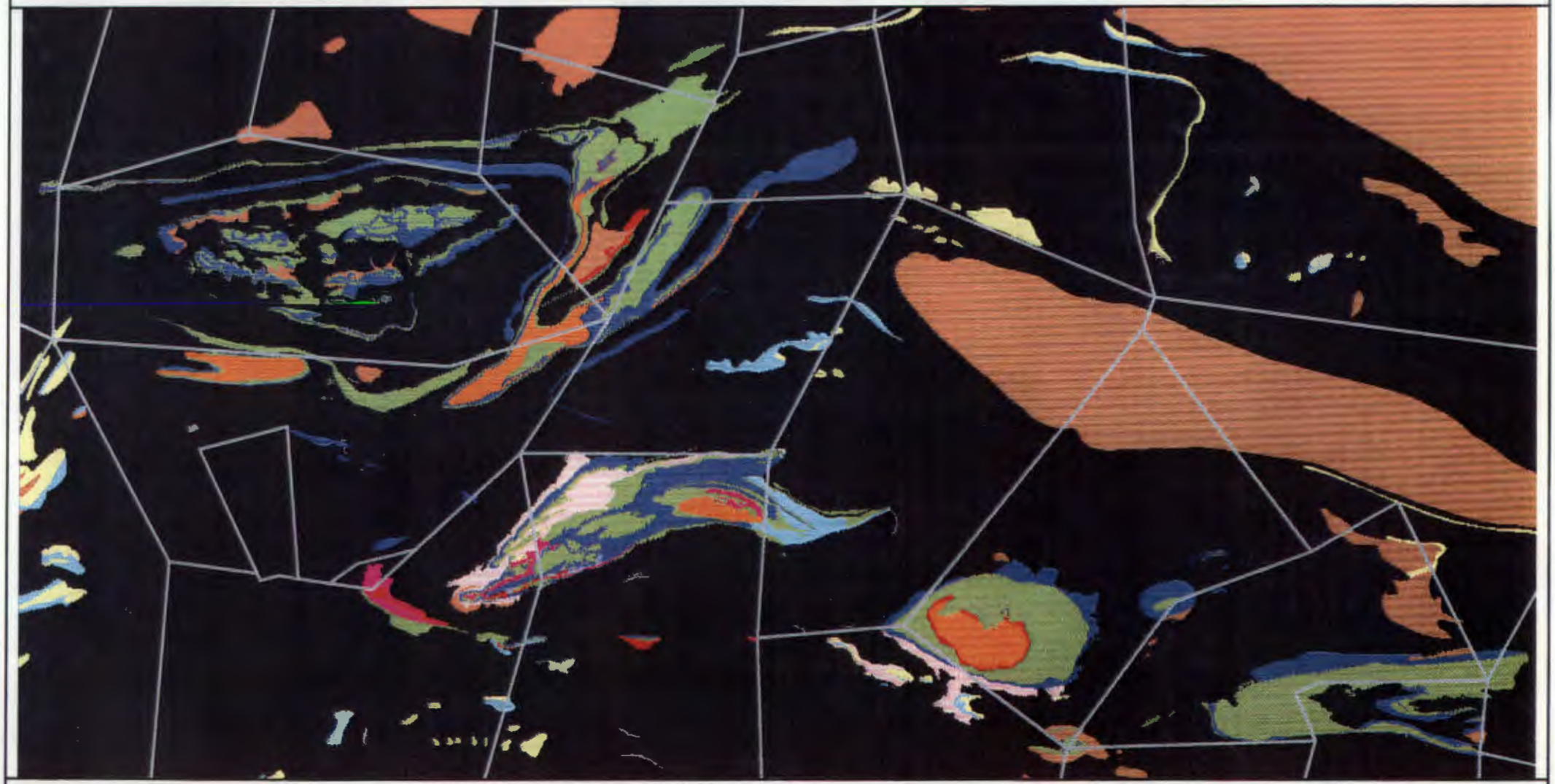

Figure 2.3 - This map summarises the lithologies of Figure 2.2 into a more simplified grouping of 11 units. Lithologies are grouped broadly into quartzite, schists, gneiss and amphibolites. Lithological horizons including magnetite-amphibolite rock, calc-silicate unit, quartz- muscovite rock and quartz-sillimanite rock, have been retained as individual groupings, because these rocks are closely associated with mineralisation in the area. The pink gneiss is also maintained as a separate group: many workers regard the pink gneiss an important (and possible basement) lithology in the area.

Bushmanland (Joubert, 1974b) . The deformation phases have subsequently been used as a regional reference framework of structural events. Each structural event has its own deformational style, orientation, intensity and associated metamorphism.

D1 is intense and eliminates primary structures in the sedimentary rocks. This event imprinted the major gneissic fabric on the supracrustal rocks (Harris, 1992). The significance of this deformation event on structural history of the Bushmanland is poorly constrained. Previous workers inferred F1 folding from indirect evidence. Odling (1983) provided the first direct field evidence for F1 folding in the Gamsberg mountains, Bushmanland. She identified the outcropping hinge zone of an F1 fold and recognised that F1 folds are generally difficult to recognise because F1 fold limbs are rapidly rotated into D2 orientations making the two almost indistinguishable.

D2 resulted in the greatest intensity of structural modification. Harris (1992) recognised that four episodes of folding are representative of the D2 event. The overall stress regime during the D2 event is compressional, resulting in north-south directed shortening and thickening (Harris, 1992, Moore, 1989). Lineations, parallel to the isoclinal fold-axis, trend ENE and plunge shallowly eastward (Moore, 1977). Thrust faulting during the D2 event (Joubert, 1978; Moore, 1989) resulted in basement gneisses overriding the supracrustal sequence from the north. Thrusting was superimposed on a system of north-west striking mylonite zones, where in the Graafwater mylonite zone an estimated a thrust displacement of approximately 80 Km occurred. (Harris, 1992).

D2 linear and planar fabrics have been greatly modified by the succeeding D3 event. McStay (1992) suggests the compressional D2 phase of deformation took place under upper amphibolite facies metamorphism and succeeding D3 shearing deformation occurred under granulite facies conditions. D3 phase of deformation is characterised by large scale open F3 folds (Joubert, 1978; Moore, 1977) associated with steeply dipping east-west trending shear zones (Joubert, 1974b). Strike-slip shearing resulted in the formation of the broad ductile shear zones in Bushmanland and Gordonia Subprovinces (Harris, 1992).

The F3 open upright folds give rise to the NW trending dome and basin (closed or synformal structures) structure of central Namaqualand. The closed (Gamsberg) and synformal (Aggeneysberge, Namiesberg) basin and dome structures are clearly visible in the outcropping inselberg contained in the study area (Figure 2.2 and Frontispiece). The most prominent shear zones occur in areas where D2 thrusting has occurred.

Odling (1987) recognises four phases of folding leading to the formation of the Gamsberg basin. The northeast plunging basin initially formed by the superposition of D2 on a major F1 fold. This was overprinted by an F3 synform, superimposed on the western portion of the basin. The interference of these 3 fold phases in the Gamsberg Mountains are shown in Figure 2.4 (overlay 1 - axial traces of major folds).

Extensional D4 strains re-deformed the F3 fold structures, causing stretching of D3 structures along NE lines and simultaneous tightening of folds in NW-SE direction (Harris, 1992). The D3 phase of deformation affects rocks of the Spektakel Suite, where both open folding and shearing is recognised. The age of the Spektakel Suite is 1200 Ma (Clifford et al., 1975 and Reid and Barton, 1983) implying that D3 deformation is younger than 1200 Ma (Moore, 1989).

In the Aggeneys, Gamsberg and Namiesberg areas, which fall within the study area, north-east trending upright open F4 folds deform the major F3 synforms (Rozendaal, 1975; Moore, 1977; Lipson, 1978). Crosscutting these folds are later upright north-south folds associated with prominent fracturing and mylonitisation (Moore, 1989).

Clockwise (dextral) rotation of lithological layering, D1 and D2 foliations, and F3 folds, during D4 event results in the appearance of NE to ENE structural trends within Bushmanland. The effects of D4 on structural grain in Bushmanland are clearly distinguishable as north-south trending magnetic lineaments (Figure 2.4, overlay 3).

The structural history of the study area records most of the above events and is summarised graphically in Figure 2.4, with overlays, and are listed in Table 2.2.
Fold phases in the study area, listed in Table 2.2, correspond to different phases of

First Vertical Derivative of the Total Magnetic Field overlain with Structural Features (1, 2 and 3)

Figure 2.4 - Interpolated image of the second vertical derivative aeromagnetic contour map with reduction to the pole. The magnetic survey covers the farms Aggeneys, Bloemhoek, and northern parts of farms Gams and Aroams (Figure 2.2). Magnetic intensities are coloured black/dark-grey = low, grey = intermediate, white = high.
Overlay 1 shows shear zones and the axial traces of major F1, F2 and F3 synformal (yellow) and antiformal (red) fold structures in the study area.
Overlay 2 delineates interpreted thrust zones (slate blue). Names of thrusts are listed in the map legend.
Overlay 3 presents structural lineaments as interpreted from magnetic images covering the Aggeneys area (blue-green).

deformation recognised by Joubert (1974b), Lipson (1978), Moore (1977), Rozendaal (1977) and Odling (1983). A correlation of fold phases proposed by the above workers, during mapping in different regions of the study area, is listed in Table 2.3.

Table 2.2 - A summary of deformation events in the Bushmanland Area and the characteristic structure developed.

First Phase of Deformation (D1) and folds (F1)

Positive identification of F1 folds at Gamsberg only (Odling, 1983). D1 is intense and eliminates primary structures. Folding (F1) is characterised by isoclinal folds with sharp tapering hinge zones.

Second Phase of Deformation (D2)

This is the most important phase of deformation in the area: most of the ore bodies are localized in the vicinity of F2 fold closures where thickening of individual zones of mineralization has occurred. Penetrative hinge zone axial planar schistosity characterises F2 folds. Plunge of F2 fold axes is generally north-east and east.

Third Phase of Deformation (D3)

This phase of deformation resulted in large scale open, asymmetric, synformal and antiformal structures in Aggeneys area. Plunge of F2 fold axes is east-north-east at 20-30 degrees. Mineralization is associated with the limbs of F3 folds.

Fourth Phase of Deformation (D4)

North and north-north-west-trending monoclinal folds, and by northerly trending faults, fractures and shear zones. These structures deform all pre-existing structures in the area.

Table 2.3 - Correlation of different fold phases(F) interpreted by workers in the study area.

Joubert (1974b) Regional	Lipson (1978) Aggeneysberge	Moore (1977) Namiesberg	Rozendaal (1977) Gamsberg	Odling (1983) Gamsberg
F1	F1	F1		F1
F2	F2	F2	F1	F2
F3	F3a	F3	F3	F3
	F3b	F4	F2	
F4	F4	F5	F4	F4
			F5	

2.1.4. Metamorphism

In the Bushmanland Subprovince, Namaqualand, amphibolite to granulite facies metamorphism and granitic to charnockitic magmatism occurred at around 1200-1100 Ma ago (Waters, 1988). The metamorphic mineral assemblages, in particular of the metapelitic and metavolcanic rock types, reveal a pattern of E-W-trending metamorphic zones (Waters, 1986; Figure 2.5). These are bound to the north and south by rocks metamorphosed in the amphibolite facies. The isograd between granulite facies and upper amphibolite appears to coincide with the Ratelpoort shear zone north of Springbok (Blignaut et al., 1983).

The granulite-amphibolite boundary has a large bulge around Springbok and swings southwards (Figure 2.5). Albat (1984) believes that this boundary is structurally controlled by late open folding. Mc Stay (1992) argues that Albat's results are poorly constrained and that, the location of the amphibolite-granulite facies boundary is uncertain.

Pelitic gneisses of the Aggeneys-Gamsberg area contain the first recognisable metamorphic mineral paragenesis (biotite-sillimanite-quartz), that belongs to the amphibolite facies (Waters, 1986). The amphibolite-granulite facies transition in Central Namaqualand is defined by the reaction isograd:

$$\text{Biotite} + \text{Sillimanite} + \text{Quartz} = \text{Garnet} + \text{K feldspar} + H_2O$$

Frimmel et al., (1993) investigating metapelites that host the stratiform deposits in Bushmanland, estimate peak metamorphic temperatures of 670° C and 4 kbars. Relating metamorphic imprints to structural events, it has been widely accepted that the major metamorphic imprint (M2) is coincident with the major structural episode (D2, Joubert, 1971; Moore, 1989). Mc Stay (1992), however, working in the Buffels-River area, records evidence for a thermal maximum at D3 outlasting the D2 deformation event.

2.1.5. Geochronology

Eglington (1989) dating metapelites in Natal obtained T_{CHUR} ages of less than 2.0 Ga, indicating that Archean crustal lithologies were not a major provenance for clastic

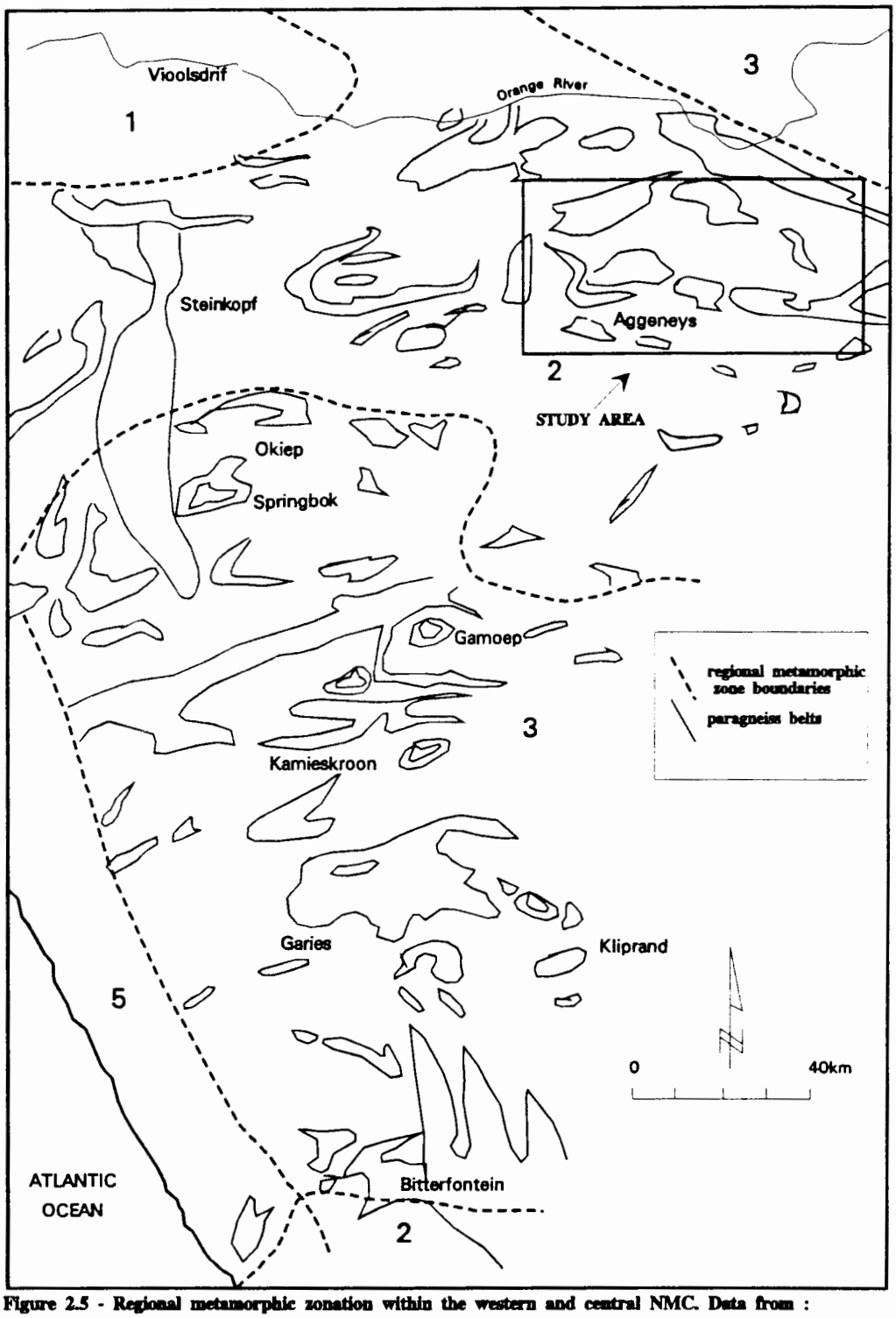

Figure 2.5 - Regional metamorphic zonation within the western and central NMC. Data from : Blignaut et al., 1980; Albat, 1984; Beukes, 1973; Waters et al., 1984; Joubert, 1971; Mc Stay, 1992.

Zone 1 - greenschist/lower amphibolite facies with the upper boundary defined by the transition from andalusite to sillimanite.

Zone 2 - amphibolite facies with the upper boundary defined by the appearance of orthopyroxene

Zone 3 - granulite facies metamorphism

Zone 4 - the polyphase high-grade metamorphism in the Geselskapbank area

Zone 5 - the superimposed Pan-African imprint along the west coast

sediments in the Namaqua-Natal belt. Eglington (1989) reports that all his data supports models involving substantial crustal accretion and differentiation, in the Namaqua-Natal belt, subsequent to approximately 1.5 Ga.

The Achab Gneiss yield Pb/Pb ages of 2020 +_ 150 Ma (Welke and Smith, 1984); and Armstrong et al., (1988) infer a 2000 Ma Pb/Pb age for the granitoid crystalline terrain from which Bushmanland sequence was derived. Data from the Achab Gneiss in the Aggeneys area, indicates that it could represent a basement to rocks in the Bushmanland Sequence (Armstrong et al., 1988). Watkeys (1986) and Moore (1977) also believe that the Achab gneissic suite forms part of the basement to the Aggeneys Subgroup. Hence an upper age constraint on deposition of the Bushmanland Group can be placed at 2000 Ma.

Amphibolites at the top of the supracrustal sequence in the Aggeneys-Gamsberg area, give a Sm-Nd isochron age 1600 Ma (Betton, 1984; Reid et al., 1987). This age provides a minimum age for the underlying sediments. Combining the upper and lower age constraints discussed above, the time of formation of the supracrustal sequence falls somewhere between 1600 - 2000 Ma. Dating of the Aggeneys-Gamsberg orebodies within the ASG has yielded significantly younger Pb/Pb and U/Pb ages of between 1200-1500 Ma (Koeppel, 1980).

2.2. Mineral Deposit Geology and Mineralisation

Within the metasediments of the Bushmanland Group, Pb-Zn sulphide mineralisation is restricted to the Aggeneys/Gamsberg ore horizon. Figures 1.1 and 2.2 outline the geographical location of the Broken Hill, Black Mountain , Big Syncline and Gamsberg deposits, all within the extent of the study area. The four deposits contain economic grade mineralisation. Table 2.4 lists the grade and tonnage of each deposit.

Two papers: "The Aggeneys Base Metal Sulphide Deposits, Namaqualand District" by P.J. Ryan, A.L. Lawrence, R.D. Lipson, J.M. Moore, A. Paterson, D.P. Stedman, and D. Van Zyl (1986); and "The Gamsberg Zinc Deposit, Namaqualand District" by A. Rozendaal, both published in Mineral Deposits of Southern Africa (1986) describes the geology of the deposits in the study area by workers very experienced with the

geology of the area. The following section summarises the main observations and conclusions of these articles.

Table 2.4 - Ore Reserve and Grades of the Aggeneys-Gamsberg Deposits.

Ore Deposit	Reserves (million tonnes)	Cu %	Pb %	Zn %	Ag (gm/t)
Broken Hill *	85	0.34	3.57	1.77	48.1
Black Mountain *	82	0.75	2.67	0.59	29.8
Big Syncline *	101	0.04	1.01	2.45	12.9
Gamsberg +	150	-	0.55	7.1	-

*** From Ryan et al. (1986) + From Rozendaal (1986)**

2.2.1. Geology of Aggeneys Area

At Aggeneys (Figure 2.2), the supracrustal sequence consists of: basal augen-gneiss, a lower unit of pink quartzo-feldspathic gneiss overlain by aluminous schist, and an upper unit of schists and quartzite. The lower unit of leucocratic gneisses are regarded as probable meta-pyroclastic deposits by Watkeys et al. (1988). The quartzite-aluminous schist couplet is an economically important lithology in the Bushmanland supracrustal sequence (Joubert, 1986a and b). The central parts of the supracrustal sequence in the Aggeneys area, particularly the quartzites, quartz-schist couplet, and iron formations are associated with Zn-Pb mineralisation.

Four separate ore bodies comprise the Aggeneys base metal deposits: Black Mountain, Broken Hill, Big Syncline and Gamsberg. Black Mountain was first recognised for its mineral potential, and initial exploration drilling, in 1971, was concentrated here. Exploration activity gradually spread to Broken Hill (1972) and Big Syncline (1973). The Broken Hill ore body proved to have the higher metal grades and was selected as a first mining exploitation target.

The Aggeneys ore-formation consists of a 200 metre thick succession of pelitic schist. Economic base metal sulphides in the Aggeneys area consist of varying proportions of

chalcopyrite, galena, and sphalerite which, with pyrite and pyrrhotite, constitute the massive sulphide concentrations.

The structural aspects of the Aggeneys-Gamsberg area are dominated by major early F2 recumbent, isoclinal synforms of east-west trends, that are refolded by later F3 synformal structures with steep, northerly-dipping axial planes and shallow easterly plunges (Moore, 1989). These synforms are deformed by north-east trending upright D4 structures, most notably the Aggeneysberge and Gamsberg synforms (Moore, 1977; Lipson, 1978).

2.2.2. Broken Hill

The Broken Hill ore-body (Figure 2.2) outcrops on the southern slopes of Broken Hill as a well defined, 600 m, east west striking, massive and magnetite rich gossan. The original depositional sequence is thought to have been overfolded (F1) and then refolded (F2).

In the Upper ore-body succession, a well-banded magnetite-quartzite is the predominant unit; and it consists of thin alternating bands of magnetite and quartz. Galena, sphalerite, and chalcopyrite are disseminated throughout this unit. The banded magnetite grades into a banded magnetite amphibolite, which has a combined base metal content slightly higher than the magnetite quartzite.

Baritic massive sulphide occurs directly below and in sharp contact with the magnetic quartzite. The sulphidic-quartzite, is preserved in the core of F2 folds, and lies stratigraphically below the massive sulphide unit. Within the footwall succession of the upper ore body, a pyritic-graphitic-biotite-schist grades into a sillimanite-quartz-biotite schist which is thought to be the stratigraphic equivalent of the Spring Schist and Quartzite member in the Aggeneys Mountains.

2.2.3. Big Syncline

Big Syncline (Figure 2.2) is situated in the south-western part of the Aggeneys Mountains. The Spring Schist and quartzite member in this area consists of a schist grading upwards into a quartzite. The well-mineralised portions of the Spring Schist

constitute the stratabound Big Syncline ore-body. Along the Southern rim of the syncline, the ore body displays higher and more consistent grades. There is a gradual drop in grade through the hinge zone.

2.2.4. Black Mountain

The most westerly deposit, Black Mountain (Figure 2.2), whose discovery sparked further major exploration in the Bushmanland area, gained its name from the characteristic black staining caused by the oxidation and weathering of the sulphide-rich gossans on the slopes of the mountain. Stratigraphy in this area is contained in a major recumbent isoclinal (F2) synformal infold into the basal gneisses. The Aggeneys Ore Formation occurs in the core of this F2 synformal structure. The stratigraphy in the upper limb of the fold is overturned causing stratigraphy to be reversed.

An Upper and Lower ore-body are present at Black Mountain. The relationship between the two is not clear. They may be at different stratigraphic positions, or they may have been structurally emplaced into their present relative positions and may in fact be laterally equivalent to the Broken Hill ore bodies (Ryan et al., 1986).

Mineralisation occurs within garnet-quartzite, magnetite-quartzite and magnetite-amphibolite. Copper concentration decreases upward and Pb and Zn increases upward within these units. The garnet-quartzite has been interpreted as a metamorphosed siliceous altered feeder zone to the deposit (Barr, 1988). Dominant lithologies of the lower ore body are garnet-quartzite, magnetite-quartzite and sulphidic-schist. The mineralised magnetite- quartzites grade laterally into barite-sulphide-schists.

2.2.5. Gamsberg

The Gamsberg stratiform Zn-Pb-Cu deposit outcrops as a large steep-sided inselberg, with an internal basin in the eastern extremities of the study area (Figure 2.2). Mineralization is exposed as a prominent gossan along the periphery of this basin. The Gamsberg deposit is being considered for future mining after mining at Broken Hill is phased out (Richard Viljoen, Goldfields, pers. comm., 1993).

The stratigraphic succession at Gamsberg consists of basal quartzo-feldspathic gneiss

overlain by a thick succession of sillimanite-bearing pelitic-schist and metaquartzite followed by an iron-formation, and succeeded in turn by psammitic schist, lenses of conglomerate, quartzite, and amphibolite.

Zn-Pb mineralization at Gamsberg occurs within the Gams-Iron-Formation. The Gams-Iron- Formation comprises mainly, banded fine-grained pelitic and calcareous metasediments. At Gamsberg, sulphides include pyrite, pyrrhotite, marcasite, marmatitic sphalerite, galena and albandite.

Major exposures of barite are found in the eastern and south-eastern corners of the Gamsberg. Barite is associated with the base metal mineralisation in this area, and both are confined to the upper part of the iron formation and interbedded with the oxide facies.

Vertical zoning of the ore-minerals in the Gams Iron Formation, is a prominent feature. This "ore-body-zoning" develops laterally into "district-zoning" if similar deposits at Aggeneys viz. Black Mountain, Broken Hill and Big Syncline are brought into consideration.

2.3. Stratigraphic Correlations

A regional trend in metal content of the Bushmanland ore deposits occurs, with progressive increase in Cu to the west and Zn to the east (Ryan et al., 1986; Table 2.5 and 2.6). Regional mapping in the Aggeneys-Pofadder region disclosed the possibility of Gamsberg being the easterly equivalent of the Aggeneys base-metal mineralisation zone (Joubert, 1974b; Rozendaal, 1986), thus placing all four deposits (Broken Hill, Big Syncline, Black Mountain and Gamsberg) potentially at the same stratigraphic position.

Moore (1989) suggests that the precise stratigraphic position of the Broken Hill iron-formations and base-metal sulphide deposits to the south of Aggeneysberge is still uncertain, and disputes previous attempts to correlate between iron formation at Broken Hill and Gamsberg. He believes that the Broken Hill iron formation

Table 2.5 - Variations in metal grade in the Aggeneys-Gamsberg orebodies.

Azimuth	Ore Body	% Cu	% Pb	% Zn
West	Black Mt	0.75	2.67	0.59
	Broken Hill	0.34	3.57	1.77
	Big Syncline	0.04	1.01	2.45
East	Gamsberg	-	0.50	7.00

adapted from Ryan et. al.(1986)

Table 2.6 - Metal ratios of the Aggeneys-Gamsberg ore-bodies.

	Gamsberg	Big Syncline	Broken Hill	Black Mountain
Zn/Pb	93	71	33	18
Zn/Cu	100	98	84	44
Pb/Cu	97	96	91	78

adapted from Lipson(1990)

represent localised iron formation units that stratigraphically underlie the white quartzite, and are not, therefore, equivalents of the Gams Iron Formation. Lipson (1978) and Ryan et al., (1986) maintained that the iron formation at Broken Hill are the equivalents of the Gams Formation. They believe that the iron formations stratigraphically overlie the white quartzite unit, but structurally underlie it in outcrop.

2.4. Discussion

The above discussion may seem confusing at times, but this merely reflects the state of stratigraphic, structural and tectonic interpretation in the Bushmanland area. Geological interpretations in the area are complicated by polyphase deformation and extensive high grade metamorphism of Bushmanland supacrustals. These events have overprinted primary fabric, making geological and genetic modelling in the area contentious.

Genetic modelling has been attempted to explain the origin of the four known stratiform massive-sulphide base-metal deposits hosted in the Bushmanland metasediments. In all four deposits there is a systematic variation in base metal content and mineralogy in both a vertical and lateral sense (Table 2.5 and 2.6). Therefore, besides being potentially at the same stratigraphic level, the four deposits may also share similar metal associations and ore-genesis. This is discussed further in Chapter 3.

Chapter 3

Origin of Namaqualand Proterozoic Sediment hosted Base Metal Mineralization

3.1. Introduction

The term "sediment-hosted massive-sulphide deposits" is used to describe massive to disseminated, conformable sulphide-ores that occur most typically within marine shales or siltstone or their metamorphic equivalents (Large, 1980; Sawkins, 1990). Volcanic material is either minor or absent in the immediate host rocks associated with the deposit. Sediment- hosted massive-sulphide deposits are predominantly Zn and Pb enriched, associated with minor (Cu, Ag) and barite. These deposits are typically associated with argillic sediments in third order continental rift controlled sedimentary basins (Meyer, 1981, Sawkins, 1990). Major world reserves of Pb and Zn are contained in sediment-hosted massive-sulphide bodies, Table 3.1 lists some of the districts containing these deposits. Details including age, metal composition, tonnage and rocks hosting the deposits are also summarised in Table 3.1.

The stratiform Pb-Zn deposits at Bushmanland are hosted in a metasedimentary succession, and the deposits display many of the characteristics conforming with exhalative models. The deposits have therefore been compared with sedimentary exhalative (SEDEX) deposits related to hydrothermal vents in a rift environment (Ryan et al., 1986; Willner et al., 1990). The Aggeneys deposits display close genetic affinities with the Broken Hill deposits in Australia, and the New Brunswick deposits of Canada (Ryan et al., 1986). Rozendaal (1986) investigating the deposit at Gamsberg, and Frimmel et al., (1993) at Broken Hill, both describe strong similarities between the Bushmanland deposits and modern sedimentary base metal mineralisation in the Red Sea. However Red Sea deposits are associated with volcanic rocks.

Salient observations regarding the spatial and genetic relationships between the occurrence of stratiform base metal deposits in the Aggeneys area, Bushmanland and various geological (lithological, structural, geochemical, geophysical) variables constitute the elements for a geological model. This chapter reviews some genetic concepts put forward for the occurrence of the Aggeneys deposits.

Table 3.1 - List of Sediment Hosted Pb-Zn massive sulphide deposits adapted from Sawkins (1990) with references cited in Sawkins.

Deposit or District	Epoc Age(Ga)	Metals	Tonnage	Host Rocks	Reference
Lik, N. W. Alaskska	Mississippian	Zn,Pb	25+	Carbonatite, shale	Forreset and Sawkins (1983)
Red Dog	Mississippian	Zn,Pb	85+	Carbonatite, shale	D.M. Moore et al (1986)
Rammelsburg, Germany	Devonian	Zn,Pb,Cu	22	Carbonatite, slates	Hannak (1981)
Meggen, Germany	Devonian	Zn,Pb	50	Carbonatite, slates	Krebs (1981)
Macmillan Pass	Devonian	Zn,Pb	20	Carbonatite, siliceous shale	Carne and Cathro (1982)
Gataga	Devonian	Zn,Pb	30	Siliceous shale	MacIntyre (1982)
Howard Pass	Silurian	Zn,Pb	?	Carbonatite, sandstone, chert	Carne and Cathro (1982)
Anvil	Cambrian	Zn,Pb	140	Graphitic phylite	Carne and Cathro(1982)
Sillivan.B.C.	Proterozoic (1.4)	Zn,Pb	155	Argillite	Ethier et al.(1976)
Mt.Isa, Australia	Proterozoic (1.65)	Zn,Pb	88.6	Carbonatite, shale, dolomite	Mathias and Clarke (1975)
Hilton, Australia	Proterozoic	Zn,Pb	35.6	Carbonatite, shale	Mathias et al.(1973)
Lady Lorreta, Australia	Proterozoic	Zn,Pb	8.6	Carbonatite, shale	Loudon et al. (1975)
Mc Arthur River, Australia	Proterozoic (1.65)	Zn,Pb	190	Dolomite, shale	R.N.Walker et al. (1977)
Metamorphosed Equivalents					
Broken Hill, NSW	Proterozoic(1.7-2.0)	Zn,Pb	180	Felsic gneiss	Johnson and Klingner (1975)
Gamsberg, S.Africa	Proterozoic(1.6-2.0)	Zn,Pb	93	Meta-pelites	Rozendaal (1986)
Big Syn., S.Africa	Proterozoic(1.6-2.0)	Zn,Pb	101	Meta-pelites	Ryan et al. (1986)
Black Mountain, S.Africa	Proterozoic(1.6-2.0)	Cu,Pb	82	Mica Schist	Ryan et al. (1986)
Broken Hill, S.Africa	Proterozoic(1.6-2.0)	Pb,Zn	85	Iron Formation	Ryan et al. (1986)

Table 3.2 - Summary of important characteristics and relations that are known or suspected to be associated with Bushmanland stratiform base metal deposits (summarised from various authors mentioned in the text).

1. Depositional Environment of host Rocks
   - deposited at a continental-edge to intercontinental environment
2. Lithological composition of Host Rocks
   - aluminous schist
   - metaquartzites
   - barite layer
   - banded iron formation
3. Character of ore bodies
   - stratabound and in most cases stratiform, of extensive strike length
   - associated with significant gossan outcrop
   - intimate association with banded iron formation
   - stratiform barytic units appear to overly sulphide rich units
   - mineralisation occurs regionally within the same general stratigraphic interval
   - concentration of base metal sulphides in aluminous schist/quartzite couplet
4. Structure
   - complex polyphase deformation of ore and host rocks
   - major structural discontinuities (thrust zones)
   - synformal and antiformal structures
   - F1 to F3 fold phases
   - overprinting by D4 metamorphism and deformation
   - the mineralised rocks are associated with F2 antiformal fold closures and the limbs of F3 folds
5. Regional Tectonic Environment
   - continental rift basin
6. Character of mineralization
   - vertical metal zoning with Cu:Pb ratios of ore-bodies increasing stratigraphically upward
   - lateral metal zoning with progressive increase in Cu to west and Zn to the east
7. Age of Host Rocks
   - Meso-Proterozoic
8. Geophysics
   - magnetic anomalies associated with ore bodies
   - known occurrences of mineralisation closely associated with magnetic bearing quartzites having pronounced magnetic signatures
9. Geochemistry
   - Pb and Zn clearly delineate the ore deposits
   - Cu and Mn do not clearly delineate the deposits, but are vaguely associated with the ore deposits

Observations relating to lithological, structural, geophysical and geochemical variables have been described by separate workers during exploration and research in the study area. Table 3.2 summarises and combines the observations of these workers.

3.2. Metallogenesis

The Bushmanland Subprovince forms a distinctive base-metal metallogenic province within the Namaqualand Metamorphic Complex in Southern Africa. Ore-formation in the Bushmanland basin occurred between 1600-2000 Ma, defining a Meso-Proterozoic metallogenic epoch. The major base-metal deposits in Australia also fall in this age bracket (Table 3.1), so that the metallogenic province may be continentally extensive. Figure 3.1 from the Gondwana-GIS, outlines the extent of Meso-Proterozoic Pb-Zn deposits within Gondwanaland.

The Bushmanland sequence is intensely deformed and metamorphosed. However, despite the state of tectonism, investigations have attempted to restore the original size and shape of the basin. There must, however, remain a large margin of error associated with such basin reconstruction. Genetic and tectonic modelling are, therefore, also limited by lack of understanding of the regional scale deformational and metamorphic overprinting in the Bushmanland area. Some genetic and tectonic models, explaining the metallogenic Pb-Zn deposits at Gamsberg and Aggeneys, in the Bushmanland, are briefly outlined below.

3.2.1. Petrographic Aspects

Gustafson and Williams (1981) speculate that most sediment hosted stratiform deposits of both copper and Pb-Zn, formed early in the diagenetic history of their enclosing sediments. The supracrustal succession in Bushmanland measures in total thickness around 1000m. This unusually thin supracrustal succession as well, as lack of associated volcanics in the area, limit modelling for the source of the metals. Metal leaching of the basement to the Bushmanland supracrustals or underlying sequences, are the most likely source for metals in Bushmanland (Lipson, 1990).

The fluid plumbing systems that transports these metals are generally thought to be associated with hydrothermal systems. Evolution of the lithospheric rift system that

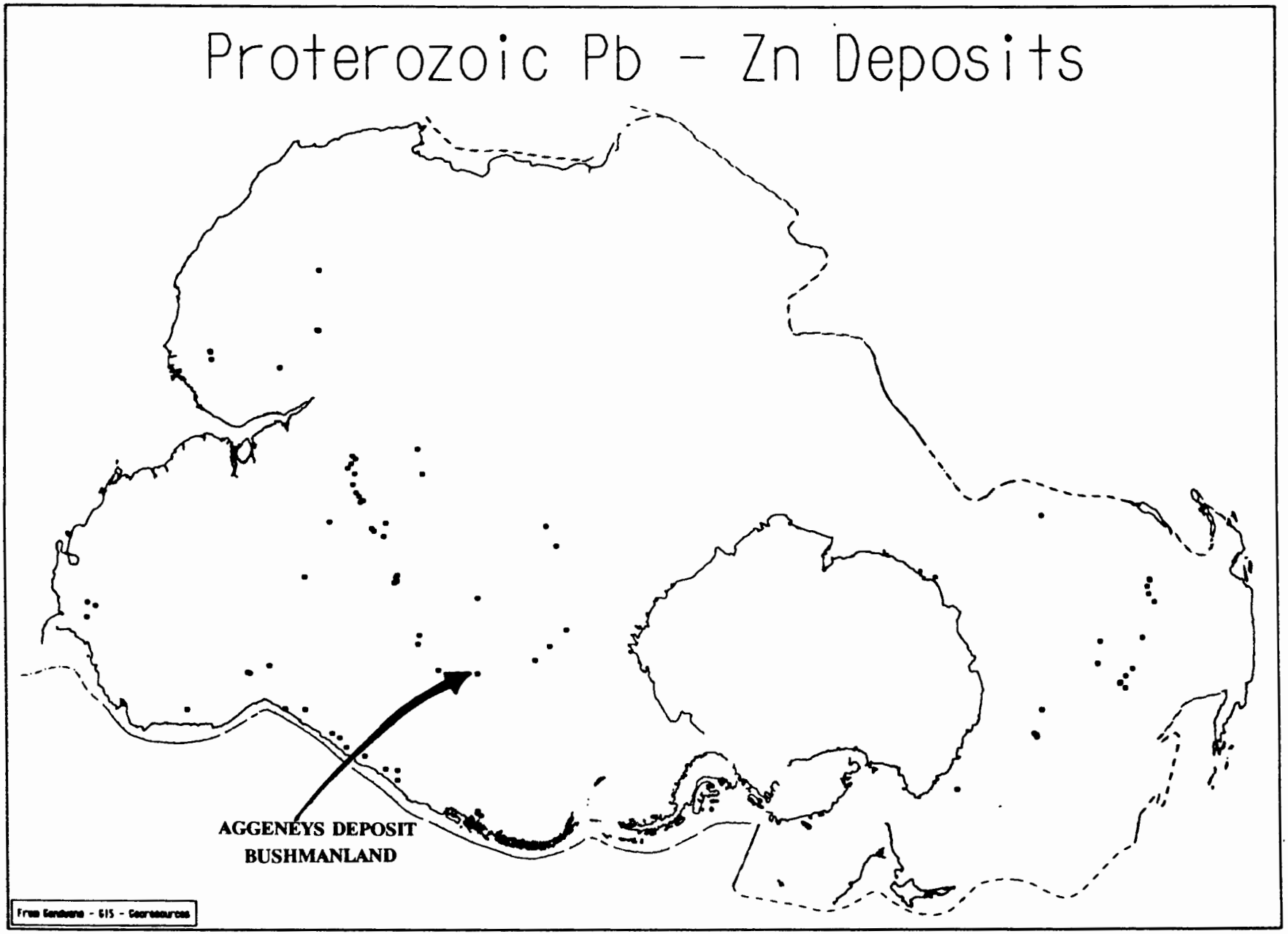

Figure 3.1 - Distribution of Proterozoic Pb-Zn deposits within Gondwanaland.

characterises deposition of the Bushmanland meta-sediments, probably also exerted strong control on metallogenesis. Lipson (1990) suggests that each of the four deposits were generated by independently operating hydrothermal fluid convecting cells. Such a model could explain the different metals ratios of each deposit, listed in Table 2.6. If the basement is considered more mafic at depth, fluids circulating to variable depths (kilometres) into the basement, probably also determined the proportions of metals leached from the basement (Lipson 1990).

Rozendaal (1982), Moore(1989) and Lipson(1990) all stress the role that lithospheric rifting played in controlling the sedimentology of the Bushmanland basin; and they believe that the conduits for basinal brines generated by convecting hydrothermal cells may correspond to faulting associated with lithospheric rifting in the Bushmanland basin. Migration of basinal brines, loaded with metals generated in the lower units of the stratigraphic sequence, are facilitated by rift faulting which creates across-basin aquifers and cross-strata-basin margin fault pathways.

Lipson (1990) suggests that trends of continental margin rift faults in the assumed basement (Achab Gneiss) at Aggeneys Subgroup are east-north-east. Tilted fault-bounded rift blocks may have created sub-basins in which individual ore deposits developed (Lipson, 1990). The greater degree of advective heat flow associated with rift faults separating individual basins could have set convective cells in motion and focused fluids during exhalations (Lipson, 1990). This energy source is proposed in the absence of gross intrusions in the area, that could have stimulated hydrothermal convection of the basinal fluids.

Lipson (1990) argues that a model involving regional fluid flow via a single convective cell driving fluid migrating tens of kilometres (Gamsberg ore body), whilst selectively precipitating out various metalliferous elements, is highly unlikely. This type of system should result in a continuous ore horizon in the sedimentary succession, instead of only having a possible ore equivalent horizon linking the different ore horizons (Lipson 1990). If one convective cell gave rise to a continuous ore unit within the stratigraphic sequence, subsequent polyphase deformation of the sequences in the area could account for the lack of continuity. In the Bushmanland area "tectonic pumping" could

also account for the migration of ore bearing fluid over hundreds of kilometres (c.f. Oliver, 1986; Duane et al., 1988) resulting in a stratigraphically continuous ore horizon which was later deformed during high grade regional metamorphism.

Rozendaal (1982) suggests that the areal concentration of iron formations at Aggeneys-Gamsberg and immediate surroundings, show that the inferred metalliferous brines were supplied in "fairly" large quantities to this area. The Aggeneys-Gamsberg was the site of a local continental high-temperature geothermal system which generated thermal brines over a considerable period (Rozendaal, 1982). Initial brines were low temperature and depleted in base metals. These low energy fluids were the precursors of hotter brines, highly charged with base metals, that later produced the Gams Iron Formation (Rozendaal, 1982).

Several vents situated along one or more approximately E-W linear zones are believed to have produced the various distal and proximal base metal deposits at Aggeneys and Gamsberg (Rozendaal, 1982). The Broken Hill and Black Mountain display characteristic of deposits situated proximal to an associated fumarolic vent, compared to distal deposits of Big Syncline and Gamsberg (Rozendaal, 1982).

Lipson (1990) envisaged the Black Mountain and Broken Hill deposits forming from higher temperature, more deeply circulating, alkaline fluids, whilst lower temperature, shallowly circulating, more acidic and H_2S rich fluids generated the Gamsberg and Big Syncline orebodies. A summary of the conditions that produced the Aggeneys-Gamsberg deposit, according to Lipson (1990), is listed in Table 3.3.

3.2.2. Tectonic Aspects

Plate tectonics provides a meaningful framework within which the geologic and geochemical processes that lead to economic metal concentrations can be more fully understood (Sawkins, 1990). Sawkins proposes the wider utilisation of plate tectonic concepts in exploration for metal deposits. Tectonic modelling has not yet been fully applied in the Bushmanland area. General ideas put forward by some workers are briefly reviewed below.

Table 3.3 - Synopsis of the Aggeneys-Gamsberg orebodies and the possible physical\chemical characteristics for their formation; modified from Lipson (1990).

Parameter	Black Mountain	Broken Hill	Big Syncline	Gamsberg
Major Metals	Cu, Pb	Pb, Zn, Cu	Zn, Pb	Zn
Accessory deposit	Barite			Barite
Basement type	silicic	potassic	gneiss	
Amphibolite Unit below	Yes	No	No	No
Amphibolite Unit above	No	No	Yes?	Yes
Basin Redox Conditions	oxidizing	moderately oxidizing	slightly reducing	reducing
Fluid Temp (°C)	300	280	180-260	100 - 150
Fluid pH	5.6 - 6.2	4.7 - 5.4	4.1 - 4.6	4.0 - 4.5

Moore (1989) envisaged that within the time span of the formation of the western NMC (approximately 2000 to 1000 Ma), some form of plate tectonics was the operative force, controlling the type of volcanicity, sedimentation and tectonism in the area. Most observations today point to plate tectonic processes operating in the Proterozoic and even Archean (Windley, 1993). Within the wide spectrum of plate tectonic environments, rifting environments (extensional tectonics) are important in spawning metallogenic provinces like the Bushmanland and analogous deposits (Sawkins, 1990). The stratiform zinc, lead and barite ores in Bushmanland basin formed well within the continents during or following plate convergence (Garson and Mitchell, 1991).

Sawkins (1990) believes that fundamental control of continental rift metallogeny is linked to crust-mantle interactions during attempted continental breakup events. Sometimes basaltic mantle melts break through the crust giving rise to major basaltic magmatic episodes, and eventual copper dominated metallogenic events. However, where the mantle-derived basalts pond and amalgamate at the base of the crust, large scale crustal melting that may be induced, and in turn cause the onset of Pb-Zn metallogenesis (Sawkins, 1990).

The evolution of the proposed rift system associated with Bushmanland mineralisation can be summarised as follows (after Moore, 1989; Rozendaal, 1986; Plimer, 1987 and Willner et al., 1990) :

Crustal anatexix resulted in extrusion of ignimbritic rhyolites (leucogneiss). Graben formation and basin filling by clastic and chemogenic silicic sediments followed, accompanied by minor basaltic extrusions. Willner (1990) documents more than one phase of rifting in the area, and peraluminous volcanic rocks were deposited in first and third order basins associated with later phases of rifting. The Aggeneys-Gamsberg deposits are believed to have formed during the late stages of rift evolution, and final ore formation probably coincides with the highest geothermal gradient for the Broken Hill deposits (Plimer, 1987).

Reid et al., (1987) describe the Bushmanland Group as evolving in a cratonic basin in a back-arc continental extension setting, closely linked to subduction. Moore (1989) also conceived the Bushmanland depository as a marginal, continental basin. However Moore (1989) postulates that the sedimentary sequence represents a peripheral basin developed during and/or subsequent to collision between a rifted continental margin and continental margin-arc (Figure 3.2). Lithospheric evolution of the peripheral basin is associated with subduction; the calc alkaline volcanics of the Orange River Group were attributed to melting above this subduction zone (Moore, 1989).

The Groothoek thrust is believed to represent the suture between the northerly "Namaqualand microcontinent", and the Vioolsdrif Suite. Bimodal acid dominated volcanism persisted after deposition of Bushmanland sediments and the metals leached from these acid volcanics precipitated as iron formation and massive sulphide in restricted anaerobic sub-basins (Moore, 1989). Moore (1989) estimates that the Bushmanland sedimentary basin has post tectonic/present day dimensions of approximately 100 by 300 km and sediment thickness between 500 -1000 m.

In contrast, Lipson (1990) suggests that major zones of rifting in the Aggeneys area correspond to a passive continental margin setting, over which sediments prograded to the south. A combination of passive margin rifting, thick felsic basement and local areas of elevated temperatures generated these SEDEX-like deposits at Aggeneys-

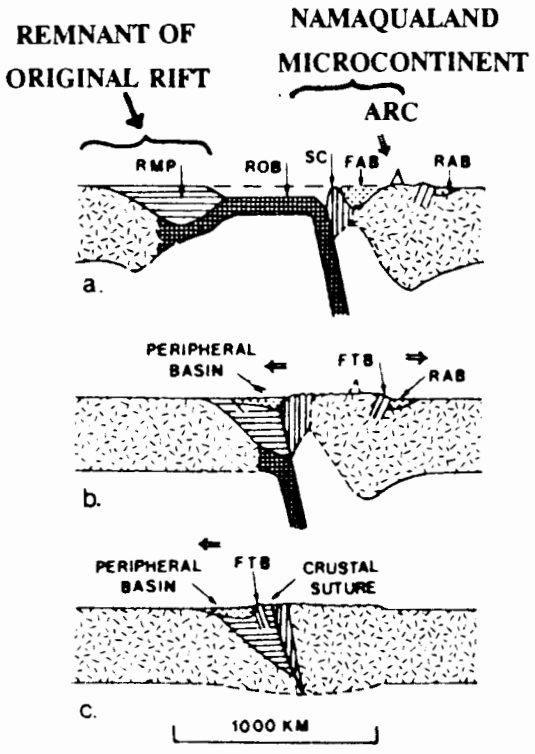

⇐ = Tectonically driven fluid migration

Figure 3.2 - Series of schematic diagrams illustrating the sequence of events during collision. Oceanic crust is cross-hatched; continental crust jackstrawed. RMP - Rifted Margin Prism, ROB - Remnant Oceanic Basin; SC -Subduction Complex; FAB - Fore-Arc Basin; RAB - Retro Arc Basin; FTB - Fold Thrust Belt(modified after Dickinson, 1974).

Gamsberg (Lipson, 1990). In all models, the deposits are subsequently overprinted by the Namaqua-Natal orogenesis and associated metamorphism at about 1.0 Ga, accounting for the highly deformed and metamorphosed state of these deposits.

In summary, although details of the models described above have not yet been fully tested, in a broad framework, sedimentation followed by basin-wide fluid migration was almost certainly induced prior to major collisional events (and associated deformation and metamorphism) at the end of the Meso-Proterozoic (1.0 Ga).

Chapter 4

Geographic Information Systems (GIS): an overview

4.1. Introduction

Geographic Information Systems (GIS) are computer packages that combine spatial database functions, with a range of analytical functions. Searching, interrogation, analysis, integration, modelling and interpretation of spatial and descriptive data, from diverse sources, derived from a range of disciplines, is possible within GIS.

A single, universally accepted definition of GIS does not exist. The above paragraph is synthesised from my own experience in GIS. Other attempts to define GIS address to varying degrees the hardware-software, toolbox, applications, database and information processing approaches. Maguire (1991) proposed a definition of GIS which would encompass three distinct but overlapping views of GIS:

a) The map view which presents the digital map-making or cartographic aspect of GIS.

b) The database view which emphasises the importance of a well designed and implemented database design.

c) The spatial analytical view which focuses on the analytical and modelling aspect of GIS

These are the three most important aspects of GIS. The power of GIS derives from the ability to unite these three important functions, in one information system.

The functional characteristics of GIS are shown schematically in Figure 4.1. The items listed represent tasks to be carried out in creating a functional GIS database. These tasks include data collection, storage, manipulation, analysis and presentation operations (Maguire and Dangermond, 1991). The data capture, transfer, validate and edit functions used in this project are expanded on in Appendix 1 (Figure 4.1 - A, B and C). Data storage and structuring (Figure 4.1 - D) influences manipulation and analysis of the data and is discussed here. The restructuring, generalisation, transformation of stored data is discussed in Chapter 6 (Figure 4.1 - E, F and G); and finally data is queried, analysed and presented in Chapter 7 (Figure 4.1 - H, I and J).

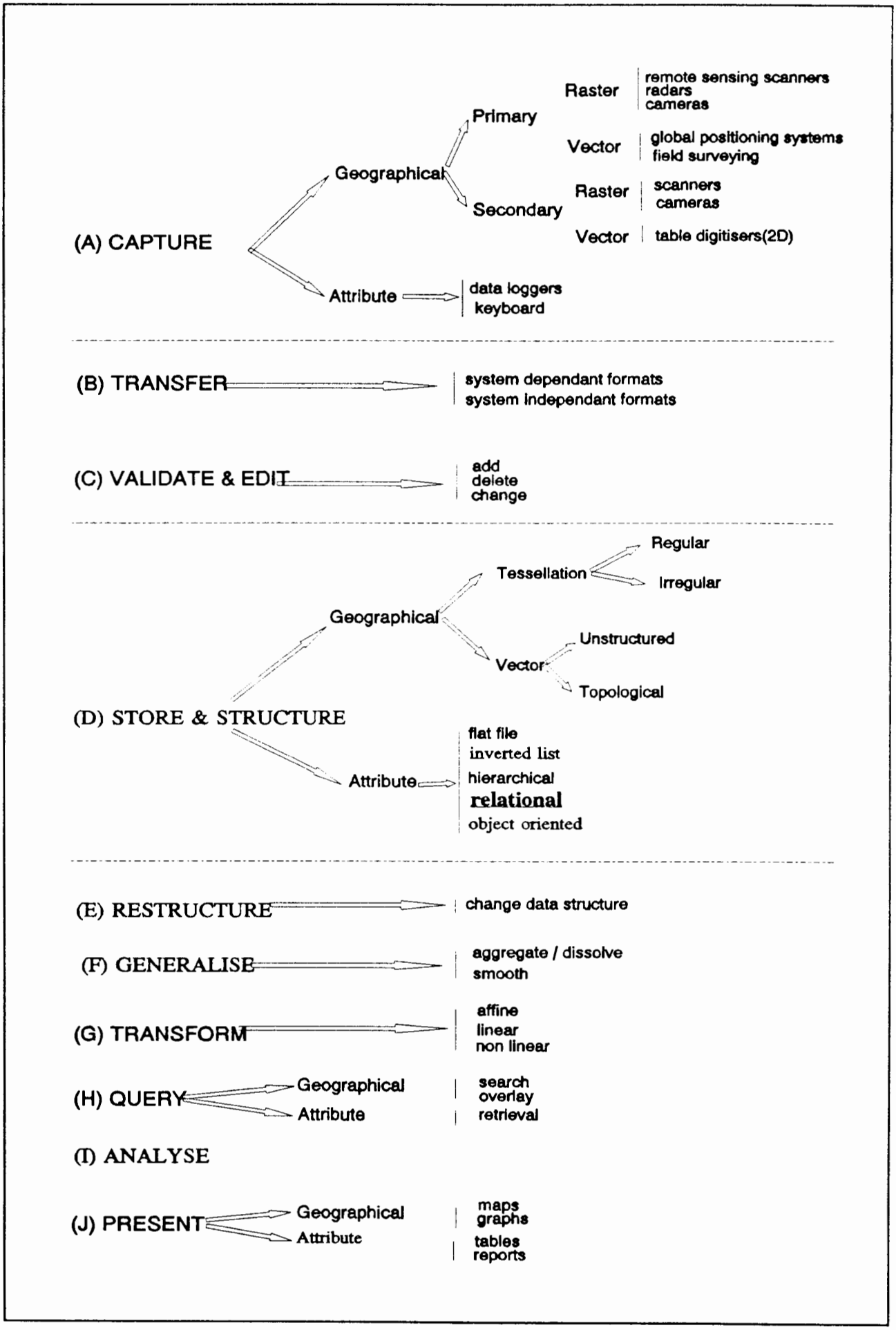

Figure 4.1 - Functional characteristics of a Geographic Information Systems (GIS) toolkit, progressing from data Capture (A) to Presentation (J). The operations are discussed more fully in Appendix 1 (Modified after Maguire and Dangermond, 1991).

Data capture, editing and validation are both tedious, and time-consuming, and occupy the greater proportion of the time set aside for any GIS project. The importance of, and labour spent performing, functions (A) to (C) is often overlooked, and the success of a GIS project is largely dependent on these functions. Data capture, transfer, editing and validation govern the quality and accuracy of data output from functions (E) to (J).

4.2. Conceptual Geographic (Spatial) Database Design

The following sections describe the conceptual spatial database design of a standard Geographic Information System. The geographical features, data models and data structures used in GIS, define its conceptual design. Conceptual database design is distinct from the physical database design, where the latter describes the storage of spatial and attribute data in the file systems of the computer.

Terminology used in GIS can be both confusing and ambiguous. The concepts described here are drawn from Peuguet (1990), Dangermond (1990), and Maguire and Dangermond, (1991). Variations in terminology and definitions may be encountered in other literature.

4.2.1. Geographical features

Geographical features use a locational (geographical) element to reference the attribute (statistical/descriptive) elements of data. The storage and analysis of spatial data, ie. the locational data element, is a distinguishing feature of *Geographical* Information Systems (Maguire and Dangermond, 1991). Four generic geographical features, based on euclidian geometry are recognised, namely point (0 D), line (1D), area(2D), and surface (3D) features (Table 4.1; Maguire and Dangermond, 1991). In this study, for example, sample location *points*, lithological *area* boundaries, and *lines* defining axial traces of folds, are used to reference sample point geochemistry, lithostratigraphy, and structural data, respectively.

Geographical features can be represented using the vector data model for point, line and area features, or raster data models for surface features. The attribute data associated with these four geographical features can be classified according to the level

of measurement (Table 4.2). The examples in Table 4.2 refer to attribute data in this study.

Table 4.1 - Four generic geographical features classified according to euclidian dimensionality adapted from Maguire and Dangermond (1991).

	Length	Dimensionality
Points	no length dimension	zero dimension
Lines	single length dimension	dimensionality = 1
Areas	two length dimensions	dimensionality = 2
Surfaces	three length dimensions	dimensionality = 3

Table 4.2 - Basic classification of attribute data using level of measurement according to Stevens (1946).

	Measurement	Example
Nominal	sufficient information to classify data into categories	lithology classified as quartzite, schists...
Ordinal	sufficient information to rank data in either ascending or descending order	favourability of rock to host mineralisation ranked: high = 10, low = 1
Interval / Ratio	distances between categories are defined as fixed sized units	geochemical element concentration categorised: eg. Zn in ppm 1 - 200, 201 - 400, 401 - 600

Linking dimensionality and measurement classification in Table 4.1 and 4.2, the basic types of data used in GIS are listed in Table 4.3. For example, stream patterns are line features with nominal measurements, and would be classified as follows,

if streams are ordered (Norton numbers) ⇒ ordered network

or have flow/volumetric data ⇒ flow lines

or just names ⇒ network.

The streams classified in the above manner have the same spatial data but different attribute data. The combination of the data model (point/line/area/surface) and level

of measurement of a particular related attribute, determines the way that data can be represented in the GIS database.

Table 4.3 - Classification of basic types geographical data used in GIS within a two dimensional table linking dimensionality and levels of measurement (adapted from Robinson et al. 1984, and Unwin, 1981).

	Point	Line	Area	Surface
Nominal	dot	network	colour class	freely coloured
Ordinal	ordered symbol	ordered network	ordered colour	ordered colour
Interval/ Ratio	graduated symbol	flow line	choropleth	contour

4.2.2. Geographic (Spatial) Data Models

A data model is a formal method of representing and manipulating spatial (locational) and attribute (non-locational) information (Date, 1986). The data model depicts an abstraction of features surveyed from the real world. Two fundamental data models for digitally stored spatial data are the vector and raster (tessellation) data models. The distinguishing features of these two models are tabulated in Table 4.4. The relational data model is most widely utilised attribute database model.

The researcher structures the data within a GIS database, selecting geographical features to represent spatial data in the vector or raster data model, and the level of measurement to represent the associated attribute data. The organisation of data into files, ie. file structure, is governed largely by the software. However, the separation of files into a directory structure is governed by the researcher. The file and directory structure used in this study is described in Chapter 5.

Different researchers will develop a different type of GIS database. Therefore every database has imperfections, and it is important to document carefully; the design of the database, the methodology of data manipulation and analytical operations, and to scrutinise the results of each analytical operation.

Table 4.4 - Summary of differences between the vector and raster data models.

Vector	Raster
1. Position of geographical features are referenced using x, y co-ordinate pairs.	1. Position is implied by the location of each pixel in a sequence. No co-ordinates are stored except as a header to locate an entire data set.
2. Data structures are boundary (map) oriented.	2. Data structure emphasises quality (contents) of areas rather than boundaries. Explicit information is provided for each pixel.
3.Data structures retain adjacency relationships between regions.	3. Position of each pixel relative to any other pixel can be determined and attributes compared.
4. Data structures facilitate geographical query and analysis such as overlay, retrieving adjacent areas and network analysis	4. Data structure facilitates map algebra, simulation and modelling in GIS spatial analysis.
5. Existing map information is encoded, and data storage volumes are smaller.	5. Data requires relatively large storage space.

4.2.2.1. Vector Spatial Data Model

In the vector data model geographic features are represented as series of x, y or x, y, z coordinates (Maguire and Dangermond, 1991). Point features are stored as a single x, y co-ordinate pair. Lines, in their simplest form are stored as two x, y co-ordinate pairs defining the begin and end point of a line segment. A string of x, y co-ordinate pairs, defining a more complex line, is known as an arc (Figure 4.2). A record for each point, or segment in a simple line or arc, is stored in an attribute table in the GIS database. These records are spatial identifiers and to obtain information about a geographic feature, the database is queried. For example, to display arcs with record-identifier 3 as a dashed line, the selected database file is searched for all arcs with record-identifier = 3, the dashed line symbol selected, and the arc displayed. Additional information describing the arc may be stored in separate tables. To link the spatial feature to information in stored in tables, each information table must contain a spatial-identifier column.

(A) Vector Data Model

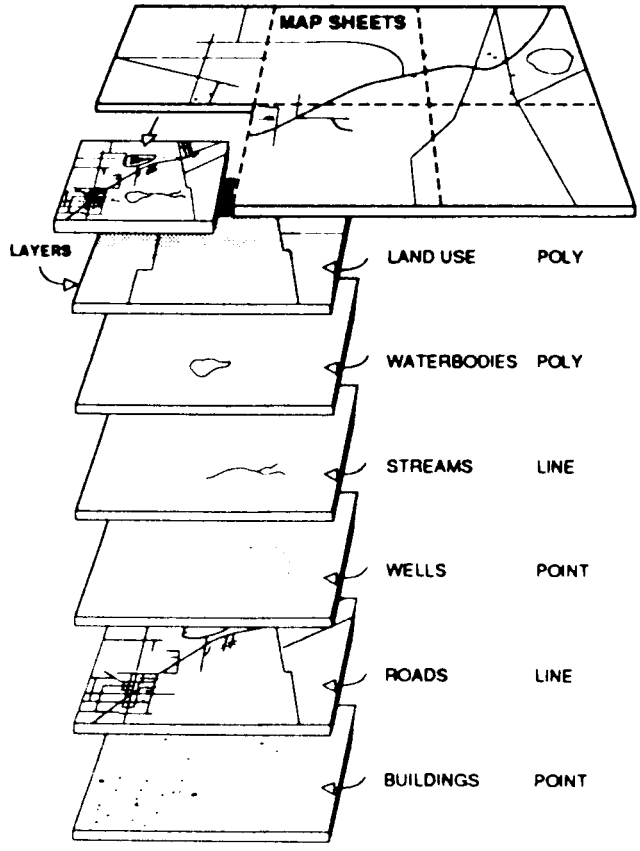

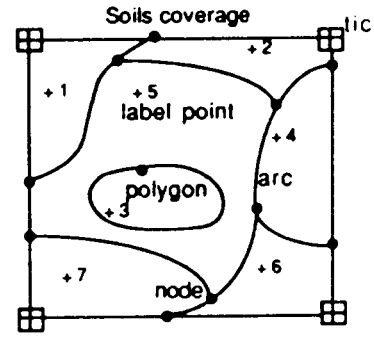

(B) Raster Data Model

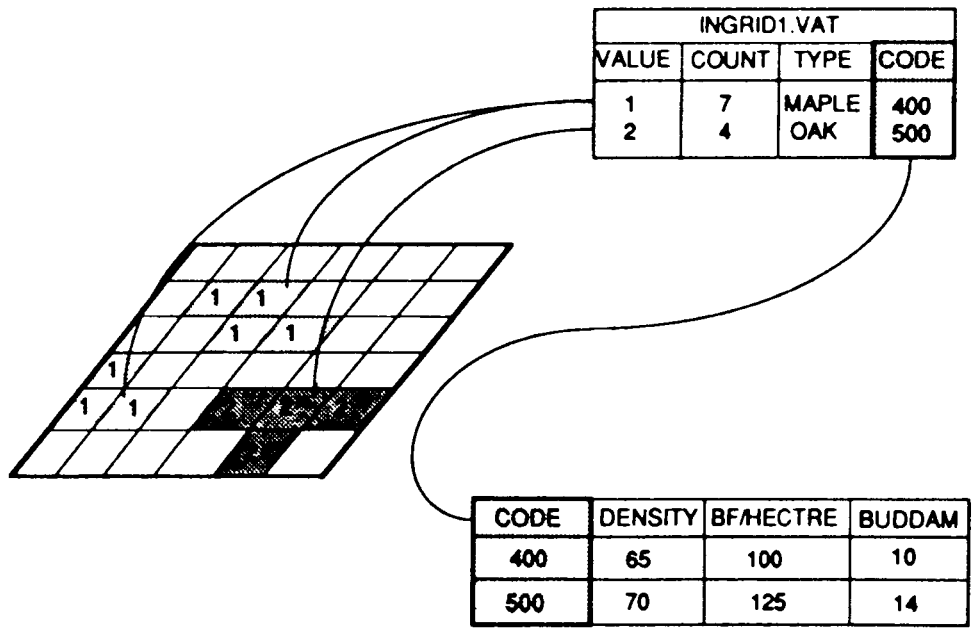

Figure 4.2 - Schematic representation of two methods of defining topological (spatial adjacency) relations in spatial data, the vector data model (A) and the raster data model (B). A illustrates how map features are organised into layers of information in vector GIS and each layer consists of topologically linked geographic features and their associated data. B illustrates a raster map representation where square cells are arranged in a matrix of rows and columns, and multiple cells with same value belong to a zone (ESRI, 1991).

Area features in the vector system are defined by a closed loop of arcs, forming a boundary polygon. The begin and end x, y co-ordinate pair of the arc is the same. Polygons define homogeneous areas, for example, an area with schists defines a polygon. The relationship of geographical features in a map is called topology, and topology concerns the way in which the geographical elements in a GIS database relate to each other in 2 dimensional space (Wilsher et al., 1993a). Topological relationships are created by identifying connecting lines in a path, and the areas contained within these lines, by identifying adjacency between area features.

To create a boundary network, junction points (nodes) are built at the points of line segments that join to form arcs, and which may form polygons (Figure 4.2 A). Within a fully topological polygon network structure polygon boundaries are encoded as arcs with node pointers. A record of each polygon, in the form point identifiers (labels) contained within the polygon, is stored in a polygon attribute table (Burrough, 1986). Arcs have direction and left and right sides, that define contiguity (Understanding GIS, 1991).

In the vector system major classes of spatial features are stored and maintained separately. Polygons defining lithological areas, are separated from a streams network, a line network defining structural zones, and sample point localities. However for the purpose of display and analysis these separate layers can be overlayed. Data overlay provides a powerful means of comparing, and analysing relationships that exist between different information stored for the same area.

GIS is based on planar geometry using the cartesian system. Geographic reference system co-ordinates (lat, long) have to be transformed to a planar co-ordinate (cartesian system) based on a particular map projection (Transverse Mercator projection for this project) using the projection function. Projection parameters include central meridian 19°,a scale factor of 1, latitude of origin 0°, no False easting or northing. Principles of the geographic and cartesian co-ordinate system is presented in Appendix 2.

4.2.2.2. Raster Spatial Data Model

The most commonly used raster data structure in GIS is the 2-dimensional square grid. In the gridded raster system, square picture elements (pixels) are organised in a line scan order of uniform pixel dimension (Figure 4.2B). Cell dimension is represented by units such as kilometres, metres, hectares and stored as header information for the entire dataset. Point, line and polygon maps can be gridded to chosen cell size. Each cell is given a value corresponding to a feature or characteristic that is located at, or describes, the site eg. drainage, lithotype, soil type.

In this study, a combination of the vector and raster data models were used: the cartographic map data were captured and stored as vector data; the remotely sensed and interpolated data are in raster format. Other raster data structures (quadtree, hexagonal) and a recently developed data model, possessing characteristics of both vector and raster models (vaster or hybrid-data-model), are discussed by Peuguet (1984, 1990).

4.2.3. Relational Attribute Data Model

The storage, manipulation and retrieval of spatial attribute data is handled by a database management system (DBMS). Relational DBMS are popular among information scientists. A common approach in GIS is to use a general Data Base Management System (DBMS) for handling the attribute information and specialised software is used for storage, retrieval and manipulation of the spatial and attribute data (Marble, 1990).

In ARC/INFO[1], for example, the spatial attribute data is managed using the INFO relational database. This is directly linked to a spatial data handling system (ARC). The data handling system may, alternatively, be linked to one of several other supported external databases. For example, the non-graphic component of the Gondwana GIS, viz. GO-GEOID (GOndwana GEOscientific Indexing Database), is constructed using the INFORMIX and INFO relational DBMS (W. Wilsher, 1993a, Wilsher et al., 1993b). Figure 4.3 summarises the features of the Gondwana spatial and

---

ARC/INFO is a registered trademark of Environmental Systems Research Institute, Redlands, CA.

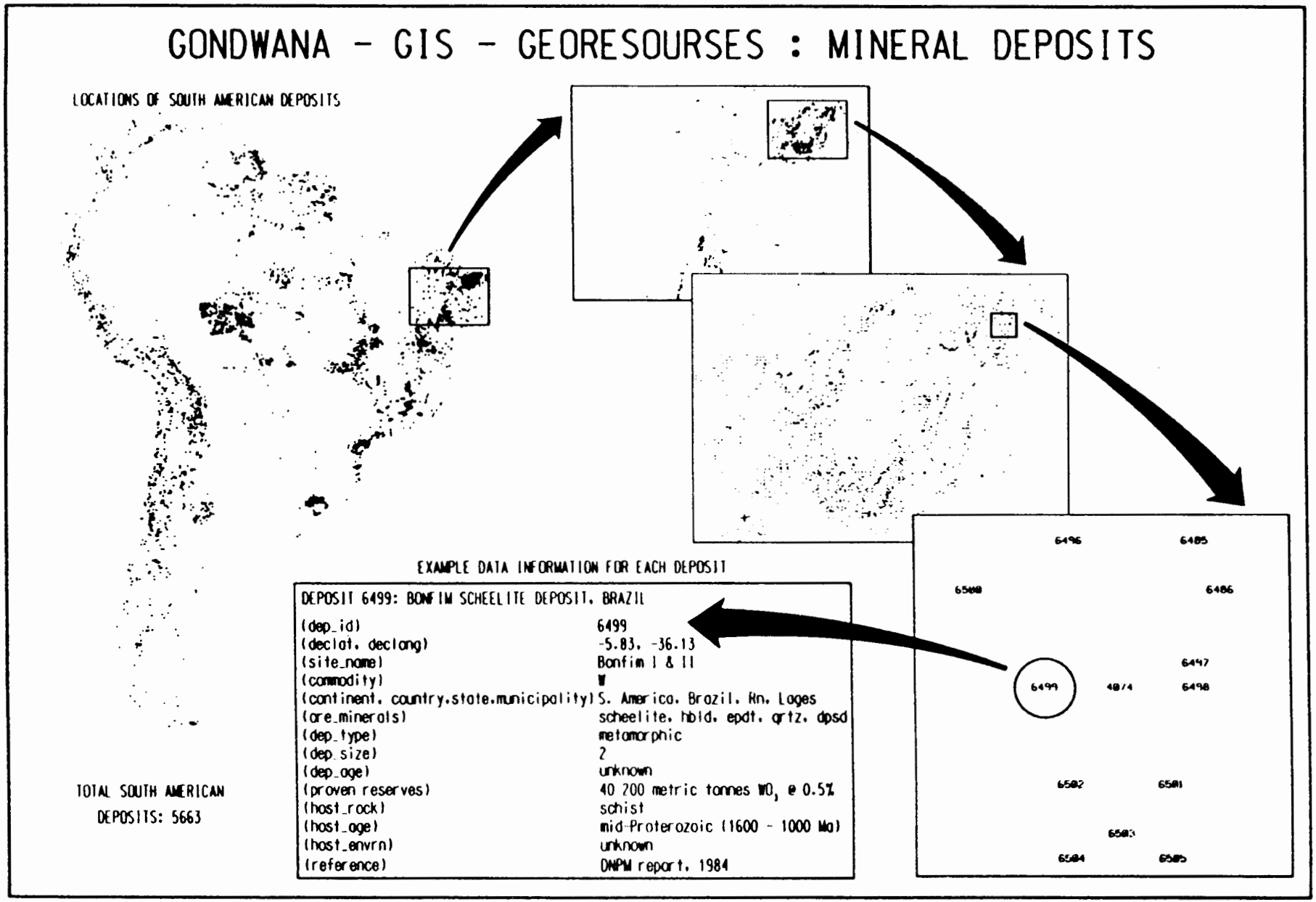

Figure 4.3 - Illustration of a query in the Gondwana GIS, linking spatial and attribute data.

attribute database related to mineral deposit locations in South America. The table summarises information for a scheelite deposit contained in the GO-GEOID database (W. Wilsher et al., 1993a).

Figure 4.4 is an example of relational tables used in this study. The GEOLOGY#, is a unique identification code that identifies a spatial feature. The co-ordinates at component arcs, polygons and points are retrieved from "spatial" files. GEOLOGY-ID identifies those map features that belong to the same class; for example, all pink gneisses have a GEOLOGY-ID of 400. Tables containing additional information associated with the Lithostratigraphic map, are linked by defining a relation using this classification item-name CODE, GEOLOGY-ID. To link database tables (or files), they must contain a common column (field). In Figure 4.4, the relational links between tables (i) and (ii), and (i) and (iii) are executed via the GEOLOGY-ID column contained in all three database tables.

The relational design de-constructs the complex logical structure of the database into a collection of simple relations. This is a flexible structure and meets the demands of queries that can be formulated using the rules of Boolean logic and mathematical functions (Burrough, 1986).

4.2.4. Combined Geo-relational Model

Using the models described above, spatial (co-ordinate) and attribute data are managed separately. However, the power of GIS lies in relational-linkage of attribute and spatial data. The integration of data in this manner allows the user to display and analyse the data using a variety of techniques. This study utilises the geo-relational model as outlined in Figure 4.4. Chapter 5 describes the structure and storage of spatial and attribute data within the geo-relational model. Processing, manipulation and integration techniques applied to the data layers, linking the attribute and spatial data, is the focus of Chapter 6.

4.3. Software and Hardware Description

A summary of the hardware and software products used in this GIS application system will help set the scene for the next two chapters.

Georelational and Relational Linkages used to Reclassify the Litho-Stratigraphic map (Gamsberg) to a Lithological map

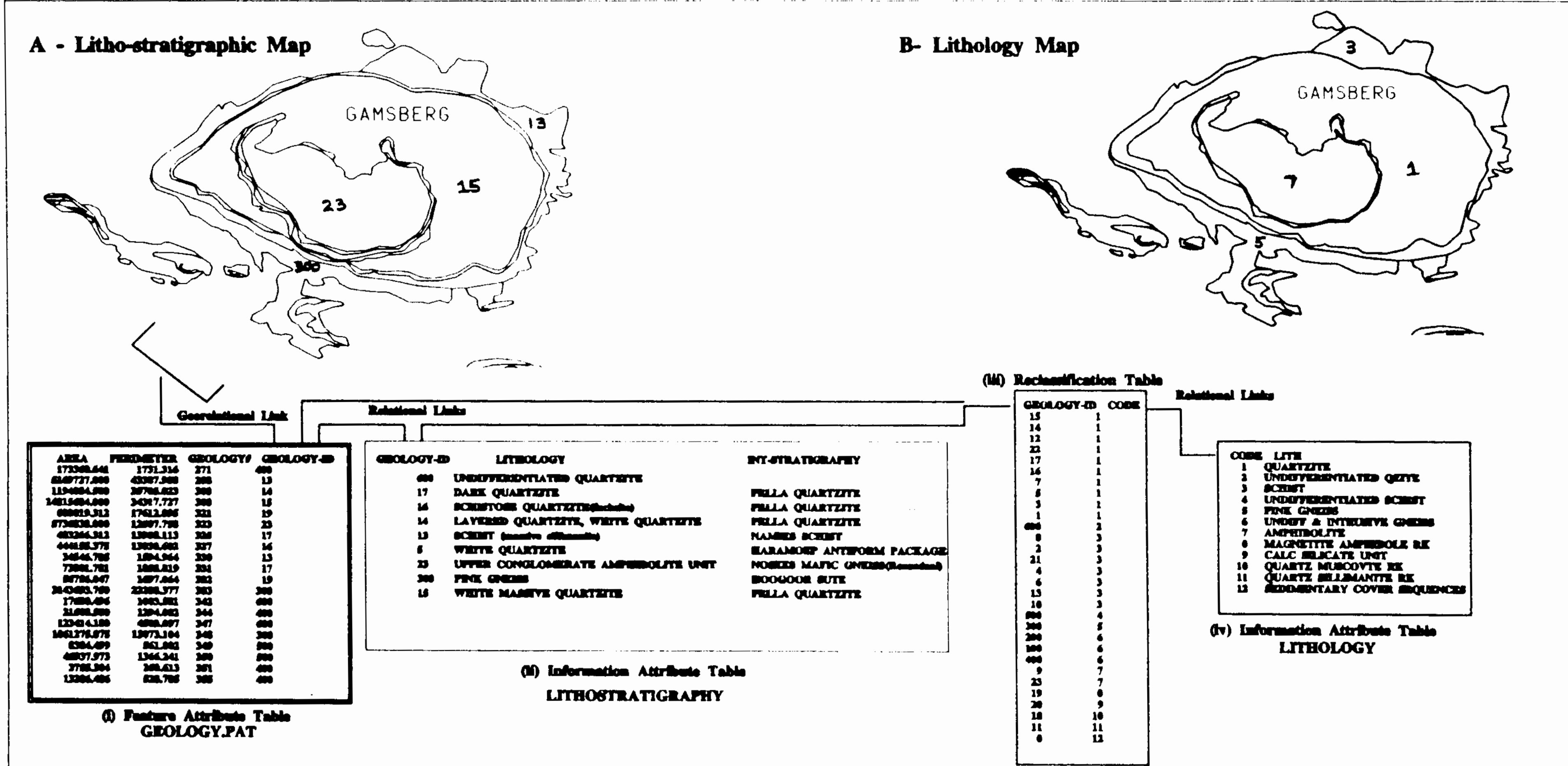

Figure 4.4 - Links created between spatial (i) and attribute (ii, iii, and iv) database tables, to attach litho-stratigraphic classification (A) to Lithological classifications (see text for detailed explanation). The Lithostratigraphic (A) and Lithological (B) Maps, describe the spatial data model stored for the Gamsberg basin and tables (i), (ii), (iii) and (iv) the data structure. Links created between data structure tables (i) and attribute tables (ii, ii, and iv) or between two attribute tables are relational links. The reclassification described here for the Gamsberg basin has been carried out for the entire lithostratigraphic map (shown in Figure 2.2.). The resulting lithological map is displayed in Figure 2.3.

In the 1990's, workstation technology combining the functions of mainframe computing and graphic computing is becoming popular (Goodchild, 1991) particularly in the field of applied geology (Wadge, 1993). In this study a SUN-SPARC2 workstation was used. This workstation is a computer with Reduced Instruction Set Chips (RISC) running a Unix operating system (SUNOS 4.1.1). This workstation has 64 megabytes of Random Access Memory (RAM), and a 1.3 Gb byte hard disk.

Since processing of large data sets is more efficient using workstation technology than minicomputer or PC technology; the large data volume of the present project (in particular the use of images) dictated this type of Unix based workstation environment. The vector data was captured in the PC environment and imported to the workstation for editing, validation, analysis, storage, restructuring, generalisation, transformation, interrogation, analysis and presentation (Figure 4.1 and Appendix 1).

The basic components of the system are, ARC and INFO. ARC performs most of the geographic functions. INFO is the relational database system, that stores and manages related attribute data. Within the ARC/INFO system ARCEDIT and ARCPLOT are subsystems. Additional external modules currently include TIN, GRID, NETWORK, COGO. For further information on the ARC/INFO system, and its all its modules, refer to the series of manuals available where any ARC/INFO system is installed. As the software is updated, new modules and operational functions are incorporated into the system. In this study, ARC-INFO version 6.01 was used.

4.4. Data Analysis and GIS

The spatial data analysis capabilities of GIS differentiates it from other information systems (Maguire; 1991). Within Computer Aided Design Systems (CAD) the computer is used as cartographic tool concerned primarily with computer graphics techniques. In CAD the actual co-ordinates of the graphics are important but spatial adjacency relationships do not exist. In GIS spatial or adjacency relationships between objects on the map is the key element of the data model. Hence spatial data analysis is possible in GIS, but not in CAD

Table 4.5 - Classification of some generic GIS analysis functions adapted from Marble and Peauquet, 1983; and ESRI's ARC/VIEW Manual, 1991. Examples of usage in this study are added.

Classification	Example
1. **Location**	What is at ...? Point out a spatial feature on screen and information about that feature is returned (ie. identify).
2. **Condition**	Where is it? Given an attribute and a map file, find all of the regions containing .... Show all spatial features with lithology attribute quartzite in the study area?
3. **Proximity**	What are the characteristics of the area around existing features? What lithologies are there within 100 metres of a copper anomaly?
4. **Dimension**	What is the areal coverage for each region in a area map? What area is covered by ore bearing schists?
5. **Intersection**	Given two overlapping area maps, what proportion of total spatial area do the two maps share specified characteristics? What proportion of aluminous schists are in the region of specified magnetic anomalies?
6. **Distance**	Given a point, p, and point or line feature in a vector map, what is the point in the vector map nearest to p? What is the distance from that point to p? What is the distance of a site suggested for future drilling from existing drill hole?
7. **Interior**	Given an area map, what is its most central point? Which is the central point on the farm Aggeneys. Point-in-poly - Is this sample point on X's farm?
8. **Trends**	What has changed .. ? How do zinc values change across an area/time.
9. **Patterns**	What spatial pattern exists...? What patterns/clustering do the magnetic anomalies display? What are the patterns of copper, lead and zinc ?
10. **Logical Operations**:	What is unique about a set of features? Examine specific magnetic anomalies that have a copper anomaly associated with them, and display their host lithologies.
11. **Spatial Join**	Where is something found? Establish composite requirements for existence of a geochemical anomaly.
12. **Boundary operations**	What exists within a specific region? Test a set of rules to a small test area before applying them to an entire area. Where is the boundary of this feature? Define a moving boundary buffer.
13. **Modelling**	What if? This may require some additional information and possibly some scientific paradigms and logical operators.

At present most analysis in vector GIS is concerned with data manipulation eg. buffering, overlay, query, search and comparison operations. Table 4.5 is a classification, with examples, of generic queries that can be explored in GIS. Analytical functions for data in raster format, for example the GRID module in ARC-INFO, are versatile. All vector data can be reduced to a raster format. GRID functions allow analysis of gridded data via map algebra, which includes mathematical operators, for example multiplication, addition, subtraction, division. Integration, modelling and manipulation operations are greatly facilitated using GRID, and processing time is considerably faster.

4.5. Using GIS as an application system for predictive Mineral Exploration

The science of mineral exploration is a cognitive science. The objective is to recognise some sort of anomalous pattern from the geological, geochemical and geophysical data surveyed in an area. Relationships and information indicative of economic mineralization may emerge through linking these patterns to lithology, structure and chemical element dispersion in the area. It is a truism that in mineral exploration ore-bodies are not found due to an individual significant response in one data set, but rather by the superposition of several, sometimes not significant, anomalies in different data sets (Ortega et al., 1990).

GIS, therefore, is an ideal tool for the mineral explorationist. The GIS database can maintain graphical and attribute information of areas delineated for mineral exploration. These include, inter alia, lithological, structural, geochemical and geophysical data sets. The ability to:

a) view these data sets individually or in relation to one another.

b) describe and query possible patterns and relationships that may exist within and between the data sets (Wilsher et al., 1993a); (Figure 4.3);

supports the understanding and interpretation of geological and metallogenic processes in exploration using GIS techniques (Ortega et al., 1990).

The presence of known mineralization, or the existence of favourable geological conditions for a particular type of mineralisation, will guide the selection of a district

for exploration. For example, when searching for massive lead-zinc sulphide deposits in Southern Africa, the Bushmanland in the North Western Cape is a more logical choice than the Witwatersrand basin in the Transvaal. Exploration relies heavily on data visualisation and pattern description. Description of variation within exploration data sets, is the first step to identifying outliers or anomalous values in the data. These variation patterns and anomalies result from unique causes. Therefore, variation patterns contribute a valuable source of information. The task of an explorationist is to:

i) identify variations caused by the presence of mineralisation, and isolate these from variations caused by other geologic processes.

ii) describe these variation patterns and apply them in other areas for predictive pattern recognition.

iii) account for the processes that may have given rise to this variation pattern.

In an exploration program the primary purpose is to locate new drilling targets. Locating drilling targets depends solely on recognising areas where mineralisation is likely to occur. Geographical descriptive statistics, data analysis and modelling capabilities in GIS can be utilised to convert the original data gathered through exploration activities, into information that will aid this decision making process (Tomlin, 1991).

A prototype map-based (spatial) expert system , Prospector III, the successor of Prospector I and II, is designed to combine map data with the descriptions of geological settings, and to compare information thus combined with a set of stored mineral deposit models (McCammon, 1989). Knowledge gained during mineral exploration projects by geologists, geophysicists, and geochemists is represented within this expert spatial database system. Areas that are permissive for specific deposit types, stored in the expert system, are delineated for further exploration. Using such a system, the geologist can examine a wide range of deposits models and thus increase confidence in deciding which models best fit the set of data collected in an area (McCammon, 1989).

Studies that utilise GIS as a tool for predictive mineral exploration have, amongst

others, been undertaken by: Bonham Carter et al. (1990), for gold exploration in Nova Scotia, Canada; Bolivar et al. (1983), for base metal exploration Montrose Colarado, USA; O'Callaghan et al. (1982), for base metal exploration Broken Hill, Australia; Pearson et al. (1991) for silver, cobalt, base metal and placer gold mineralisation in the Dillon 1° by 2° quadrangle, Idaho, Montana, USA.

4.6. GIS and Remote Sensing

GIS and remote sensing are linked, both in an historic context and functionally (Star et al., 1991). Remotely sensed data, which include satellite and flight (airborne) data, provide a significant source of input to GIS. The synergy between remotely sensed data for *updating* GIS information, and the use of GIS for *improving* the extraction of useful information from multi-sensor data, is a major advantage of combining GIS and remote sensing (Star et al., 1991). Development of improved integration of these two powerful technologies, GIS and remote sensing is receiving impetus from a range of fields, including mineral exploration.

4.7. Discussion

Developments in GIS technology are occurring at a rapid rate. Attempting an overview of a rapidly developing technology is difficult. Although there are some standard terms, the terminology varies according to the software, and new developments bring with it changes in terminology and concepts.

New data models, data structures, analysis functions and visualisation techniques are being researched, and these are briefly reviewed in the conclusion of this thesis. During the eighties and early nineties GIS technology was commercially driven. Vendors "boasted" systems with a wide-range of sophisticated functions, attempting to please a range of users in different fields. To make GIS a practical tool for geoscientists and explorationists, the impetus for development should be governed by geoscientists. Only we know the type of problems we face and the solutions to these problems.

Coppock and Rhind (1991) believe that the current phase of GIS development is one of user dominance and will be facilitated by agreement on the users' perception of

what GIS should do and look like. At the current stage of development in GIS technology it is opportune for the geoscientist to offer valuable suggestions and ideas as to where the technology should be going. Mutual understanding is important, and should be encouraged through consultation and debate on issues relating to GIS, for example what GIS can offer geoscientists; where GIS is at, what functions of GIS should be developed; and, also important, what GIS cannot offer presently.

Chapter 5

Construction of the AGGeneys Exploration Database (AGGED)

5.1. Introduction

The aim of constructing a spatial database was to integrate and analyse of exploration data sets for predictive mineral exploration in the Aggeneys area. Spatial databases and GIS tools do not provide black box solutions for problems of data integration and analysis, and many possibilities for ill-considered data combinations exist. However if the following two stages are implemented properly, successful and meaningful results should be forthcoming. First, careful reasoning on the aims to be achieved in creating the spatial database. Second, the careful planning of the design of the database and implementation thereof. Database design is the most time consuming and tedious stage, but is crucial to the success of a GIS project.

Table 5.1 - Phases of Exploration activity in the Aggeneys area.

DATE	AREA SELECTION
1929 to 1970	definition of favourable localised areas
	DELINEATION OF ORE BODY
1971	discovery of ore body in synformal fold closures Black Mountain by P.J. Ryan of Phelps Dodge
1972 and 1973	discovery of ore bodies at Broken Hill and Big Syncline in quick succession
	FOLLOW UP
May 1971	Property Acquisition
	SUBSEQUENT EXPLORATORY AND DELINEATION DRILLING
June 21 1971	one hole drilled at Black Mountain
1971 to 1986	detailed surface mapping
1974	regional stream sediment geochemical surveys
1985	regional traverse geochemical surveys in
1972	first local airborne geophysical surveys
1973	regional airborne magnetic survey flown by S.A. Government
1990	localised helicopter magnetic survey over Black Mountain flown
	BUILDING A SPATIAL GEOSCIENCE DATABASE
1993	incorporation of exploration data in a multidisciplinary, single media database

Sensible selection of data for input to the spatial database and careful the design of the database, both govern the data analysis and analytical results derived from a spatial database. Database design and data selection, are described here. The latter two activities, data analysis and analytical results are expanded in Chapters 6 and 7.

Geological, geophysical and geochemical exploration data exist, from two decades of exploration in the Aggeneys area (Table 5.1). The AGGeneys Exploration Database (AGGED) incorporates a subset of this geological, geophysical and geochemical data, from the Aggeneys area, in a spatial database structure. Geographically referenced map and image data, with associated attribute data are stored in a structured manner within a spatial database. The agencies or businesses that supplied the data used in this study; and the structure of AGGED are described.

5.2. Data Sources

AGGED incorporates data from a spectrum of storage media acquired from diverse agencies. A large proportion of the data used in this investigation was supplied by Black Mountain Mining corporation (BMM), which is a subsidiary of Gold Fields of South Africa (GFSA; head office in Johannesburg, South Africa) operating in the Aggeneys area. BMM presently exploits the Black Mountain stratabound Pb-Zn-Cu deposit and has a regional exploration office in Springbok. Hard copy geological data, including a BMM compiled geological map (now converted to Figure 2.2), structural maps (Figure 2.4 overlays 1 to 3), field reports, as well as magnetic data files containing sample location and element analyses of geochemical surveys (listed in Appendix 3) were obtained from Springbok Exploration offices. Processed images of TM satellite data and magnetic surveys were supplied by Gold Fields remote sensing department based at their head office in Johannesburg, South Africa.

The above data was supplemented with the following data:

a) Contoured element concentration maps of Pb, Zn, Cu, Ni and Mn (Figure 5.1) from the South African Geologic Surveys'(SAGS) regional stream sediment geochemistry survey in the North Western Cape

b) Cadastral data (hard copy maps) and an elevation model (on magnetic tape) from the Department of Surveys and Mapping, Mowbray, Cape Town, South Africa.

5.3. The AGGED Database Structure

A main concern of the project was to develop an organisational scheme which could highlight the sub-disciplines which were to be integrated viz., geology, geochemistry, geophysics, geomorphology. This was accomplished by maintaining separation of these themes at a storage level. Consequently the data sets are organised into geological (GLY), geophysical (GPHY), geochemical (GCHM), topographic (RLF) and cadastral (CDSL) working levels. The spatial (vector and raster) and attribute data, within each sub-level, are managed using different data handling models, and are described separately. Table 5.2 lists details of the files stored in AGGED, highlighting the separation of themes (columns) and data models (collection of rows).

The physical (file) design schema (Table 5.2) separates data for effective storage and management, but access to the data is seamless. That is, data from separate working areas is accessible for analysis and display within any working level of the exploration database.

Tables 5.3 and 5.4 describe the spatial data files stored in the raster and vector data models respectively. Table 5.3 and 5.4 are divided into the 5 sub-layers (rows) even if the layer contains no files in that data model. Full descriptions of the data included in each sublayer of AGGED follows. Files names in listed Table 5.2 derive from the description of their contents, listed in Tables 5.3 and 5.4.

5.3.1. Geological Layer

The geological data-space contains a stratigraphic map (Figure 2.2) and structural map (Figure 2.4 overlays 1, 2 and 3). The bedrock geologic map of the Bushmanland area (Figure 2.2), was compiled by Thorpe and Hobbs (1984) from mapping carried out on a regional scale by Joubert (1974b); in detail at Aggeneys by Lipson (1978), at Gamsberg by Rozendaal (1975), and in the Namiesberg by Moore (1977; Table 2.3). Areas remapped by Thorpe and Hobbs (1984) include the Haramoep antiform, the Hotsan antiform, the Rozynbosch synform, the Koeris-Witteberg synform, the Aggeneys East-Dabbiespoort, and the Vogelstruishoek and Achab portion of the Namiesberge.

Table 5.2 - AGGED file storage layers (columns) in the different data models (rows).

	GLY	GCHM	GPHY	RLF	CDSL
Raster	TMIMAGE		AGDRV1 BRPRES REGMAG	LAT50	
VECTOR	GEOLOGY STGEN STOFS	TREG GSPB GSZN GSCU GSMN GSNI	AMIBODY AMIBOUND AMIDYKE AMIFAULT PROSPDAT	RELIEF	PTMINE RDS TLPL FARMS FARMOPTN

Table 5.3 - Description of raster data files in the five sub layers of AGGED.

	File Name	Description	Coverage
GLY	TMIMAGE	landsat TM three band composite	study area
GCHM			
GPHY	AGDRV1	ground magnetometer survey - 1st vertical derivative	farms Aggeneys, Aroams, Blomhoek and Gams
	BRPRES	airborne magnetometer survey - residual magnetic field (reduced to pole)	farm Aggeneys adjacent to Black Mountain
	REGMAG	government aeromagnetic data	study area
RLF	LAT50	grid of elevation values in 50m cells	study area
CDSL	-		

The structural maps are composites of structural interpretations in the study area, correlated with four major phases of folding (F1-F4) identified by Joubert (1974b). Table 2.3 tabulates the correlation of Lipson (1978), Moore (1977) and Rozendaal (1975) and Odling (1983) with Jouberts' nomenclature. Structural overlays in Figure 2.4 outline the axial traces of major folds and shear zones (overlay 1), thrusts (overlay 2) and linear features interpreted from magnetic data including, dykes, sills and faults (overlay 3).

Table 5.4 - Description of vector data files in the five sub-layers of AGGED.

	File Name	Description	Feature
GLY	GEOLOGY	stratigraphic compilation	p
	STGEN	structural composite	l
	STOFS	structural data of UOFS (University of Orange Free State)	l
GCHM	TREG	regional traverse survey	pt
	GSZN GZPB GSCU GSMN GSNI	contoured regional stream sediment survey data for elements Zn, Pb, Cu, Mn, Ni (all in ppm)	l
GPHY		AMI - aeromagnetic interpretation	
	AMIBODY	magnetic bodies	p
	AMIBOUND	magnetic boundaries	p
	AMIFAULT	fractures or faults	l
	AMIDYKE	dykes or sills	l
	PROSPDAT	prospecting data compilation	p +l + pt
RLF	RELIEF	contoured elevation data	l
CDSL	PTMINE	location of mines	pt
	RDS	major roads network	l
	TLPL	telephone and power lines	l
	FARMS	boundaries defining farms	p
	FARMOPTN	boundaries of farms or pieces of farms optioned	p

p = polygon, pt = point, l = line

5.3.1.1. Spatial Data

The hardcopy maps were available at 1:50 000 scale. The structural maps were digitised, edited and relevant attribute data was added during the project. The more detailed geological map was scanned and vectorised for this study, to convert it to digital format ready for incorporation into AGGED. The scanned data was cleaned, edited and attribute data was added during this project.

To create topological relations between adjacent features, lithological units are represented as closed polygon features. In areas where geologists interpreted the sequence continuing under cover, or where these workers were unsure of continuation on the ground, line boundaries were added on the map to create closed polygons. This procedure maintains unique representations of three dimensional supracrustal sequence in a two dimensional representation. A graphical file containing discrete lithological polygons identified by unique numeric codes was thus created. Structural data are symbolised as vector line features representing thrusts, shear zones, axial traces. Graphic line data are identified by unique numeric codes referenced in data structure attribute tables (see Figure 4.2 a).

Gridded spatial data consists of Landsat TM data covering the Aggeneys area. Landsat is an unmanned satellite system which acquires images of the entire earth. The data are archived at the Earth Resource Observation Site (EROS) data centre in the United States, and all images are available for purchase by the general public. A world wide database of images is thus available in digital format suitable for digital processing (Sabins, 1978), a valuables source of information in GIS. The first generation of Landsat satellites, 1 2 and 3 have ceased operation. The second generation Satellites 4 and 5 include multispectral scanner and thematic mapper imaging systems on board.

Landsat thematic mapper acquires data at a spatial resolution of 30m in the extended visible and infrared regions of the electromagnetic spectrum (Sabins, 1978). The visible and infrared regions are divided into seven spectral bands, recorded by TM systems. Table 5.5 describes the visible and infrared spectral regions, recording the electromagnetic wavelength of the visible and infrared regions, on the logarithmic scale, corresponding to the spectral bands 7, 4 and 1 in a TM image.

Information recorded in bands 7, 4 and 1 from a standard Landsat TM quarterscene covering the Black Mountain area, was acquired from EROS and processed at Gold Fields. The image details are:
WRS 176-80 Quadrant-4
Scene Identity 5103507592

Acquisition date 31-12-86

The original seven band raw data was processed at Gold Fields remote sensing department (Appendix 1A). The image in AGGED is a false colour composite of bands 7, 4 and 1, in red green and blue. Table 5.5 describes the characteristics of TM spectral bands 7, 4 and 1. These bands were selected because they show up the contrast in geology well, particularly in this semi-arid region rich in gossans (Frontispiece and Figure 5.1).

Table 5.5 - Characteristics of TM spectral bands 1, 4 and 7 in the visible and infrared wavelength region of the electromagnetic spectrum (adapted from Sabins, 1978).

Region	Wavelength	B	Description	Band Wavelength
Visible	0.4-0.7 um	1	energy reflected from the earth - daytime. max reflectance 0.5	0.45-0.52 um
Infrared	0.7-100 um	4 7	earth radiates energy day and night. max radiation 9.7	0.76-0.90 um 2.08-2.35 um

B - thematic mapper spectral band number; band 7 represents reflected infra-red and coincides with an absorption band caused by hydroxyl ions in minerals; band 1 - useful for distinguishing soil from vegetation; band 4 - blue spectral band enabling production of normal colour composite images

The Landsat TM image data was used as a background to visually drape over other data sets. This provides a valuable reference to geologic location as well as structural details, so that relationships between the geochemistry and geologic structure, and drainage patterns can be more efficiently studied.

5.3.1.2. Attribute Data

Vector polygon and line features are linked to the graphic files via the numeric codes stored in attribute data files (Figure 4.4). Spatial data are identified on the basis of polygon and line identities, and queries and analysis functions can be performed on the selected data.

Descriptive attributes for geological data, displayed as legends to Figure 2.2 and 2.4, include litho-stratigraphic units, and stratigraphic formation nomenclature adopted by SACS (1990), fold phases (F1 to F4) and shearing events (thrusts and shears zones). The link between the graphical file and the database table, established via the numeric coding system, allows queries and other GIS analysis functions to be performed.

5.3.2. Geochemical Layer

This layer includes regional stream sediment surveys of the South African Geological Survey (1975), as well as regional soil traverse surveys of Gold Fields (1985). Elements lead, zinc, copper and manganese are known pathfinder for deposits containing these

Table 5.6 - Geochemical elements examined in this study.

Sym	Group	Classification [1]	CA [2]	DispSS [3]	Mobility [4]
Cu	Copper	Chalcophile	57	5-80 >80 = A	High ph < 5.5 else low
Pb	Lead	Chalcophile	0.13	5-50	low
Zn	Zinc	Chalcophile	93	10-200	high but readily scavenged by Mn oxides
Ba	Barium	Lithophile	5.1		
Ni	Nickel	Siderophile	2.04	5-150	fairly high
Mn	Manganese	Lithophile	590	100-5000	Low-mobile under acid reducing conditions

1. Goldschmidths' geochemical classification of the elements based on distribution in meteorites

2. CA - Crustal Abundance of elements (in ppm), summarised in Taylor and McLennan (1985)

3. DispSS - dispersion in stream sediments in the secondary environment (ppm)

4. Mobility - of elements in the secondary environment (Reedman, 1979)

elements (Beeson, 1978). Thus, these four elements plus nickel are incorporated into the data layer. Nickel, a comparatively immobile element, was chosen to compare

distributions between Ni and the more "mobile" pathfinder elements (Table 5.6 summarises selected properties of lead, zinc, copper manganese and nickel).

5.3.2.1. Spatial Data

Traverse survey sample locations are plotted in Figure 5.1 overlaid on the stream pattern over the study area. Each sample location is represented as a point feature with a unique numeric code, similar to vector line and polygon data described above.

The South African Geological Survey contour maps of elements lead, zinc, copper and nickel are plotted as separate overlays 1 to 5 on the stream pattern in Figure 5.1. The interpolated contours join areas of equal element concentration. The numeric line codes identify the element concentration represented by the contours.
A litho-geochemistry survey of the study area was undertaken by L. Thorpe of BMM during 1984-1985; the sample locations of this survey are also plotted in Figure 5.1.

5.3.2.2. Attribute data

Element concentration data are recorded in separate database table. Traverse soil sample data (-80 mesh fraction) were analysed using Atomic Absorption Spectrometry. Samples were collected at between 0-15 m depths and analytical results for each sample are stored in database tables associated with the numeric code of each sample from the spatial data file (Appendix 3).

The South African Geological Survey (SAGS) stream sediment sampled data was analysed using simultaneous X-Ray Flourescence Spectrometry of pressed pills at a 5ppm detection limit. This data was available from the SAGS as interpolated contour maps.

5.3.3. Geophysical Layer

Geophysical exploration methods are usually used in the advanced stages of exploration programme when the necessary geological control has been established. In the Aggeneys area, the mineralised formations are preserved in isoclinal folds closures, infolded into basal augen-gneiss, and are directly associated with banded iron formation (Ryan et al., 1986). Once this was recognised detailed ground magnetic

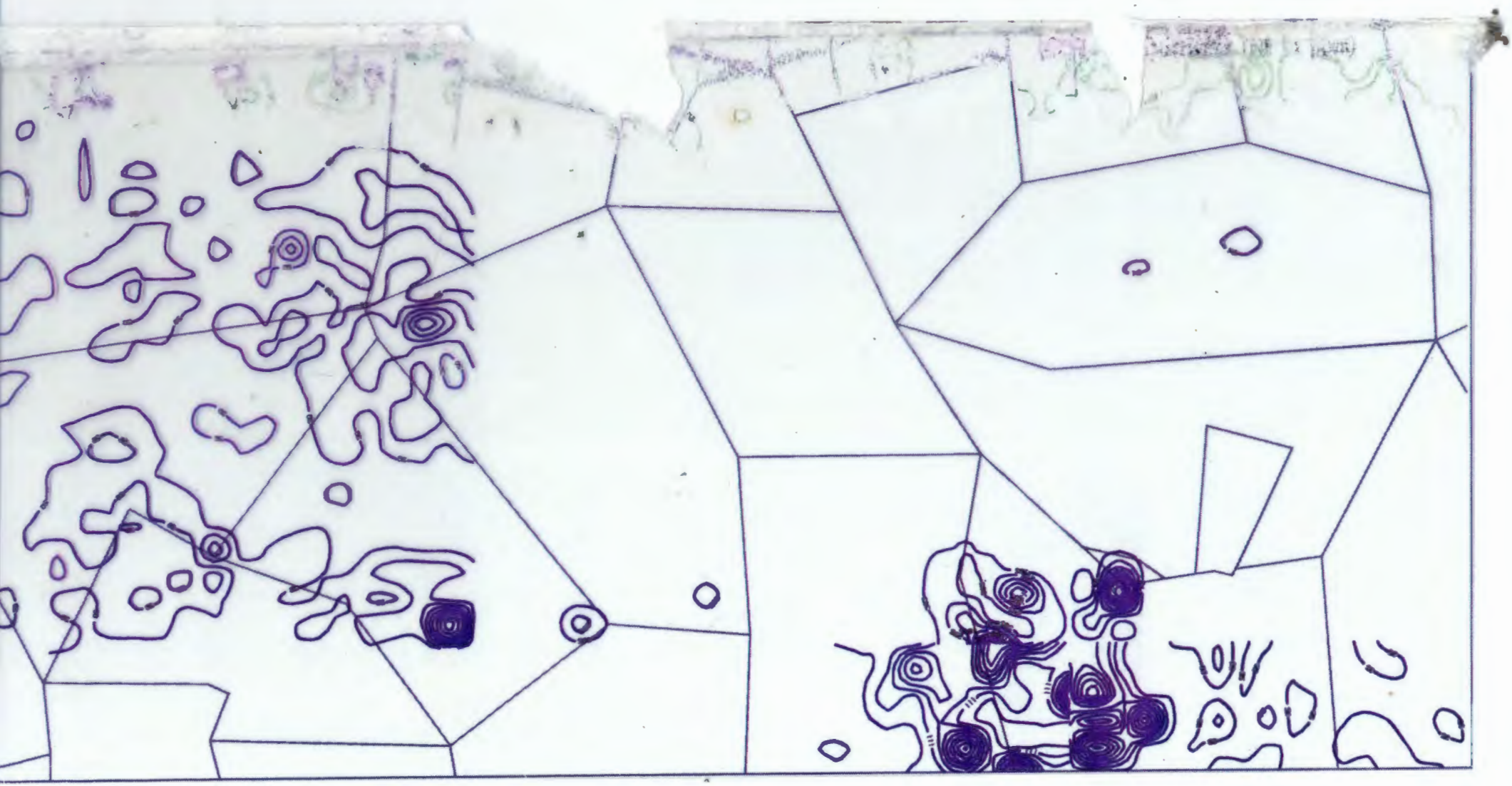

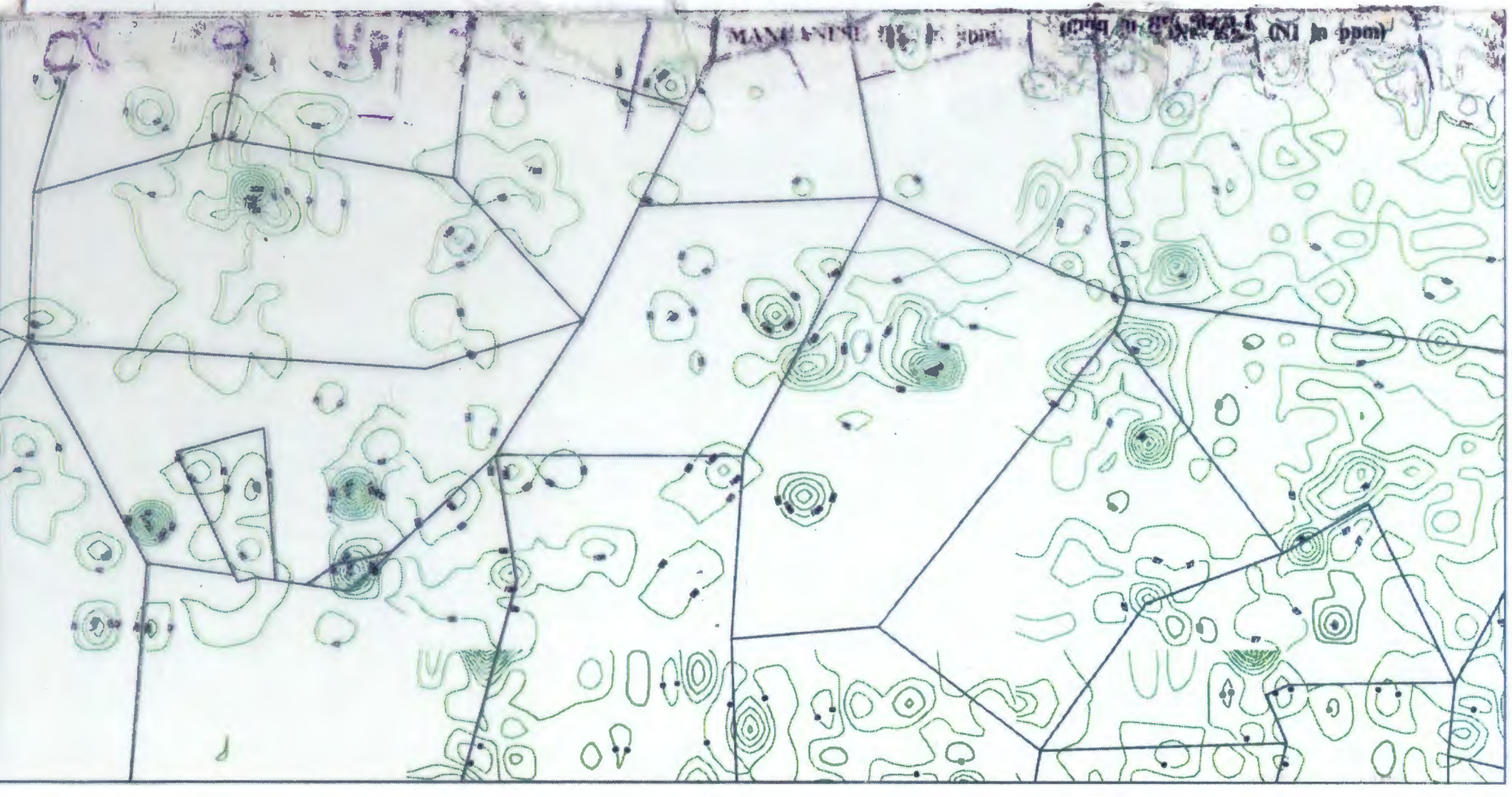

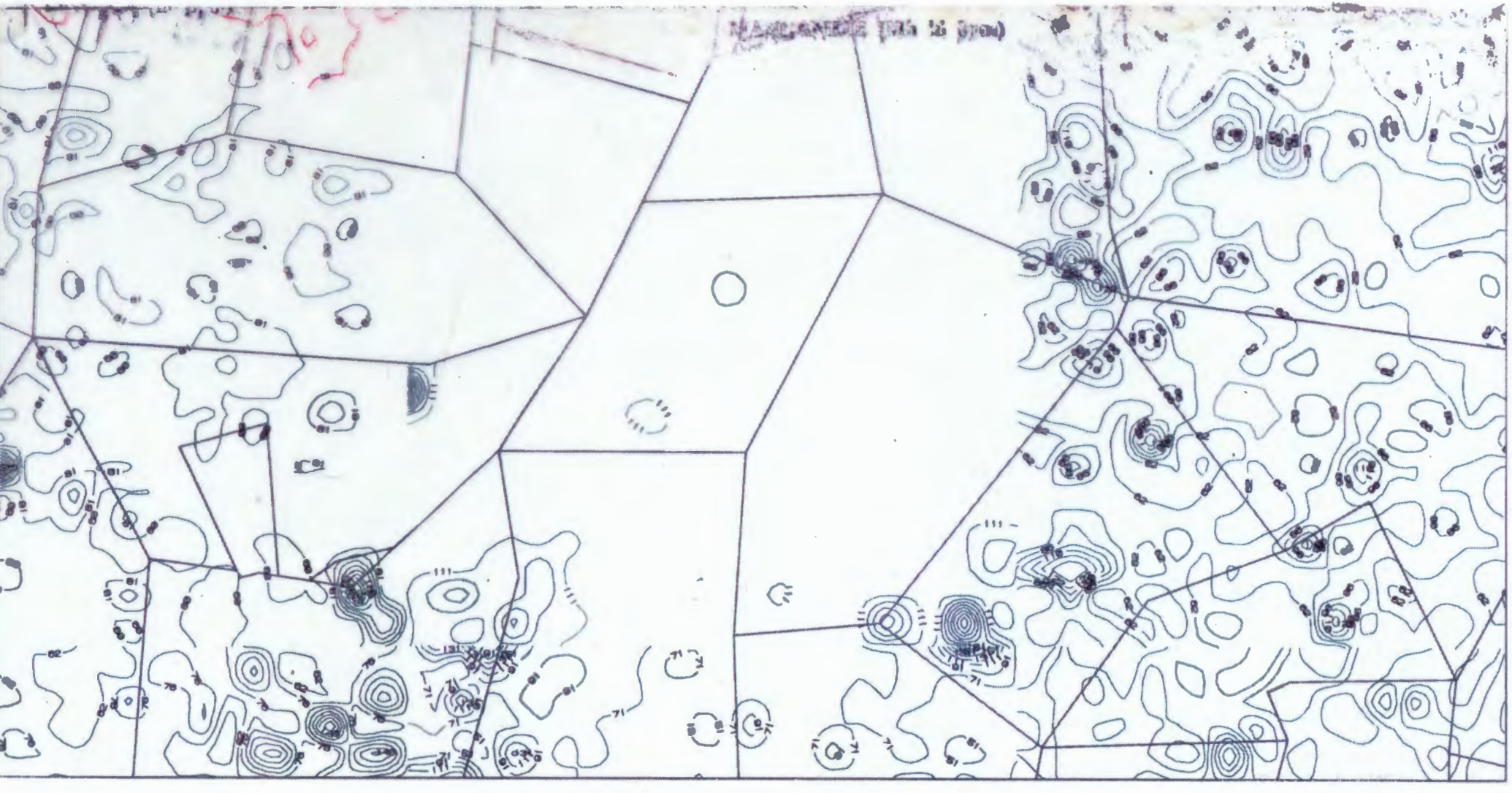

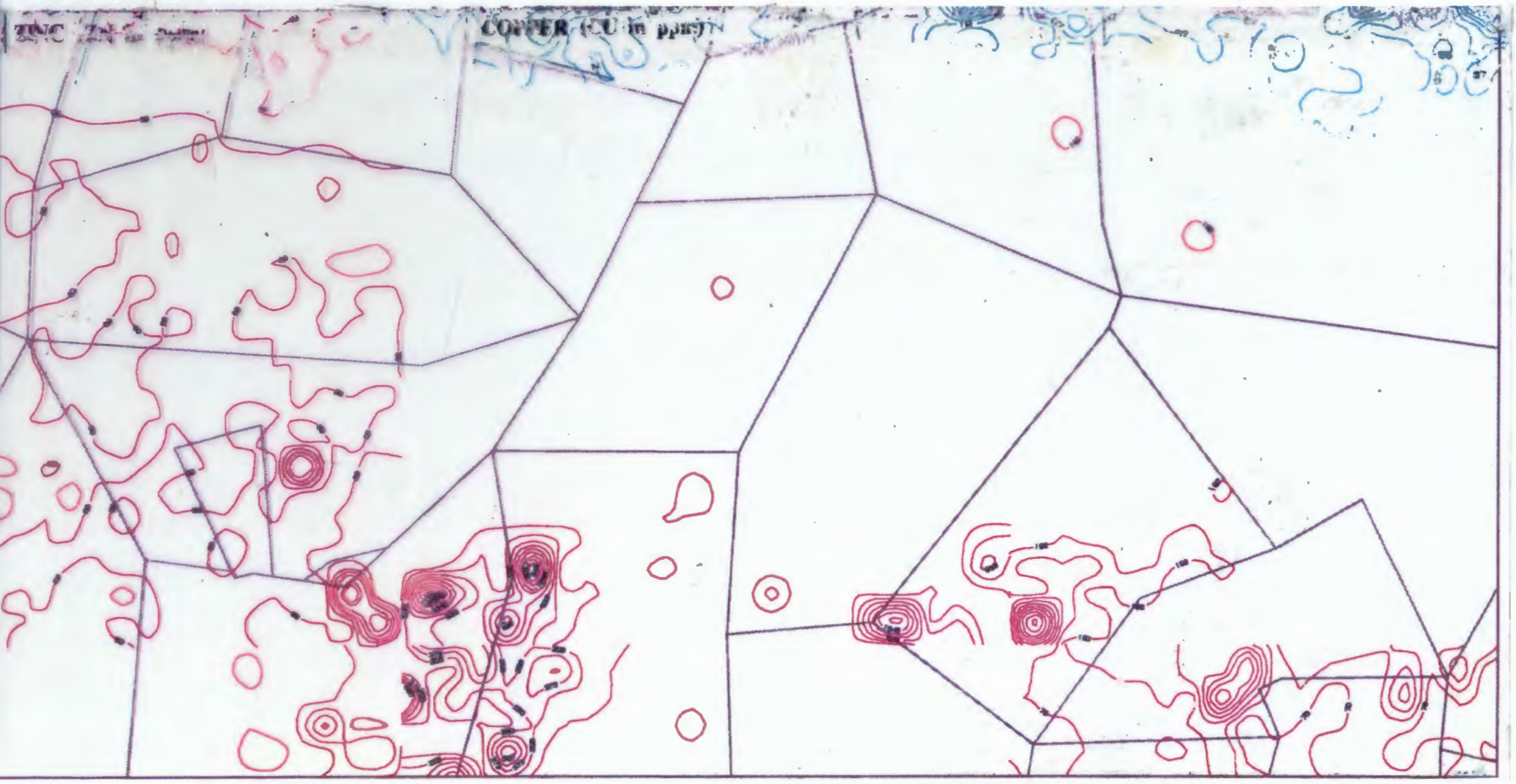
ZINC (Zn in ppm)
COPPER (Cu in ppm)

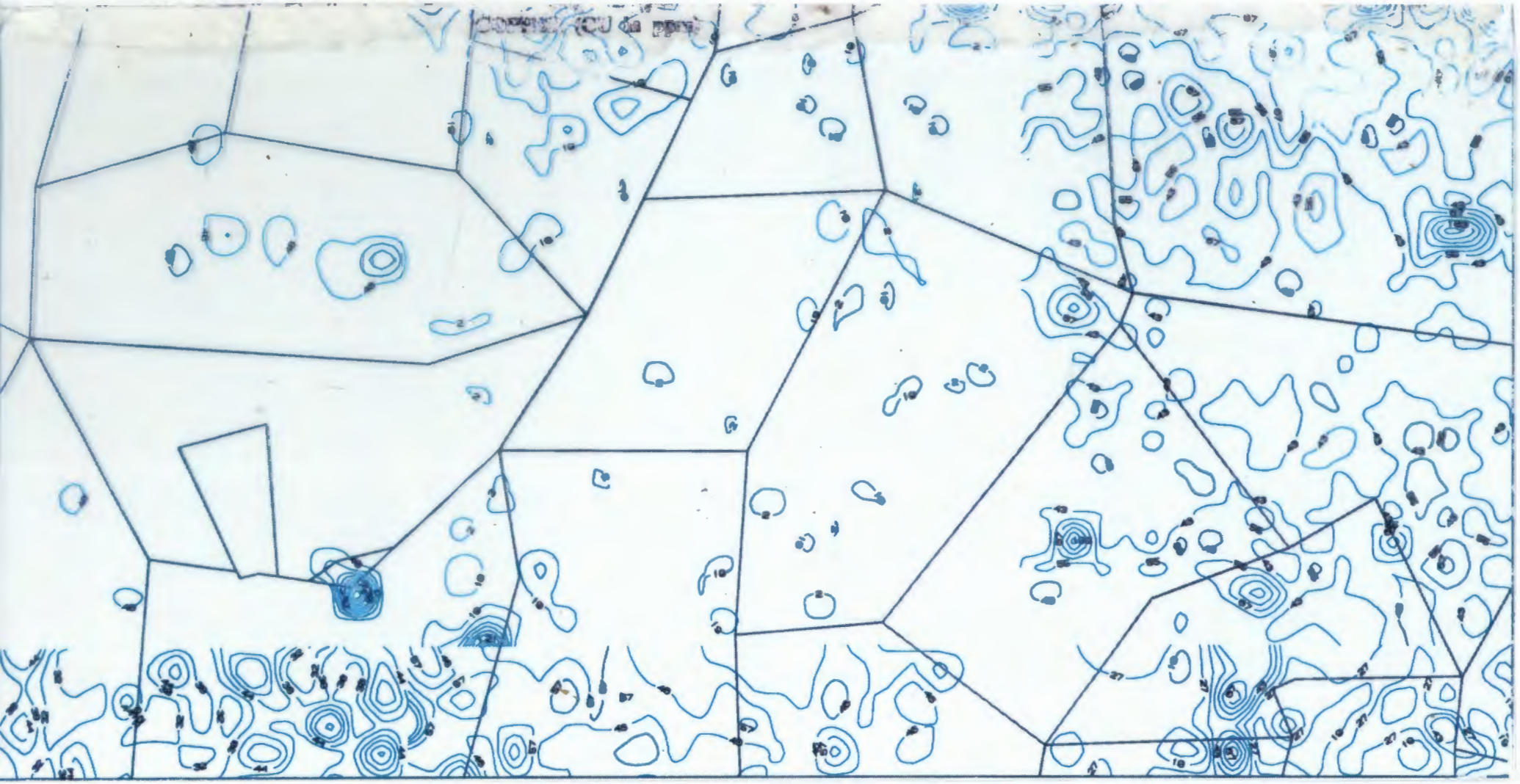

TM Image three band (7 4 1) composite overlain with stream pattern, traverse and lithogeochemical sample locations

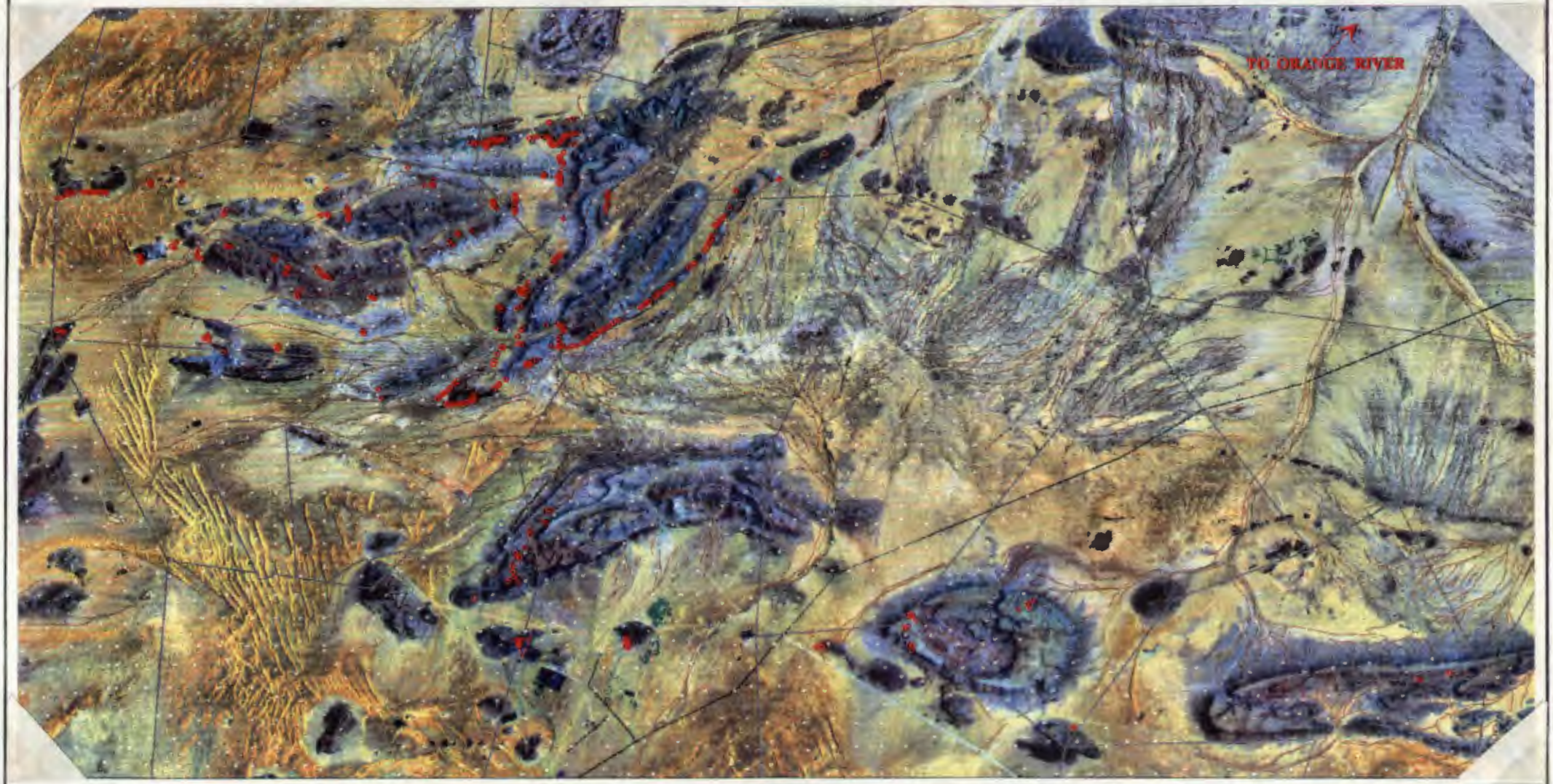

Figure 5.1 - Stream network (brown lines) overlain on TM image composite which highlights the local geology. Minor streams run-off the ore bodies and inselbergs. In the Gamsberg basin, streams merge and drain the basin through a narrow gap in the North. The major drainage is to the north where streams converge, and drain into the Orange River. Sand dunes occur in the Koa valley, to the south, which is a paleo-drainage. Traverse sample point locations are marked with white dots. Red markers indicate where lithogeochemical sample data has been collected, but this data is not used in this study. The four stratiform Pb-Zn deposits located in the southern part of the study area are marked by triangles. The green markers to the north locate Sillimanite mines.

surveys of the ore body, low level helicopter borne surveys around the initial discovery site and regional fixed-wing aeromagnetic surveys (Figure 2.4) were undertaken. The regional aeromagnetic data sets were incorporated into AGGED, but only the Phelps Dodge regional survey data was analysed.

5.3.3.1 Spatial Data

The geophysical spatial data are stored primarily as images. A Proton Precession magnetometer with sensitivity 2 nT was used, during an airborne magnetometer over the Aggeneys area in 1972, by Phelps Dodge of South Africa (BMM unpublished reports, 1983-1986). Data was captured at sensor height of 50 feet and at a 0.166 mile line spacing. Data is recorded as images interpolated from contour maps at 2 nT interval.

A local aeromagnetic survey, adjacent to Black Mountain, was flown in January 1991. A Cesium Vapour magnetometer was used, and data was captured every 5 meters from a sensor height of 35 meter at line spacing 100 meters (D. Mourant, pers. comm., 1993). Data is recorded at a pixel resolution of 50 meters.

A regional aeromagnetic survey was flown by the South African Geological Survey in 1973. Their data is recorded at 250 m pixel resolution. The images are in Gauss Conform Projection, (Longitude of Origin 19°). Co-ordinate registration problems were encountered when georeferencing this dataset. This dataset is therefore not used for analysis and details of this registration problem are outlined in Appendix 4.

Interpretation of linear features from the gridded image data, derived from the Phelps Dodge helicopter magnetic survey (1971), by R. F. Loxton, Hunting and Associates (1972), are stored in vector data files. These are interpretative outlines of magnetic bodies (AMIBODY), magnetic boundaries (AMIBOUND), dykes or sills (AMIDYKE) and fractures or faults (AMIFAULT) . These linear features are incorporated overlay 3 on Figure 2.4. Figure 5.2 summarises the prospecting data collected over the study area but not yet incorporated in AGGED.

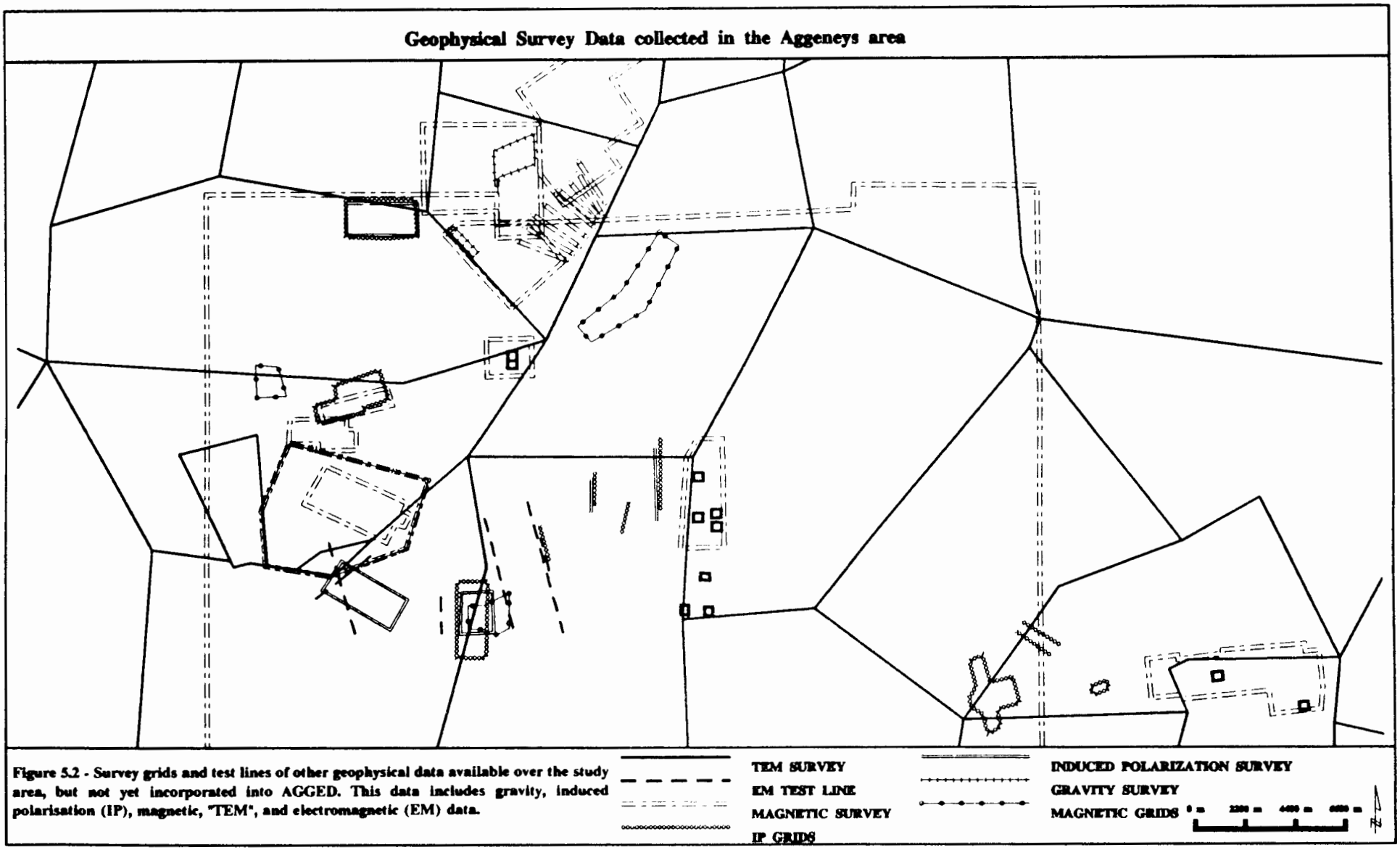

Figure 5.2 - Survey grids and test lines of other geophysical data available over the study area, but not yet incorporated into AGGED. This data includes gravity, induced polarisation (IP), magnetic, "TEM", and electromagnetic (EM) data.

5.3.4. Topographic and Cadastral Layer

5.3.4.1. Spatial Data

Contoured relief maps acquired from the Regional Department of Surveys and Mapping topographic map sheets are plotted in Figure 5.3. A Digital Elevation Model (DEM) graphically models the change of elevation over an area. The above agency has produced a DEM covering the entire Southern Africa. Although a DEM, covering the extent of the study area, was acquired, this was not included in the AGGED database. Appendix 5 outlines the reasons for this decision. A separate DEM was produced using data captured during this study. The methodology used to create this DEM is discussed in Chapter 6.

Cadastral data contained in AGGED include maps showing the roads network, telephone lines, location of mines and buildings and outlines of farm boundaries, in the study area. Farm boundaries and mine locations are overlaid on all the maps for easy referencing.

5.3.4.2. Attribute Data

A separate database table lists the details of each farm, such as the name of the farm and of the mining company presently holding mineral and exploration options on the farm.

5.4. Sources of error in AGGED

Error from hard copy cartographic map data captured and stored in AGGED cumulate from:

i) Initial data capture (geological mapping). The maps produced from mapping surface features in outcrop, record an over-simplified representation of the complex physical detail actually observed. This introduces a level of interpretive error.

ii) Storage of paper maps causes stretching, shrinking and creasing. Errors are introduced from digitizing and scanning of analog paper maps distorted in such manners.

The processing of data, for example geochemical analysis of sampled data, may

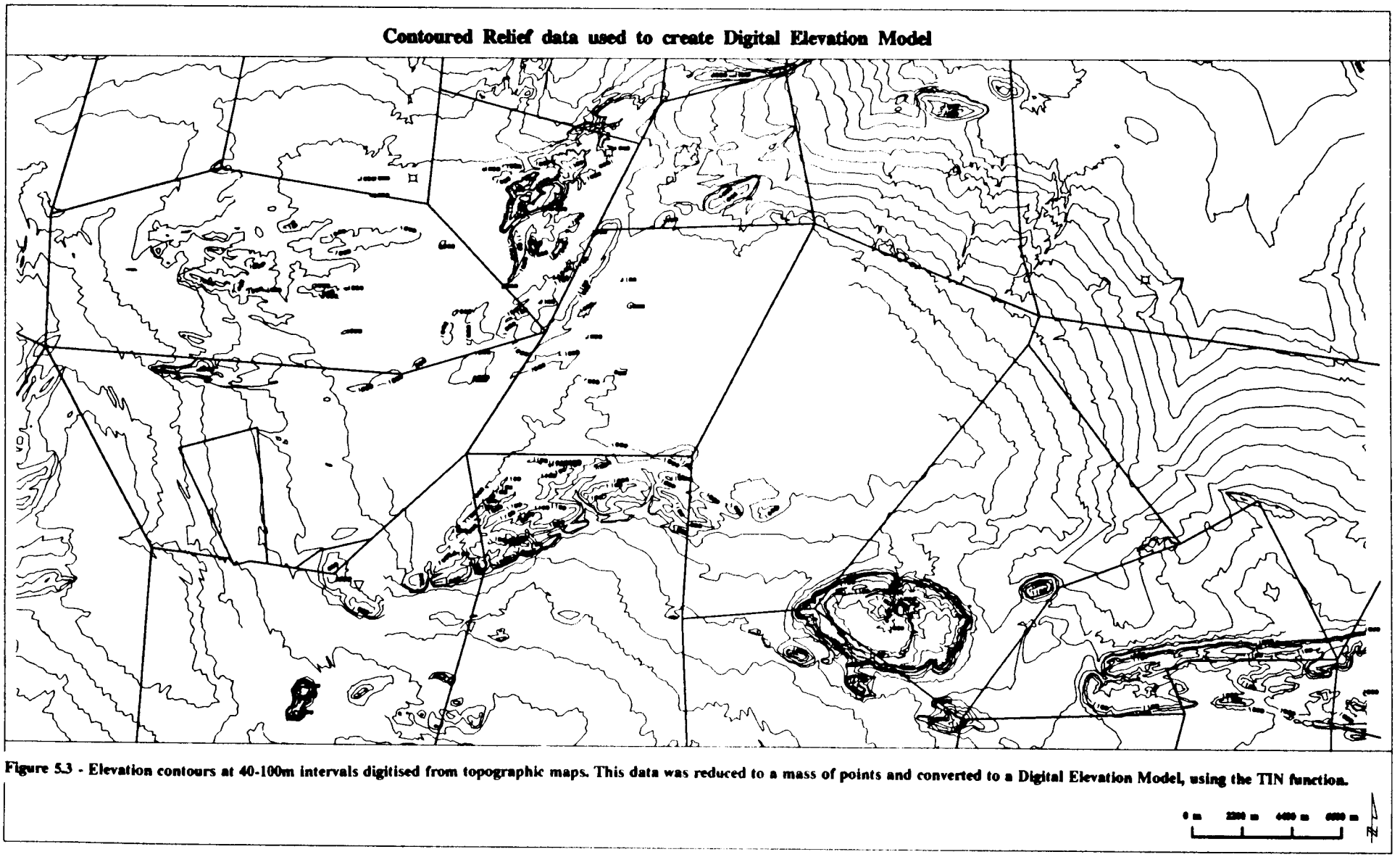

Figure 5.3 - Elevation contours at 40-100m intervals digitised from topographic maps. This data was reduced to a mass of points and converted to a Digital Elevation Model, using the TIN function.

introduce interpretive errors when detection limits for elements are set. Mis-typing of sample data values during data capture also introduces errors.

Most spatial data are available in a spherical co-ordinate system in the Geographic projection. They are subsequently transformed to cartesian co-ordinates in Transverse Mercator projection. Appendix 2 describes the spherical and cartesian co-ordinate system, and registration from the Geographic to Transverse Mercator projection.

Data captured from airborne and satellite remote sensors are in geographic co-ordinates and need to be referenced to a cartesian co-ordinate system. With photographic image data, reference accuracy poses a problem. For example, air photography is oblique to the earth, and projection problems arise as a result of varying scales over the image (Flowerdew, 1991). With satellite photography, scale (vertical) distortions are acute, because the greater the altitude the greater the effect of the earths curvature on image distortion (Flowerdew, 1991). Conversion from a spherical co-ordinate system which considers the curvature of the earth to a flat planar cartesian co-ordinate system also introduces distortion.

5.5. Discussion

AGGED currently consists a number of subsets of exploration data, selected to develop a methodology for predictive analysis of Bushmanland type sediment hosted base metal deposits. Once created, a spatial database has various implications for time and economy saving. Interactive and rapid data processing and interpretation is possible. Reduction in fieldwork and manpower is facilitated by the ability to delineate exact areas that require further and/or added data to aid in intelligent decision making.

The ability to investigate large areas with a small team of experts in a short time is aided by having large datasets from diverse disciplines geo-referenced and stored in a single spatial database. Data from old exploration campaigns can be easily and readily reinterpreted, as is done in this study. Previously collected data can be readily combined and compared with recently collected data input to the database. The spatial dimensions of the study area, incorporated in a GIS database, can be expanded or

decreased readily.

The data is stored collectively on a single storage device (magnetic media), and can be accessed, manipulated, analysed and displayed at sites where the relevant ARC-INFO software is available. Alternatively the data can be converted to variable formats used by other spatial databases, and utilised according to the functionality of that spatial database.

AGGED contains information stored in vector and raster data structures, geographically referenced to the Transverse Mercator system, with associated attribute data stored in a relational database. The time taken to create the edited, cleaned and validated GIS database, together with analysis of the database and map-creation, is summarised in Table 5.7.

Table 5.7 - Time taken to create, analyse and present data from AGGED.

Function	Time Taken (months)
data capture	10
training	5
database design	6
data analysis	3
map creation	2

Chapter 6

Methodology of Data Processing and Analysis within AGGED

6.1. Introduction

Data processing and analysis involves transforming spatial data into legible patterns, commonly called structure or signal, and illegible patterns, commonly referred to as noise (Burrough, 1986). First, the analytical methods used to extract pertinent information from the original data, using appropriate statistical and numerical functions, are described. These methods include interpolation, classification, enhancement, manipulation and merging.

The statistical and numerical methods employed on the spatial and attribute data contained in AGGED, represent a small subset of the full range of analysis tools presently available in GIS. The methods used in this project were developed to extract the type of information which may help to delineate possible targets for base metal exploration. This constitutes a digital refinement on previous examination of the data and is facilitated by using the GIS analysis toolkit and graphic display capabilities.

A clear understanding of principles inherent in the analytical tools used facilitates a better understanding of the results generated. This encourages scientifically sound inferences to be drawn from the data. The description of methodology is therefore assigned Chapter status in this thesis, and is not relegated to an Appendix. Here, the implementation of analytical tools within the different data layers, as separated in Chapter 5, are described. Results of data analysis are presented in Chapter 7.

6.2. Geological Data Sets

6.2.1. Classification

Figure 2.2 summarises litho-stratigraphic divisions in the Bushmanland area. As discussed in Chapter 2, present stratigraphic interpretations in the area are controversial. A map purely reflecting lithology, as opposed to litho-stratigraphy, is represented as Figure 2.3. This figure "reclassifies" the original litho-stratigraphic map

by merging common lithologies, some of which may be assigned to different stratigraphic units. Moore (1989) and Joubert (1986a) emphasize that the lithostratigraphic subdivisions of the Namaqualand Metamorphic Complex are based on geographical regions and tectonic boundaries. These divisions are subjective and may not be correct. A pure lithological classification, reflecting rock compositions and mineral variations is more suitable for objective mineral exploration. That is, until better chrono-stratigraphic control becomes available through, for example, precise U/Pb zircon analysis.

The reclassification procedure utilises the relational attribute and geo-relational data models; illustrated in Figure 4.4. The Lithostratigraphic Spatial Attribute Table (i) manages the geographic information stored for the Lithostratigraphic Map (A). The Information attribute table contains information describing the spatial features (polygons here) stored for the Lithostratigraphic Map. The Reclassification Table (iii) contains the codes that will redesign the Lithostratigraphic Map to a Lithological Map (B). The Reclassification Table (iii) is designed with a column containing the classification code describing the litho-stratigraphic polygon features in Map A, Spatial Attribute Table (i) and associated Information Attribute Table (ii).

First, a relational join between Table (ii) and Table (iii) is executed on this classification code (GEOLOGY-ID). A geo-relational join between Table (i) and table (ii) then effectively joins the spatial feature of the Lithostratigraphic map (A), managed in Table (i), with the previously joined tables. A function that dissolves boundaries between adjacent polygons containing identical reclassification codes, was then processed. The 31 litho-stratigraphic classes of Figure 2.2 are re-defined to the 12 lithological classes in Figure 2.3. Table (iv) in Figure 4.5 manages information pertaining to this reclassification. Additional data describing these lithologies can be added in separate columns within the same table.

6.3. Geochemical Data Sets

6.3.1. Interpolation

To optimise the information contained in the irregularly sampled point data, interpolation techniques were utilised. Interpolation converts spatial data in the form

of discrete points, to a continuous surface by finding the function that will best represent this surface, and predict values at intervening or unspecified (unknown) points (Lam, 1983). Data representation from a discrete vector data model is converted to a continuous raster data model, allowing for better visualisation, integration and analysis of the data sets.

Analytical traverse soil geochemical data is available in AGGED as vector point data sets. Interpolation procedures were used to estimate the value of geochemical element concentrations at an unsampled point from measurements made at surrounding sampled sites (points on Figure 5.1). This involves fitting a plausible model of variation to the values at sampled data points and calculating values for a continuous surrounding area using. The task was to choose an appropriate interpolation method that models the variation of values in the geochemical data optimally.

Specific interpolation methods were available in the GIS analytical toolkit to interpolate irregular point data to a regular grid. These interpolation methods included Trend Surface Analysis, Inverse distance weighting, Kriging and Triangular Irregular Networks. The geochemical data in this study was interpolated using Kriging, a local fitting technique based on the regionalised variable theory of D.G. Krige (1976) and Matheron (1971). A detailed summary of why the Kriging method was used, and its theoretical basis is described in Appendix 6.

Kriging of the geochemical data sets produced floating point grids displayed in Figure 6.1 a. After some experimentation, classification and linear colour coding were used to improve the graphical display and analysis of the data.

6.3.2. Classification

Meaningful data patterns can be disguised, or alternatively revealed, in graphical representation of surface grids. Classification allows easy comparison of different areas by highlighting the maximum and minimum values in gridded data. However, the data values and colour that highlights this maximum-minimum range need to be classified.

6.3.2.1. Colour Display

Continuous gridded data are most effectively displayed using colour representation. Colour is represented on the computer display screen by combining controlled amounts of primary colour spaces, red, green and blue. To take advantage of the full colour display range of the computer (0-255, Appendix 7), linear colour scaling was used. This modifies the colour display range by spreading the grid data values using maximum-minimum linear scaling.

Stretching parameters for the linear coding are calculated from the mean cell value over the entire image and standard deviations of the data surface being tested. The cell values below the mean (+ 2 SD) are assigned the digital value 0. Cell values above the mean cell (+ 2 SD) are assigned to 255. The cell value between the two parameters calculated above are stretched along the digital range 0 - 255. Some areas are not coloured, when the data is displayed without linear colour coding, because the colour range is not stretched to represent all the data values (Figure 6.1 A). When displayed using linear colour coding the full range of data values are clearly represented (Figure 6.1 B)

6.3.2.2. Data Values

Before classifying the data, the frequency distribution of the sampled data was inspected. The frequency distribution of point geochemical data for Zn, Pb, Cu, Mn and Ni are shown in Figures 6.2 A-E. All the datasets display skewed distributions. For maximum-minimum data classification a normal distribution of data with equal number of data values falling below and above the mean value, calculated over the entire area, is preferable. Logarithmic transformation of the element data, shown in Figure 6.3 A-E, change the data to more gaussian-like distributions.

If the data sampled over the study area, displays a skewed distribution, then so do the corresponding interpolated data sets. Hence the interpolated geochemical element grids were transformed using the logarithmic function. This takes each cell value in the grid and calculates its equivalent logarithmic value. This operation takes approximately 3 minutes in a grid, with 1184 columns and 630 rows of grid cell dimension 50 metres. Figure 6.4 illustrates interpolated surface Pb data displayed with linear colour coding

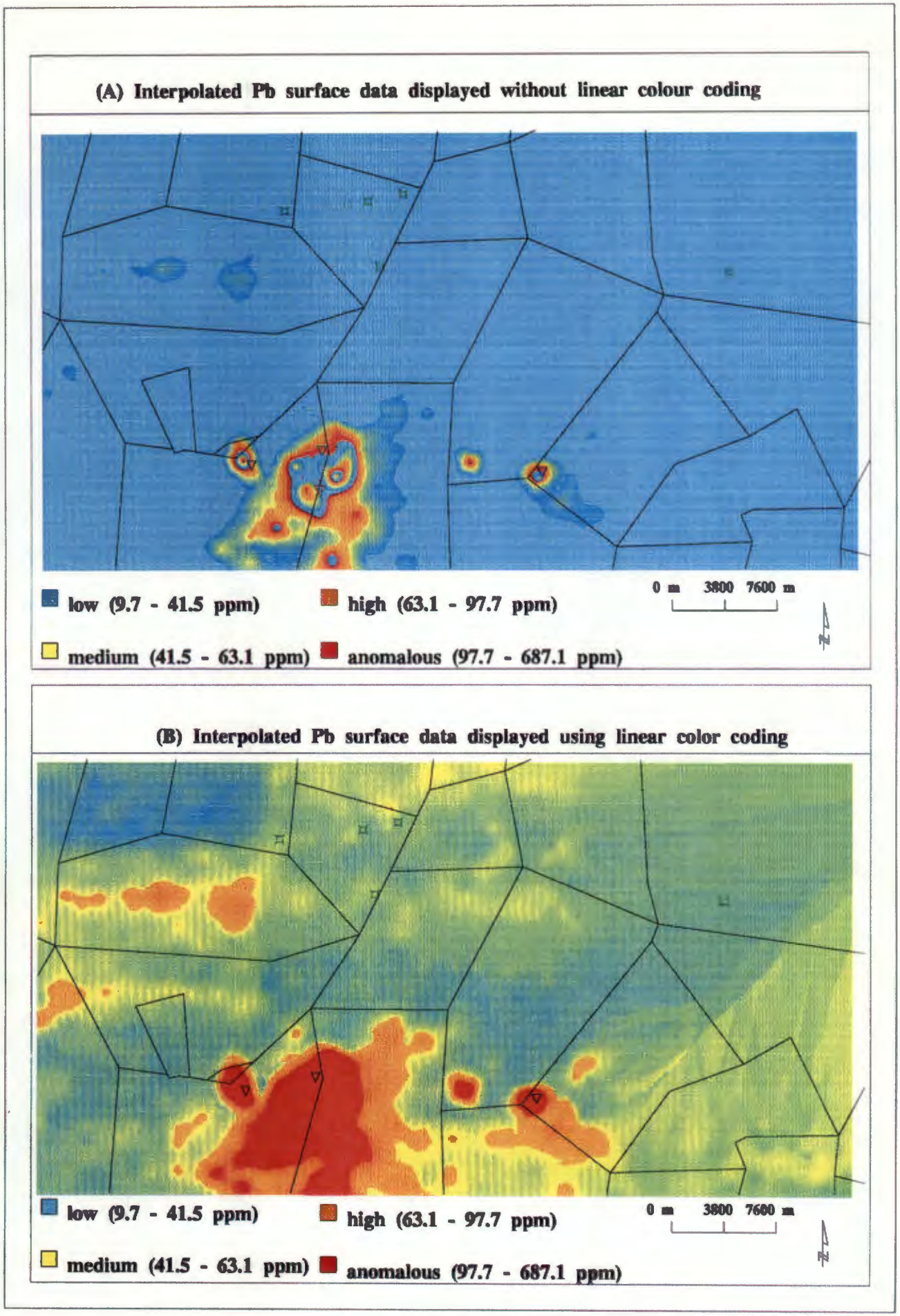

Figure 6.1 (A-B) - (A) Interpolated Pb data displayed without colour or data classification. The data thus displayed is not optimally contrasted, since most of the cell values fall within a narrow range of values. All the available colours are used to display the higher ranges of data-values, resulting in intermediate to lower data ranges not being plotted, even though this information exists. (B) Linear-colour-coding classifies the digital range(0-255) of the colour screen to the range of data values, allowing all data values to be displayed using 255 different colours.

Traverse Geochemistry - Bushmanland

A - Frequency of Pb(ppm) values

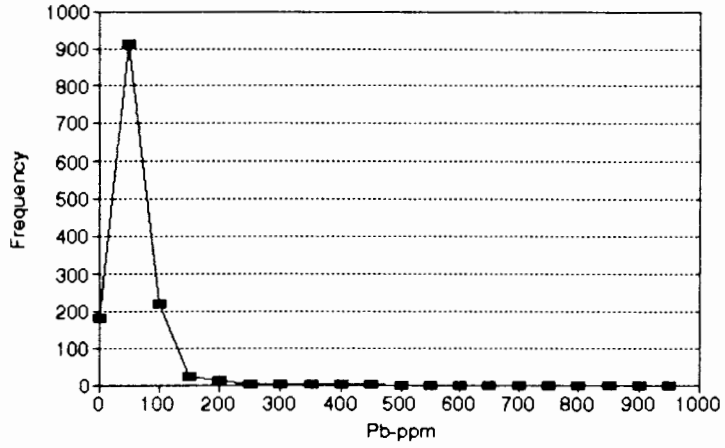

Traverse Geochemistry - Bushmanland

B - Frequency of Zn(ppm) values

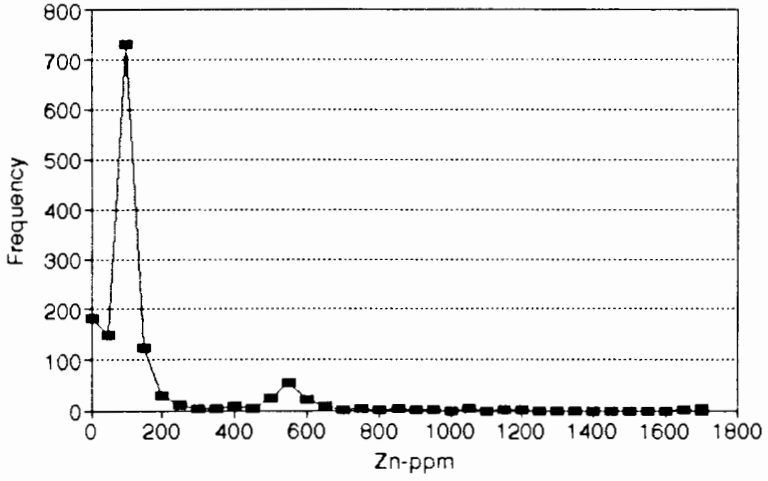

Traverse Geochemistry - Bushmanland

C - Frequency of Cu(ppm) values

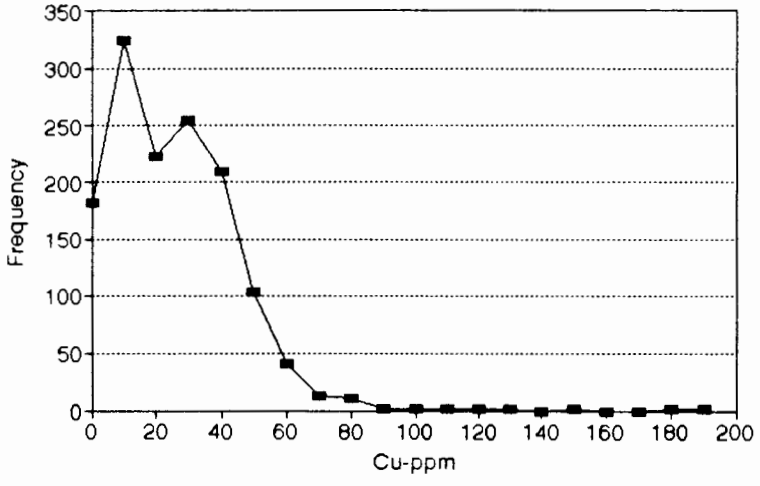

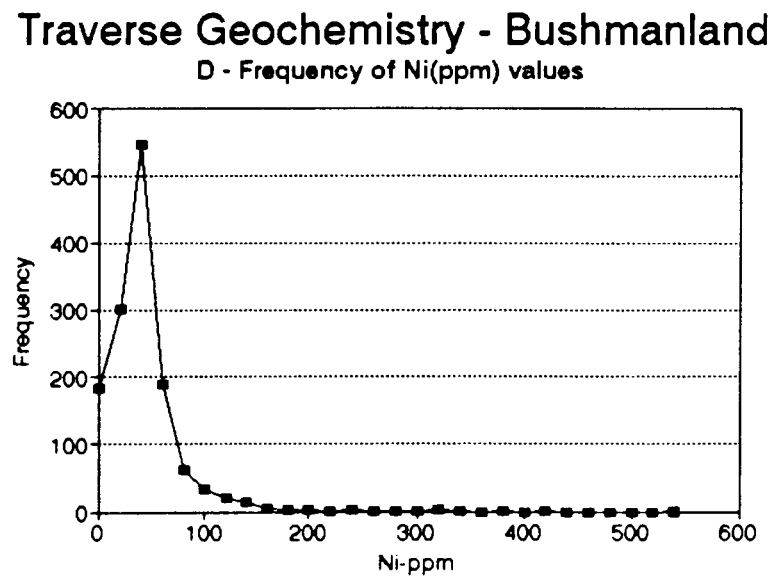

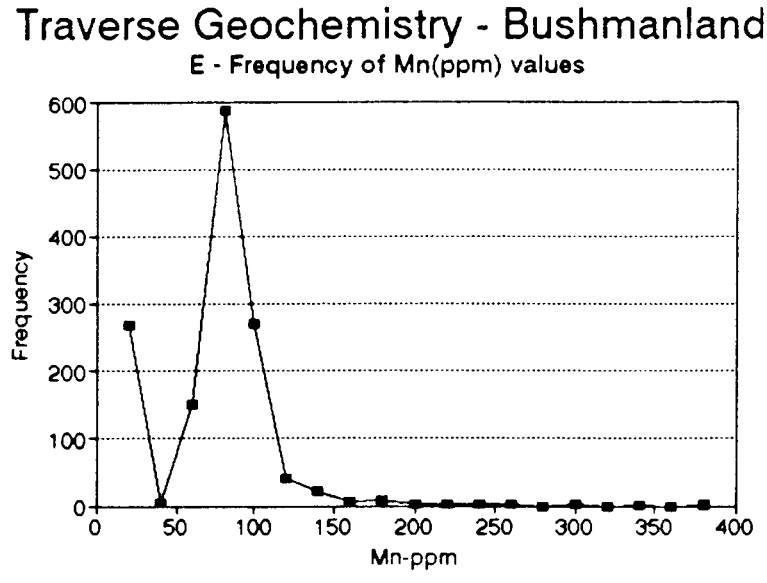

Figures 6.2 (A-E) - Graphed frequency distribution of 1374 traverse soil sample data points for Pb, Zn, Cu, Ni and Mn, all in ppm, collected over the study area and analysed. The frequency distribution of values are skewed in all data sets. The extreme range from low to high values cause element values to cluster around low values, since low values occur most frequently. In mineral exploration the high element values are of interest.

Traverse Geochemistry - Bushmanland

A - Logarithmic Transformation Pb(ppm)

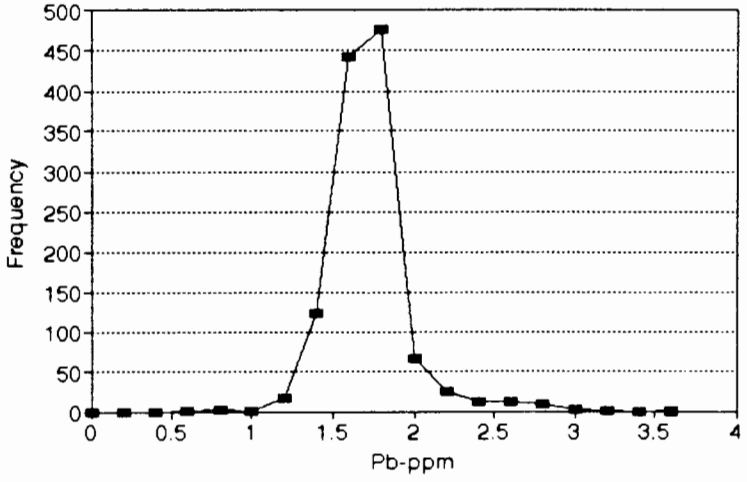

Traverse Geochemistry - Bushmanland

B - Logarithmic Transformation Zn(ppm)

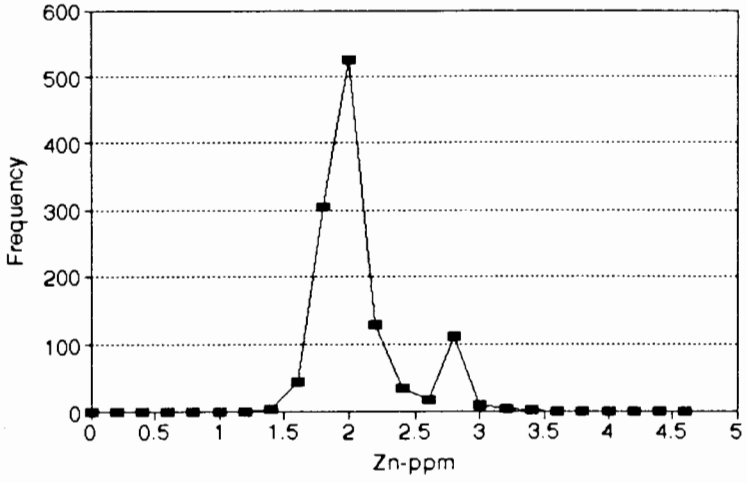

Traverse Geochemistry - Bushmanland

C - Logarithmic Transformation Cu(ppm)

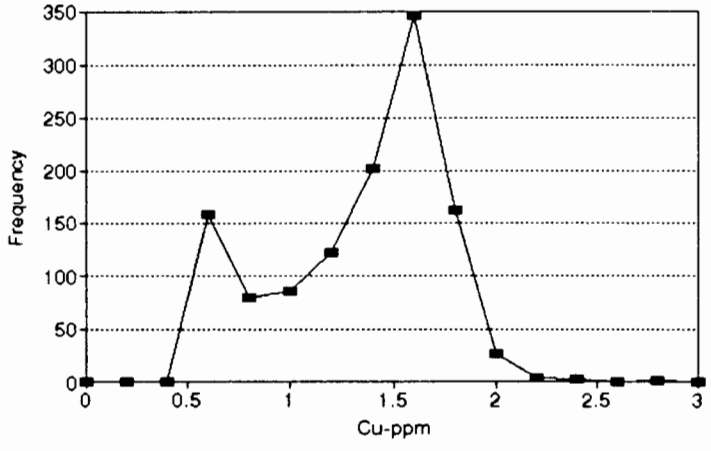

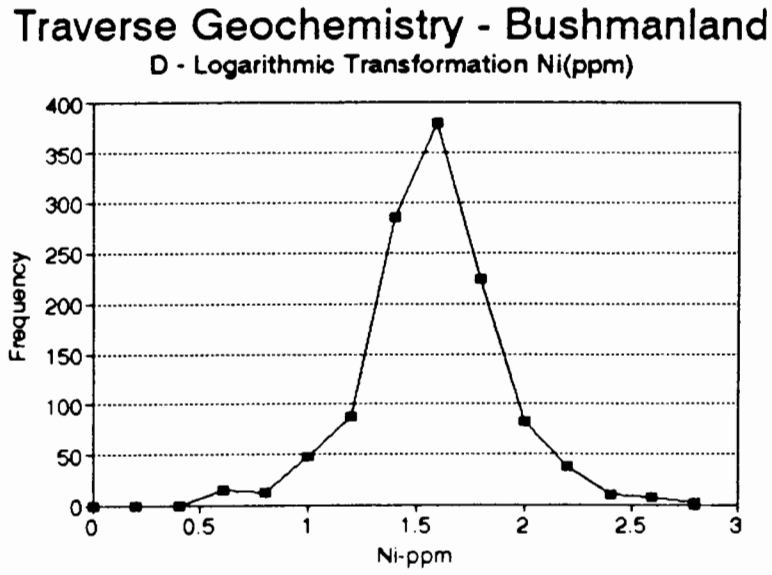

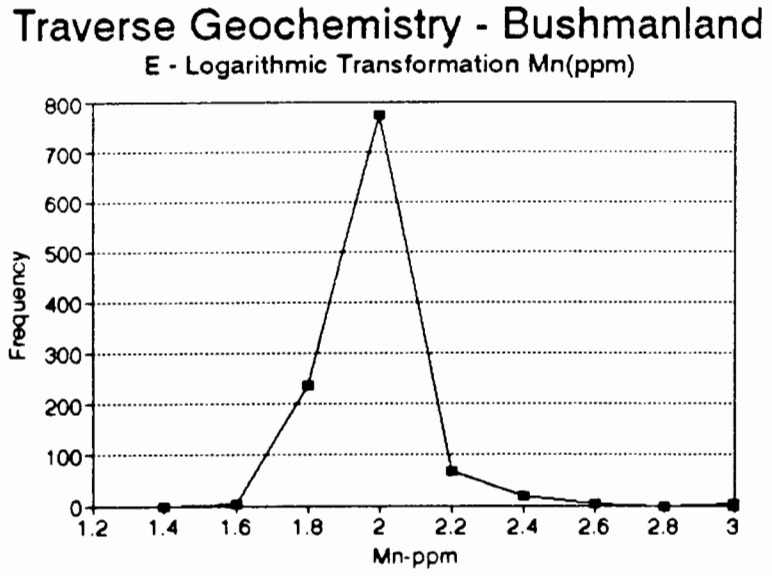

Figures 6.3 (A-E) - Logarithmic transformation of 1374 traverse soil sample data points, for elements Pb, Zn, Cu, Ni, and Mn, produces a more gaussian distribution of element values, within the high-low range of values. Logarithmic transformation of the data decreases the extreme spread in data values, resulting in a smoother frequency distribution of values. All interpolated datasets are logarithmically transformed to eliminate skewed distributions. The smoothing of element concentration values, permits the spatial variation (ranging from low to high) in the element data to be clearly displayed. Also, the signal to noise characteristics of the data area improved by getting rid of spatial clustering.

(A), and logarithmically transformed (B).

6.3.2.3. Data using Colour

By creating a colour shading file that describes the shade and value (0-255), data can be colour classified by assigning the range of grid data values to different colours. Geochemical data is colour classified by selecting classes considering descriptive statistics of the summarising mean and standard deviations (SD) of data values over the entire study area. Descriptive statistics of the sampled element data (S) and interpolated element data (I), are presented in Table 6.1.

Table 6.1 - Descriptive statistics of traverse sampled data (S), surface data interpolated through kriging (I).

	Pb	Zn	Cu	Mn	Ni
Mean (S)	79.43	251.19	39.81	158.49	31.62
M + 1SD (S)	91.12	273.91	47.65	162.02	38.49
M + 2SD (S)	102.81	296.63	55.49	165.55	45.36
Maximum	687.65	1170.55	86.95	203.93	523.78
Mean (I)	41.5	98.2	18.8	77.3	32.6
M + 1SD (I)	63.1	182.0	37.2	91.2	56.2
M + 2SD (I)	97.7	331.1	72.4	107.2	100.0
Maximum	687.1	1169.5	86.9	203.7	523.6
Background	14	47	19	150	-

SD - standard deviation

I - interpolated

S - sampled

Red plots values above mean + 2 SD, to maximum value; turquoise reflects values between minimum and mean value, which is interpreted as non-anomalous element values in an area characterised by mineralisation. These should not be confused with background values (Table 6.1) which are calculated from samples not affected by the mineralisation (Beeson et al., 1978). Green reflects values that fall between mean and mean plus 1 SD and yellow values between the mean (+ 1 SD) and mean (+ 2 SD).

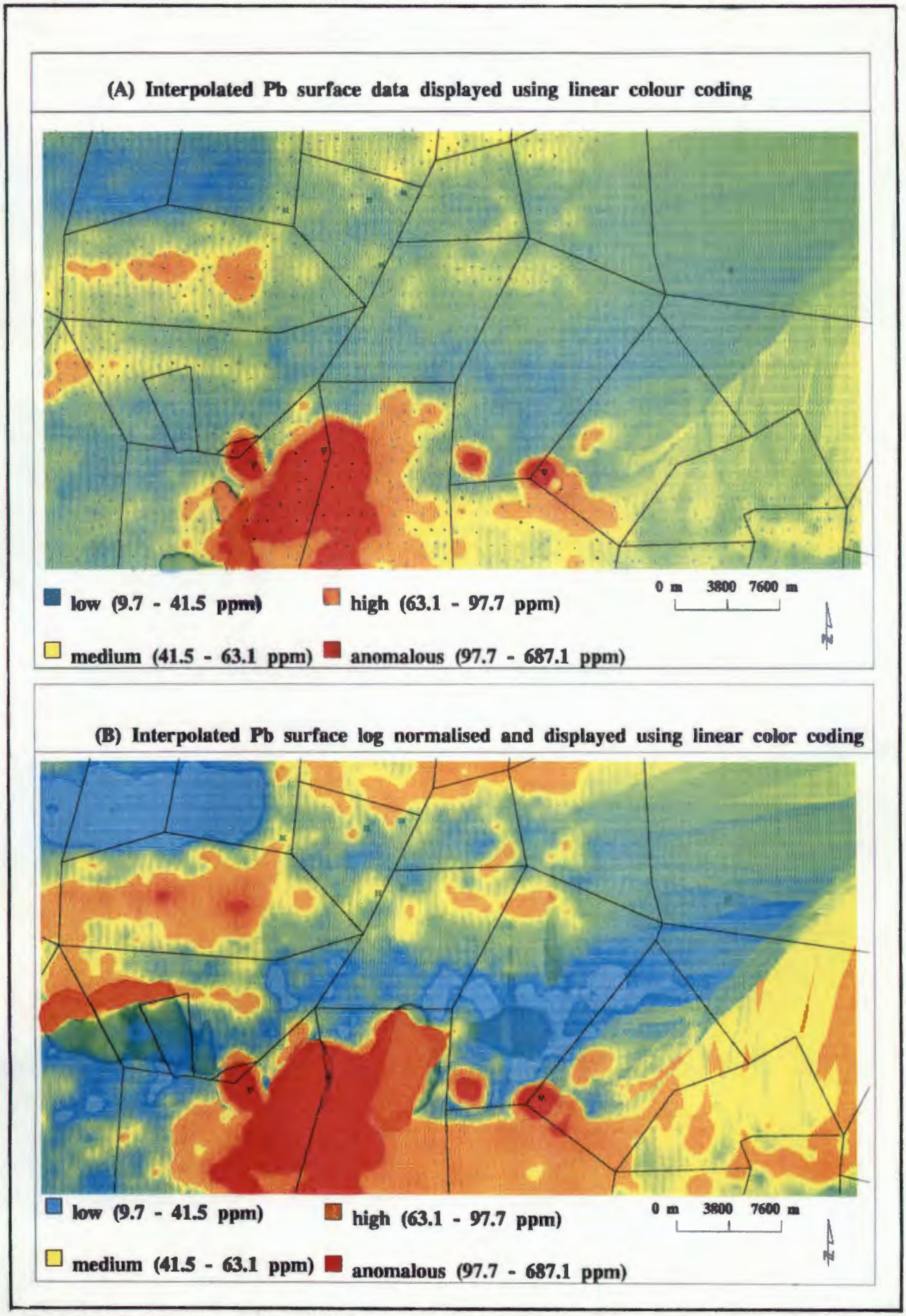

Figure 6.4 (A-B) - Comparison of interpolated surface data for Pb displayed with linear colour coding before and after logarithmic normalisation of the data, (A) and (B) respectively. Compared with images in Figure 6.3, the graphical display of data is vastly improved using these techniques. Logarithmic normalisation of the data improves the signal to noise characteristics by smoothing the interpolated sample concentration values frequency distribution around the most frequently occurring values. Red outlines areas with high values which represent anomalous element concentrations. Turquoise outlines areas of low Pb values. High values in the south-central areas correspond to the locations of the four known deposits (marker with triangles). Yellow to gold colours outline areas with values grading from low to high, ie. intermediate concentrations.

Yellow to red colouring depicts anomalous geochemical areas, in the study area.

Element classes are reflected in the colour legends of respective interpolated element component maps (Figure 6.5 A-E). These maps were created using a combination of linear colour scaling, logarithmic transformation and colour classification. A combination of this linear stretch and logarithmic stretch improves the signal to noise characteristics. Whenever any surface data was processed for display, a linear-coding contrast stretch of data was performed.

6.3.3. Contouring of interpolated surfaces

Computer generated geochemical contour maps at 50 meter intervals were generated after the following three steps were completed:

i) Studying the control point data for insight into data distribution (Figures 6.2A-E)

ii) Interpolating point data to a grid overlay using a chosen algorithm (Kriging).

iii) Contour the interpolated grid using the surface contouring function in GIS.

Each grid cell is tested by the program to see how many, if any, contours should pass through it (Hess and Herkommer, 1993). Contour lines join cells that define areas of equal concentration. The results of this contouring are presented as overlays on the interpolated surfaces in Figures 6.5 A-E. Contours maps generated by the Geological Survey of South Africa from stream sediment analyses of Pb, Zn, Cu, Mn and Ni in the Aggeneys area are presented as overlays 1 to 5 in Figure 5.1.

6.4. Geophysical Data Sets

The magnetic map reflects induced or remnant magnetisation of rocks in the surveyed area. These maps were derived from raw data collected using airborne magnetometers.

Magnetisation can be used to locate specific rock types or mineral deposits by virtue of their variable magnetic responses. The Bushmanland deposit contains magnetic minerals magnetite, illmenite, pyrrhotite with ferromagnetic properties which strongly affect the magnetic susceptibility of these rocks. Hence magnetic surveys can reveal the presence of magnetite- bearing formations, geological boundaries, and linear features (Figure 2.4 overlay 3 - magnetic faults). Pb-Zn deposits and associated rocks

(A) Pb surface interpolated from traverse geochemical analytical data

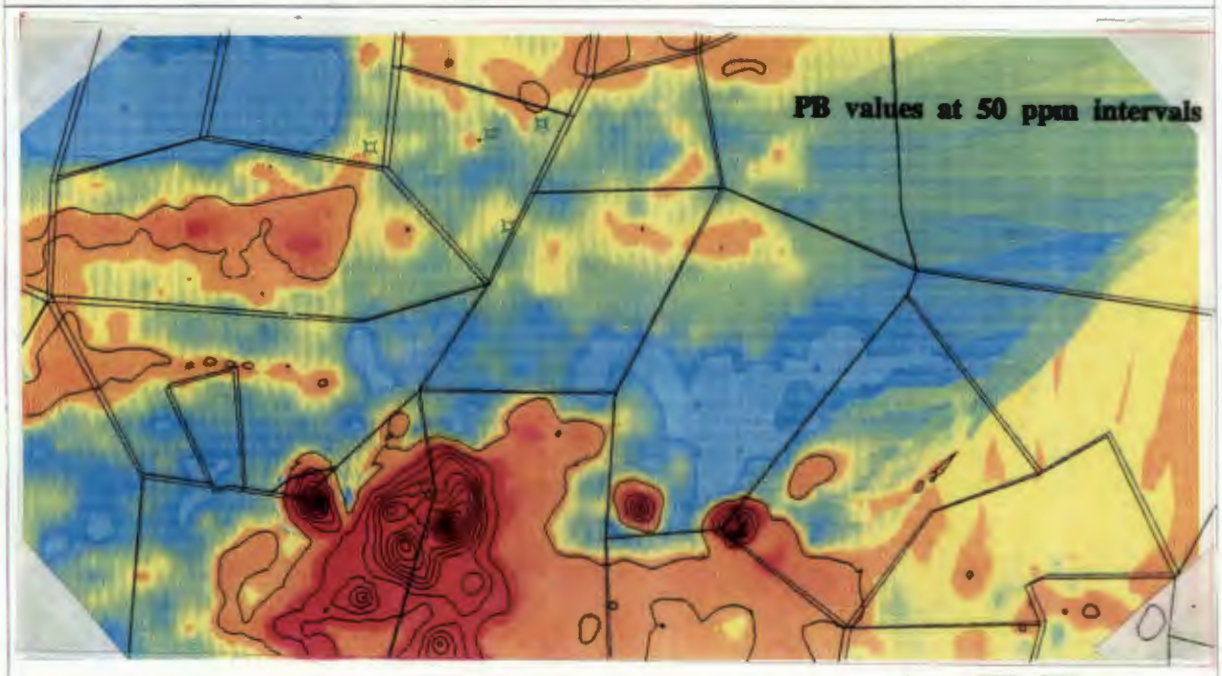

(B) Zn surface interpolated from traverse geochemical analytical data

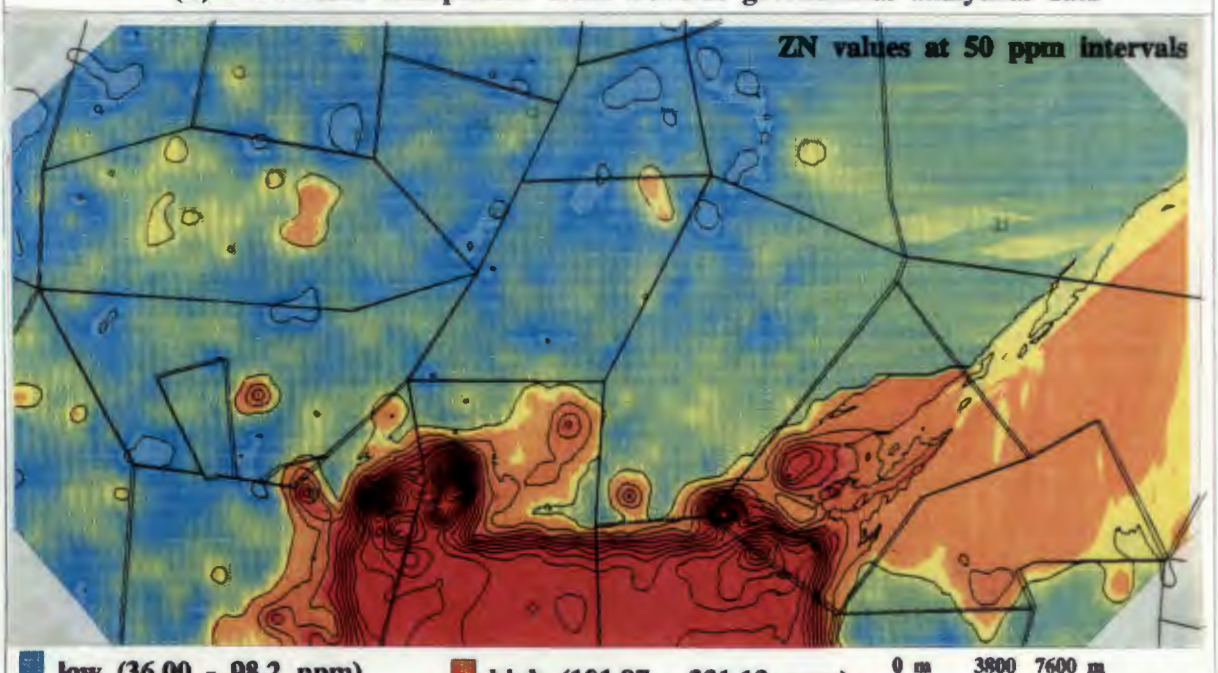

(C) Cu surface interpolated from traverse geochemical analytical data

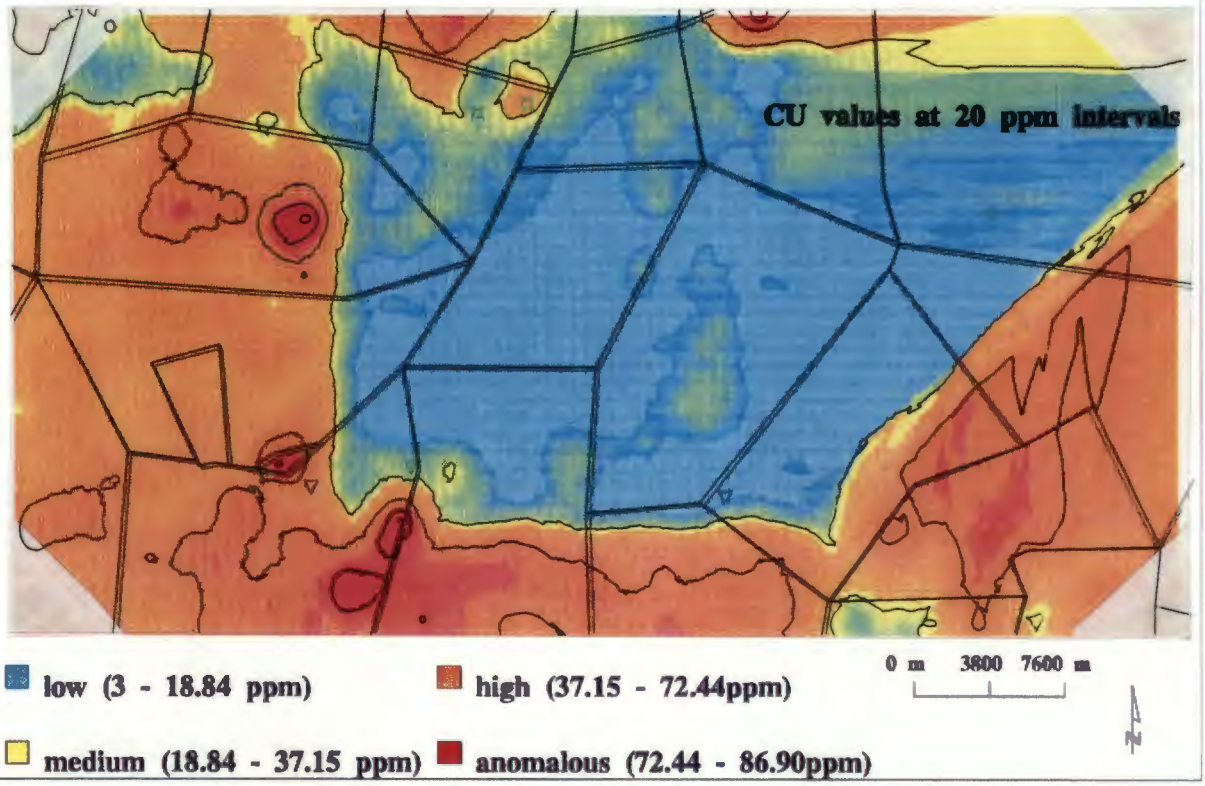

(D) Mn surface interpolated from traverse geochemical analytical data

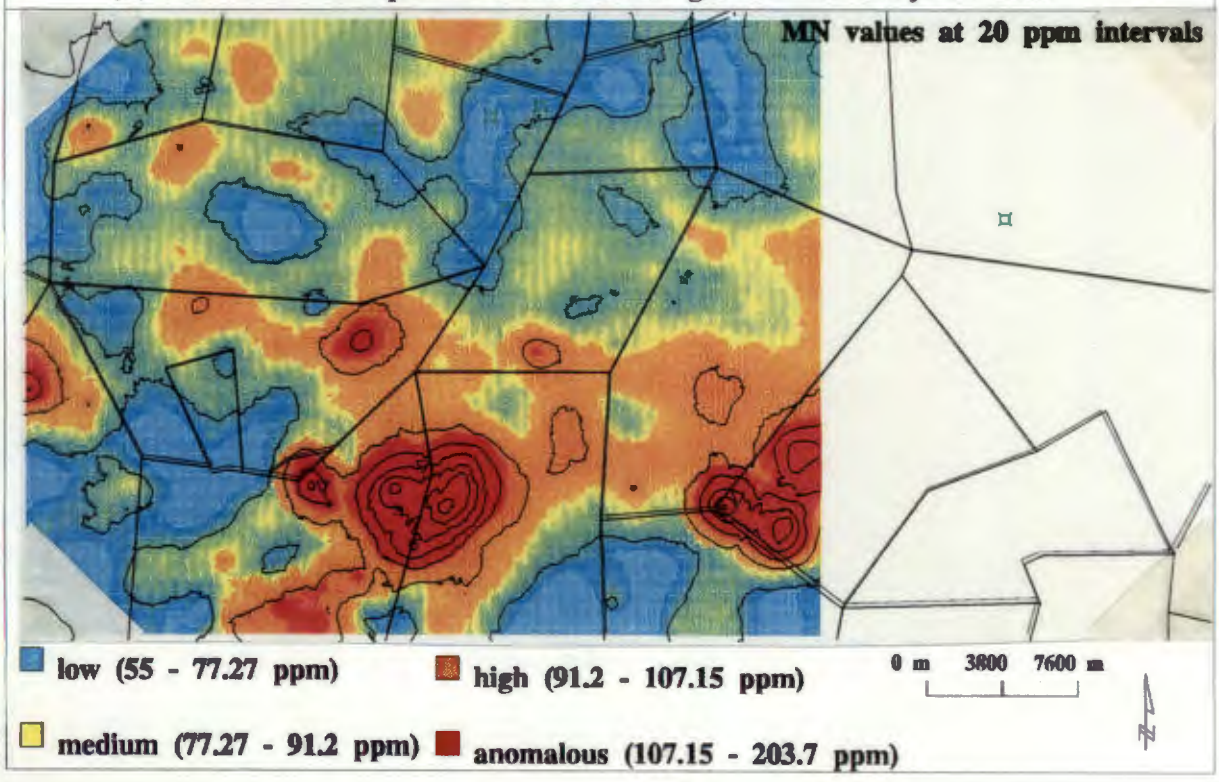

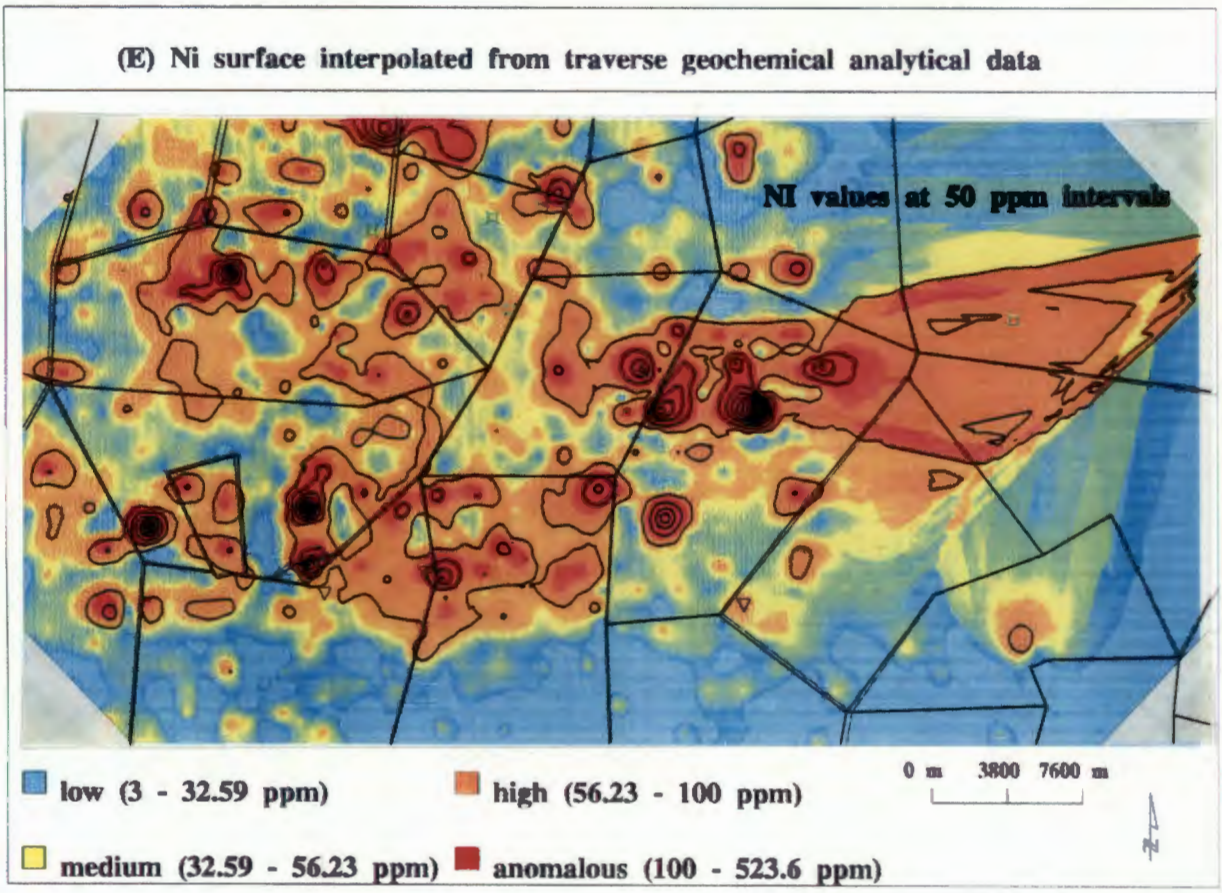

Figure 6.5 (A-E) - Displays interpolated data grids (in ppm), logarithmically transformed and linear-colour-coded, for Zn, Pb, Cu, Mn and Ni in Figures A-E, respectively. The continuous interpolated grids A to E were generated using the Kriging function. Interpolated Pb (A) and Zn (B) data values range from low (turquoise) concentrations in north to intermediate (yellow to gold) and high (red) values in the south. Areas of high Pb-Zn values correspond to the location of the four known mineral deposits in the area (marked with triangles). The values of Cu (C) and Mn (D) display slight association with the four known deposits. Ni (E) displays a more random variation over the study area.

have strong magnetic anomalies, and magnetic surveys have been used to delineate these deposits.

6.4.1. Classification

When geophysical data are rendered as images, digitized data are interpolated to assign values of a particular force field to each square cell within the grid (Drury and Walker, 1991). This is similar to interpolation using Kriging methods, described above. In magnetic data, the range of interpolated values covers negative and positive values for magnetic field intensity.

The image in Figure 2.4 represent interpolated magnetic field surface, of first vertical derivative aeromagnetic map over the four deposits in the study area, with reduction to the pole. Processed images of the total magnetic field, residual magnetic field, and first derivative of the residual images of the magnetic field, all reduced to pole, are stored in AGGED. The first derivative image was chosen for analysis since long wavelength features associated with deeply hidden magnetic source effects are removed. This isolates short wavelength features associated with shallower magnetic body sources, which, in this study are assumed to be of importance to the exploration for mineral targets.

The magnetic field intensities (Figure 2.4) were plotted using a "rainbow" range of colours; from dark blue colours, representing low magnetic intensity areas, to red and magenta representing areas with high magnetic intensities. Linear colour coding, as described for geochemical data, was also used on the geophysical datasets.

6.5. Topographic data

6.5.1. Digital Elevation Model

A digital model displaying spatial variation in surface elevation data, termed a Digital Elevation Model (DEM), was generated. Elevation data, stored as digitized contour data at 40-100m intervals, was interpolated using the Triangulated Irregular Network (TIN) data module to create this DEM (Figure 5.5; Appendix 8).

The tin data structure are based on irregularly spaced point, line, and polygon data

interpreted as mass points and breaklines. The x,y (locational) and z (elevation or attribute) values of geographical features are assembled in a discrete altitude matrix. Triangulation is used to produce a set of adjacent overlapping triangles from irregularly spaced points having x,y co-ordinate and z values.

Elevation contour data were converted to a tin surface by first converting them to a mass of points. These mass points are then used to calculate the altitude matrix and define the TIN surface. Interpolation using the Triangular Irregular Network (TIN) function within GIS best preserves the original topographic map data by retaining the geometric fidelity of this data (Burrough, 1986). DEMs provide quantitative data on elevation, slope and aspect of slope. DEMs are used to aid in 3-dimensional visualization of thematic and image data by overlaying them on perspective views of the elevation data or by illumination of the DEM from a particular angle (ie. see the Frontispiece). The DEM data was used to analyse slope and aspect of slope in Bushmanland area.

6.5.2. Slope and Aspect of elevation data

Relief shaded surface maps of the Bushmanland area were created (Figure 6.6). The Digital elevation model is a grid surface containing z-values representing surface elevation at associated x, y locations. A slope and aspect image is derived from this data by shading (illuminating) the surface using a projected light source. The location and angle of the light source mimics the position of the sun at different times during the day. A light source positioned at azimuth 160° (south east of true north), 27 meters above the surface (low on the horizon) was used to shade the surface in Figure 6.6. Areas shaded in colours white to light grey indicate areas with maximum slope at an aspect of 160°. The slope at different aspects can be examined by rotating the light source through 360°.

6.7. Integrating Grids using the Hue-Saturation-Value (HSV) Colour Model

The human eye can discriminate many more shades of colour than tones of grey. The colour space is defined by a co-ordinate system designed to allow colour to be measured and quantitatively specified (Kay, 1993). In the Red/Green/Blue colour

Digital Elevation Model (DEM) of Bushmanland surface at Aggeneys, with relief shaded from South East

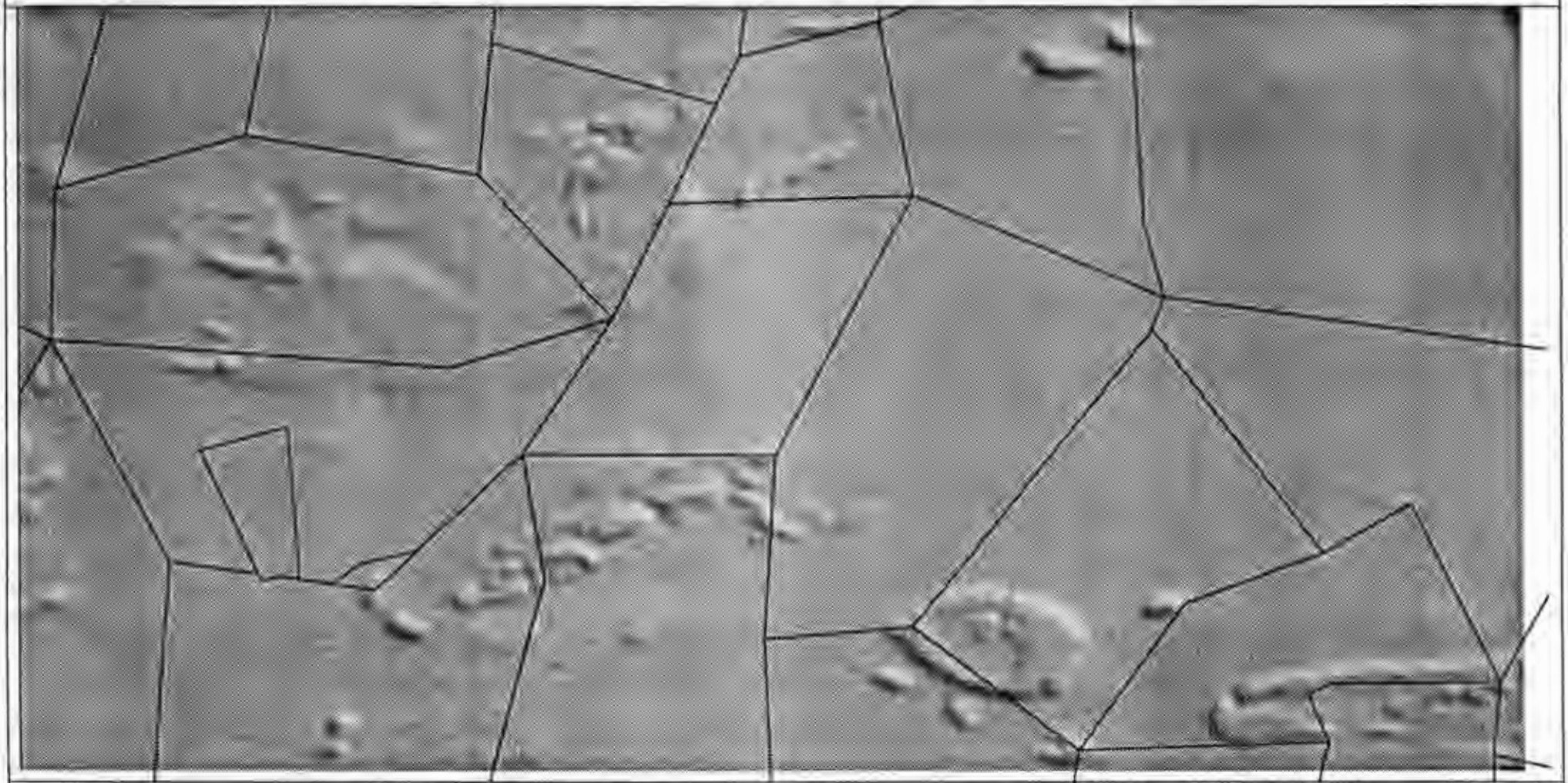

Figure 6.6 - Slope and aspect image of the study area created by shading cells of the Digital Elevation Model with a light source positioned at azimuth 160° (south east) and altitude 27°. Topography is expressed on a planar map surface, by varying shades of grey. Light grey to white highlight areas with maximum slope (8 m); and dark grey to black areas reflect areas of minimum slope (0 m). The aspect of the slope in this image is 160°. Mean slope in the area is 4 m.

Azimuth Angle of Light Source is 45 (NE)

Altitude Angle of Light Source above horizon is 30 (low on horizon)

0 m 2200 m 4400 m 6600 m

N

space varying intensities of red, green or blue result in variable colours representation by RGB values. The Hue-Saturation-Value (HSV) colour model is derived from the RGB system. Interactions of the three colour components are described by a change in hue (eg. blue, green, red), saturation (colour purity) and value (degree of brightness defined by mixture with greyscale colours ranging from black to white) (Figure 6.7). In Figure 6.7, triangles (A) to (C) illustrate the definition of hue, saturation and value respectively. Triangle (D) illustrates the colour space defined when the three components are combined.

Using the colour capabilities of the computer display monitor, three different raster (grid) datasets are combined, by assigning them to either the hue, saturation or value component of the colour model (Figure 6.7 and Appendix 8). The colours, intensity of colour, and brightness produced represent the relative intensities of the hue, saturation and value component channels, and give an indication of how they covary in the three datasets combined.

Predictable colorations for occurrence of favourable combinations, produced using the above method, aids in the recognition of patterns associated with, for example in this study, Pb-Zn mineralisation. Tanaka and Segal (1989) use a similar procedure to combine bands ratios derived from TM imagery. Their aim was to use band ratios that qualify the spectral characteristics of iron-oxide staining and clay mineralisation for gold exploration in Round Mountain Nevada, USA. Colour model transformations were used to identify the location of probable occurrence of the two alterations products (viz oxide staining and iron mineralisation), associated with gold mineralisation.

6.8. Summary

The results of geographical data (vector and raster) processing, integration and analysis are presented as hardcopy maps or tables and discussed in Chapter 7. All data derived from processing and analysis are stored in the AGGED database, together with the original data. Further analysis of the datasets can be performed, at a later date, using a wider range of GIS analytical tools available in GIS.

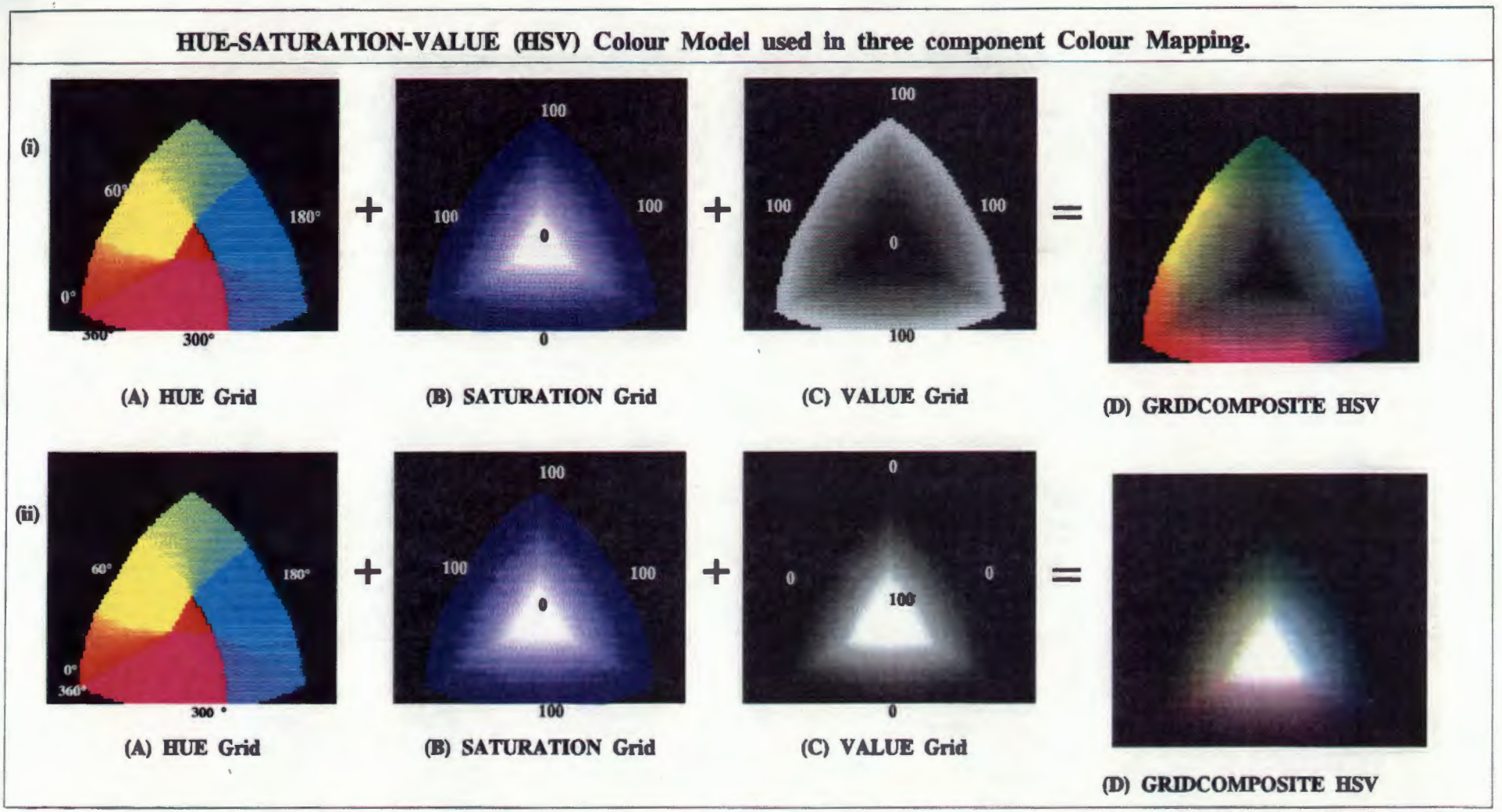

Figure 6.7 - Graphical representation of the HSV colour model. Colour variations contained in the (A) hue, (B) saturation and (C) value component grids are combined into a single (D) grid-composite. The hue component grades in a "rainbow" of colours from 0-360 degrees, with 0° representing red, 60° yellow, 180° blue and 300° magenta. Value and saturation range from 0-100 percent, with 0 representing low saturation and value, graduating to high saturation and value at 100. In series (i) changing hue is combined with increasing saturation and value component grids. In series (ii) hue is combined with increasing saturation and decreasing value component grids, respectively. In (ii) describes tonal variations produced when different. The grid-composites in series (i) and (ii) show the tonal variation produced when these component grids are integrated.

Chapter 7

Integration and Analysis in AGGED - Results

7.1. Introduction

The results of integrating the analysed data sets, are partially governed by the elaboration and reliability of previous geological models. Partially governed, because previous models may overlook important relationships describing the nature of Pb-Zn mineralisation in Bushmanland. This oversight is perpetuated if further examination of the model is entirely controlled by a particular geological model.

Reviewing some of the observations contained in Table 3.3, and experimenting with new ways of examining and integrating data in AGGED, several spatial patterns observed in the data are analysed in detail. Analysis of spatial relationships at regional scale (Figure 7.1 to Figure 7.4) and local scale (Figure 7.5) are described, in the following sections. Figures 7.2 to 7.4 are plotted at a regional and local scale.

7.2. Regional Analysis

7.2.1. Geochemical Patterning

Maps graphically display statistical distributions in the geographical landscape, and can therefore be effectively used in the analytical process to compare continuous spatial distributions. Spatial associations observed between geographical features and attributes on the spatial map, provide a summary description of spatial map patterns. In contoured maps (Figure 5.1 overlays 1 to 5 and overlays on Figures 6.5 A-E) dense concentric circles of contours, referred to as "bulls-eyes", identify areas where element values (ppm) rise abruptly, defining anomalous areas. In the linear colour coded display of interpolated surfaces (Figure 6.5 A-E) yellow to red identify anomalous areas.

Examination of spatial patterns in interpolated, classified and integrated geochemical and lithological data sets provided the following results: Pb, Zn, and Cu display distinctive spatial patterning where high concentration of these elements cluster in the south of the study area, low values elsewhere. Ni values, by contrast, are more randomly distributed over the map. Mn values contain high-low pairs that alternate

regularly over the study area.

Ore deposits Aggeneys and Gamsberg type, can be detected by stream sediment and soil geochemistry (Beeson et al., 1978). The metallogenic mineral deposits of Bushmanland have an associated characteristic geochemical signature to a greater degree for Pb and Zn, and to a lesser degree for Cu and Mn. These base metal deposits can, therefore, be detected by anomalous values of one or more of these elements in soils (Beeson et al., 1978). Thus the spatial patterning in these element datasets are described.

In the contoured geological stream sediment (Figure 5.1 overlays A-E) and kriged traverse survey analyses (Figure 6.5 A-E) the following spatial patterns and relationships in Pb, Zn, Cu and Mn data were observed. Distinct anomalies of Pb and Zn, correspond to the four known sub-surface deposits viz. Black Mountain, Big Syncline, Broken Hill and Gamsberg (marked with triangles in Figures 5.1 and 6.5 A-E). Anomalies of Mn and Cu correspond vaguely with location of known mineralisation, consistent with the geological model (Table 3.3). Interesting Pb and Zn anomalies are located on the farms Haramoep, Aggeneys and Aroams. The anomaly on Aggeneys farm is at Easy Canyon, and the anomaly on Aroams farm is between the SE tip of Aggeneysberge and Gamsberg (marked with circles in Figures 7.1 to 7.5).

Ni concentration maps (Figure 5.1 overlay 5 and Figure 6.5 e) show no obvious spatial relationship with known mineral deposits. Ni is a relatively immobile element (Reedman, 1979) and comparing Ni with Zn, Pb and Cu patterning in the maps shows the comparative mobility of the latter elements in both soil and stream sediments samples in the Aggeneys area. In the Bushmanland environment element mobility due to mechanical effects are important in geochemical exploration (Wheatley, 1978). Zinc has a higher mobility than Pb in stream sediments (Reedman, 1979; Table 5.5) and in the Aggeneys-Gamsberg area, Zn shows a significant dispersion in soils, especially downslope from the ore-bodies; but Pb and Cu do not migrate far from the source. Soil sample information is significant in areas of outcrop or shallow sub-outcrop, because the samples detect bedrock metal contents (Wheatley, 1978).
High concentrations of zinc, relative to Pb, in the sediment samples from ephemeral

streams running of the ore bodies are explained by its increased mobility. The new anomalies outlined correspond to areas of rock outcrop or sub-outcrop. In the case of the Aroams farm anomaly, lithology is not mapped on the available maps (Figure 2.2 and 2.3), but outcrop does exist and can be seen on the TM image (Figure 5.1).

7.2.2. The relationship between Lithology and Geochemistry

Assessment of spatial relationship between lithological units presented in Figure 2.3 and Pb, Zn, Cu, Mn, and Ni values in soils, are listed in Table 7.1. Lithologies including magnetite-amphibole rock, calc-silicate unit and quartz-muscovite rock show high mean values for elements Pb and Zn, in areas where these rock types occur. Amphibolites display high Pb and Zn mean values, although not as high as the above-mentioned lithologies. A definitive spatial relationship exists between the four lithologies mentioned; magnetite-amphibole rock, calc-silicate unit, quartz-muscovite rock, amphibolites, and the chemical elements Pb, Zn and Mn. This is implied since the mean element concentrations of these elements are comparatively low in the remaining lithologies. Also, the mean Ni and Cu concentrations (Table 7.1) show no marked variations associated with the eleven lithological units.

7.2.3. Three Component Colour Mapping

7.2.3.1. Integrating Pb, Zn and Cu data

The elements Pb, Zn and Cu are combined in Figure 7.1 using three component colour mapping (see method discussed in Chapter 2). The predominance of Zn (red) at Gamsberg and Pb (green) at Aggeneys (lateral zoning) is evident. Copper displays a more even graduation between the two areas. The copper data displays a distinct linear pattern to the north; where an area with a distinct rectangular shape displays very low copper values compared to the surrounding areas (Figure 6.5 C). This linearity corresponds with the extent of a topographic map sheet (2918 BB). This pattern, therefore, is probably not an artefact and probably delineates sampling or analytical error in the data. The spatial analysis of quantitative Cu data clearly delineated this false patterning.

The three map composite displays a digital integration of geochemical maps attempted by overlaying transparent geochemical maps in Figures 5.1 and 6.5 A-E. The digital

Table 7.1 - Mean, minimum and maximum concentration (in ppm) of elements Lead (Pb), Zinc (Zn), Copper (Cu), Manganese (Mn) and Nickel (Ni) in the eleven lithological zones described in Figure 2.3.

LITHOLOGY	MEAN	MIN	MAX
LEAD (Pb)			
QUARTZITE	55.837	16.073	494.087
UNDIFFERENTIATED QUARTZITE	49.808	28.389	218.560
SCHIST	54.647	16.657	469.687
UNDIFFERENTIATED SCHIST	52.757	23.392	495.671
PINK GNEISS	68.928	22.660	379.223
UNDIFF + INTRUSIVE GNEISS	38.189	13.667	391.357
AMPHIBOLITE	51.606	18.557	286.764
MAGNETITE AMPHIBOLE ROCK	126.798	28.721	512.157
CALC SILICATE UNIT	246.282	53.649	318.315
QUARTZ MUSCOVITE ROCK	191.205	42.985	531.626
QUARTZ SILLIMANITE ROCK	32.636	29.460	42.212
ZINC (Zn)			
QUARTZITE	146.888	42.892	1011.795
UNDIFFERENTIATED QUARTZITE	134.164	44.715	628.002
SCHIST	129.277	46.180	1046.084
UNDIFFERENTIATED SCHIST	127.424	53.846	972.482
PINK GNEISS	303.988	66.102	1091.601
UNDIFF + INTRUSIVE GNEISS	89.109	37.587	1128.161
AMPHIBOLITE	196.402	50.460	772.056
MAGNETITE AMPHIBOLE ROCK	275.633	48.331	938.000
CALC SILICATE UNIT	594.516	166.508	943.625
QUARTZ MUSCOVITE ROCK	273.143	100.859	998.657
QUARTZ SILLIMANITE ROCK	63.474	55.637	71.422
COPPER (Cu)			
QUARTZITE	21.674	4.176	82.974
UNDIFFERENTIATED QUARTZITE	24.654	6.056	75.920
SCHIST	19.946	4.229	82.639
UNDIFFERENTIATED SCHIST	19.171	5.312	80.471
PINK GNEISS	16.590	4.108	41.956
UNDIFF + INTRUSIVE GNEISS	19.722	4.591	84.164
AMPHIBOLITE	16.543	6.048	35.372
MAGNETITE AMPHIBOLE ROCK	19.000	6.516	80.319
CALC SILICATE UNIT	15.407	6.616	19.402
QUARTZ MUSCOVITE ROCK	27.249	6.067	61.348
QUARTZ SILLIMANITE ROCK	15.954	14.632	19.734
MANGANESE (Mn)			
QUARTZITE	84.143	56.625	177.325
UNDIFFERENTIATED QUARTZITE	79.600	62.689	141.438
SCHIST	81.753	57.270	176.694
UNDIFFERENTIATED SCHIST	79.762	62.592	166.928
PINK GNEISS	93.437	69.819	174.985
UNDIFF + INTRUSIVE GNEISS	79.811	56.522	171.133
AMPHIBOLITE	99.525	61.743	166.523
MAGNETITE AMPHIBOLE ROCK	104.662	63.512	176.916
CALC SILICATE UNIT	138.720	83.032	159.141
QUARTZ MUSCOVITE ROCK	110.962	79.037	171.235
QUARTZ SILLIMANITE ROCK	63.595	60.745	75.404
NICKEL (Ni)			
QUARTZITE	39.293	4.610	293.067
UNDIFFERENTIATED QUARTZITE	34.582	11.289	296.585
SCHIST	45.041	3.266	217.091
UNDIFFERENTIATED SCHIST	43.792	8.609	165.588
PINK GNEISS	42.513	15.003	104.896
UNDIFF + INTRUSIVE GNEISS	43.712	9.601	303.314
AMPHIBOLITE	43.785	21.377	87.426
MAGNETITE AMPHIBOLE ROCK	44.355	8.569	187.551
QUARTZ MUSCOVITE ROCK	101.654	55.591	185.299
QUARTZ SILLIMANITE ROCK	70.144	26.225	279.869
QUARTZ SILLIMANITE ROCK	57.977	25.602	117.141

Three Component Colour Map integrating Zn, Cu and Pb data grids, Using the HSV colour model

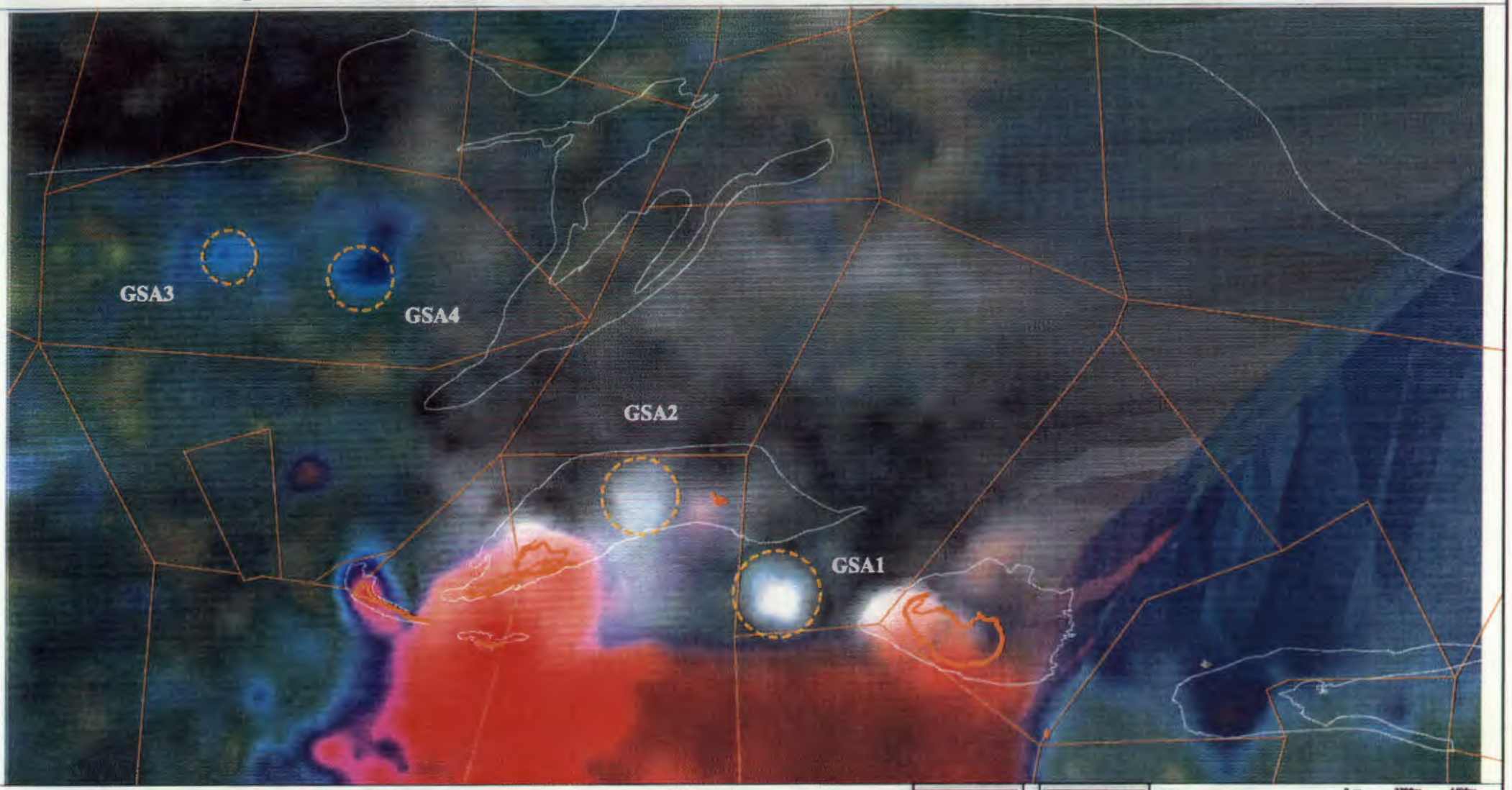

Figure 7.1 - Zinc, lead and copper data interpolated using kriging are combined. Consistent low copper (low value component) occurs to the north. Clear high Pb and Zn zonation around the four known deposits are visible. The green, red, blue and white triangles mark the location of deposits, respectively.

integration represents a more manageable way of integrating these data sets. Because the geochemical data does not have to be generalised using contouring, the additional information content is also beneficial.

7.2.3.2. Integrating Geochemical and Magnetic data

Magnetic data in Hue component is combined with Pb and Zn in the value and saturation component (Figure 7.2). Elements Pb and Zn are analysed because they clearly delineate the four existing deposits. Increasing values of Pb and Zn (bright areas reflecting high saturation and value) correspond spatially with patterns of magnetic highs (coloured magenta). Anomalies delineated by integrating different geo-scientific data are referred to as "Geoscience" Anomalies (GSA1 to GSA4; Figures 7.1 to 7.5) .

The areas around the four deposits are effectively delineated. Two new "geoscience" anomalies are visible in the south of the study area, GSA1 between Easy Canyon and Gamsberg, on the farm Aroams and GSA2 at Easy Canyon in the Aggeneysberge, Aggeneys Farm. In the north, on the farm Haramoep, anomalous lead and zinc patterns also occur (Figure 7.2, anomaly GSA3 and GSA4), but are not as pronounced as the Pb-Zn patterns in the south.

The structural overprint in the Aggeneys area is discernable from the magnetic data, and thus magnetics are useful for tracing features, discernable in outcrop, under sand cover (Stevenson, 1985). Magnetic highs (magenta; Figure 7.2) display an E-W trend, corresponding to axial traces of F2 and F3 folds (Figure 2.4 overlay). These fold patterns are extrapolated along the magnetic signature, under sand cover where structural information does not exist. Structural extrapolation from known structural traces, is attempted at a smaller scale 1:1130, and shown in Figure 7.5.

Geochemical anomalies correspond with fold patterns of magnetic highs. The magnetic data used in this composite was subjected to Upward Continuation (UC, Stevenson, 1983). The upward continuation process in geophysics simulates the effects on magnetic data if the survey was flown at a higher altitude. Stevenson (1983) found that 200m upward continuation removed or reduced surficial anomalies caused by, for

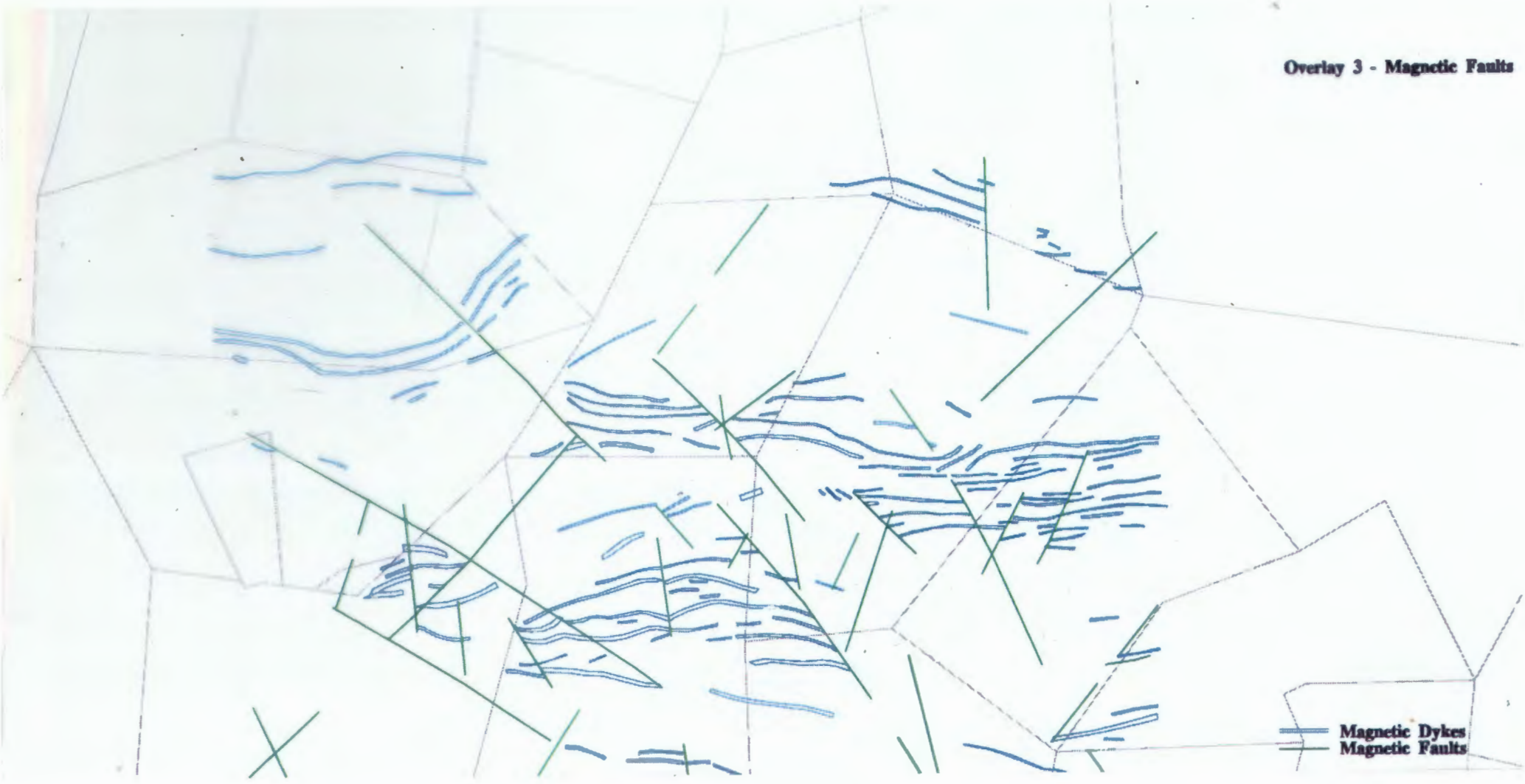
Overlay 3 - Magnetic Faults
Magnetic Dykes
Magnetic Faults

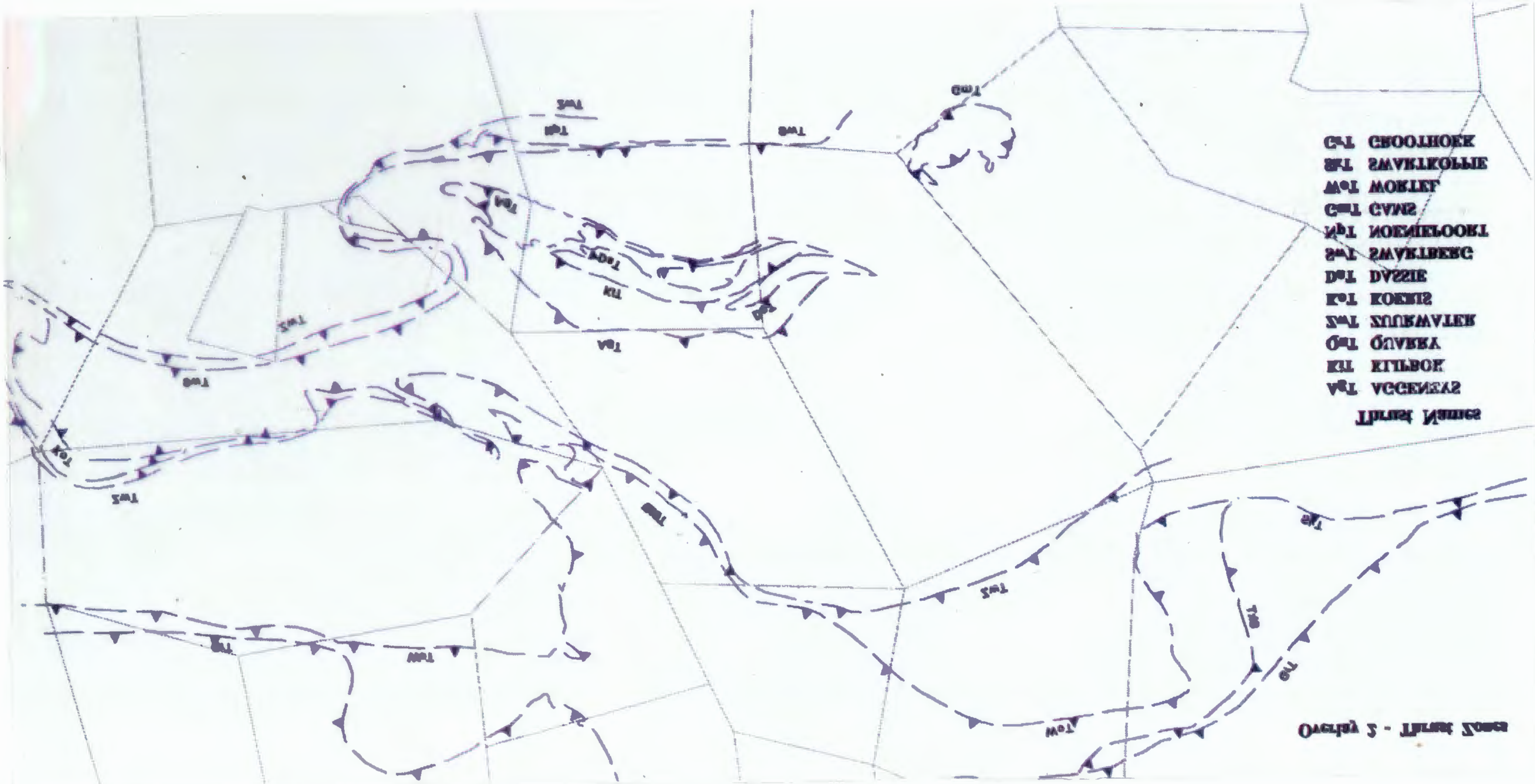
Overlay 2 - Thrust Zones
Thrust Names
GrT GROOTHOEK
SkT SWARTKOPPIE
WoT WORTEL
GmT GAMS
NpT NOENIEPOORT
SwT SWARTBERG
DaT DASSIE
KoT KORRIS
ZwT ZUURWATER
QuT QUARRY
KlT KLIPBOK
AgT AGGENEYS

Overlay 1 - Foid Axial Trace
Synform
F1 Axial Trace
F2 Axial Trace
F3 Axial Trace
Antiform
F1 Axial Trace
F2 Axial Trace
F3 Axial Trace
Shear Zone
Thrust Faults

Three Component Colour Map integrating Magnetics (1st derivative), Zn and Pb data grids

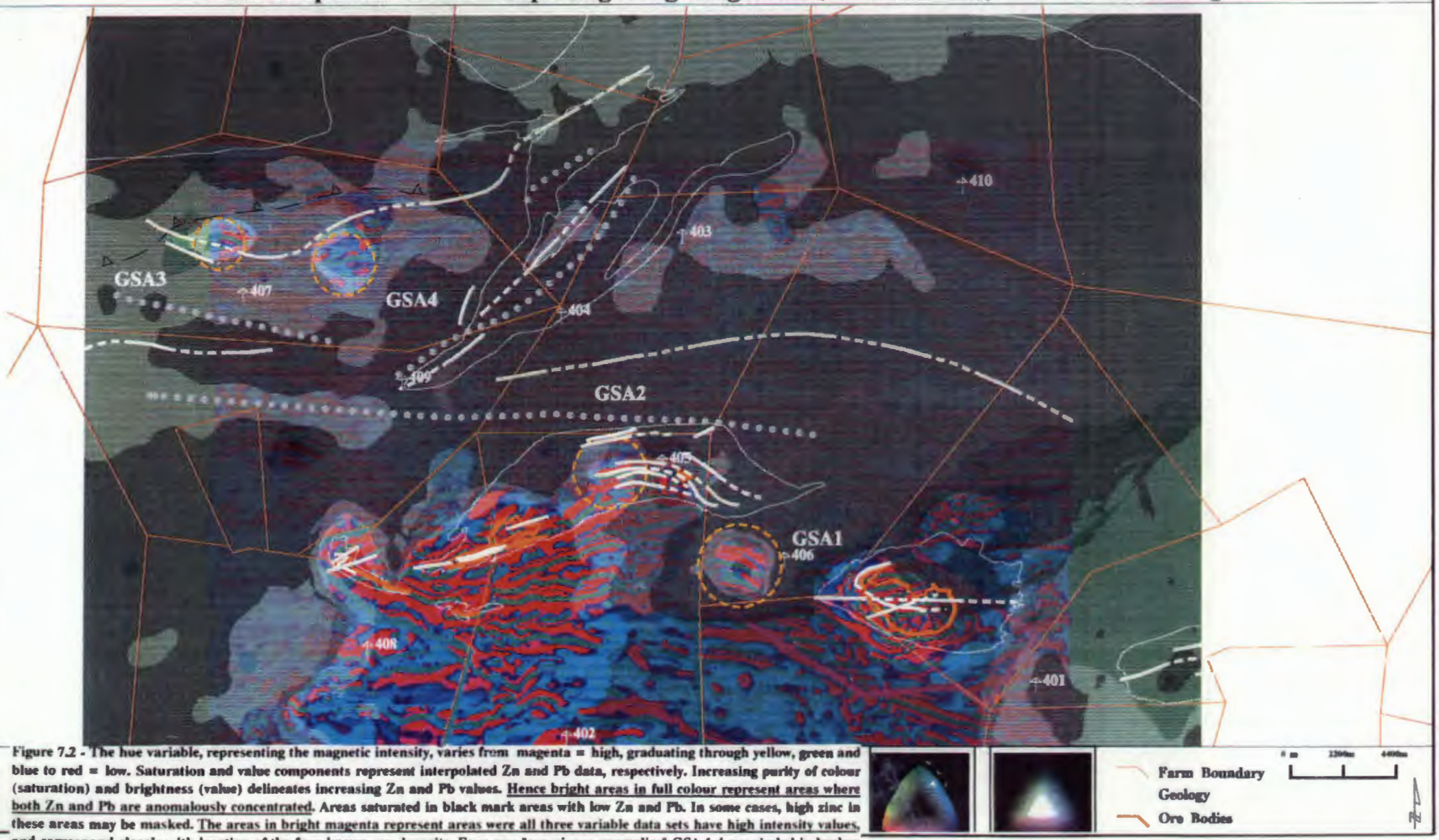

Figure 7.2 - The hue variable, representing the magnetic intensity, varies from magenta = high, graduating through yellow, green and blue to red = low. Saturation and value components represent interpolated Zn and Pb data, respectively. Increasing purity of colour (saturation) and brightness (value) delineates increasing Zn and Pb values. Hence bright areas in full colour represent areas where both Zn and Pb are anomalously concentrated. Areas saturated in black mark areas with low Zn and Pb. In some cases, high zinc in these areas may be masked. The areas in bright magenta represent areas were all three variable data sets have high intensity values, and correspond closely with location of the four known ore-deposits. Four new "geoscience anomalies" GSA 1-4 are circled in broken orange, fold-axial traces = white.

Three Component Colour Map integrating Magnetics (1st derivative), Zn and Pb data grids

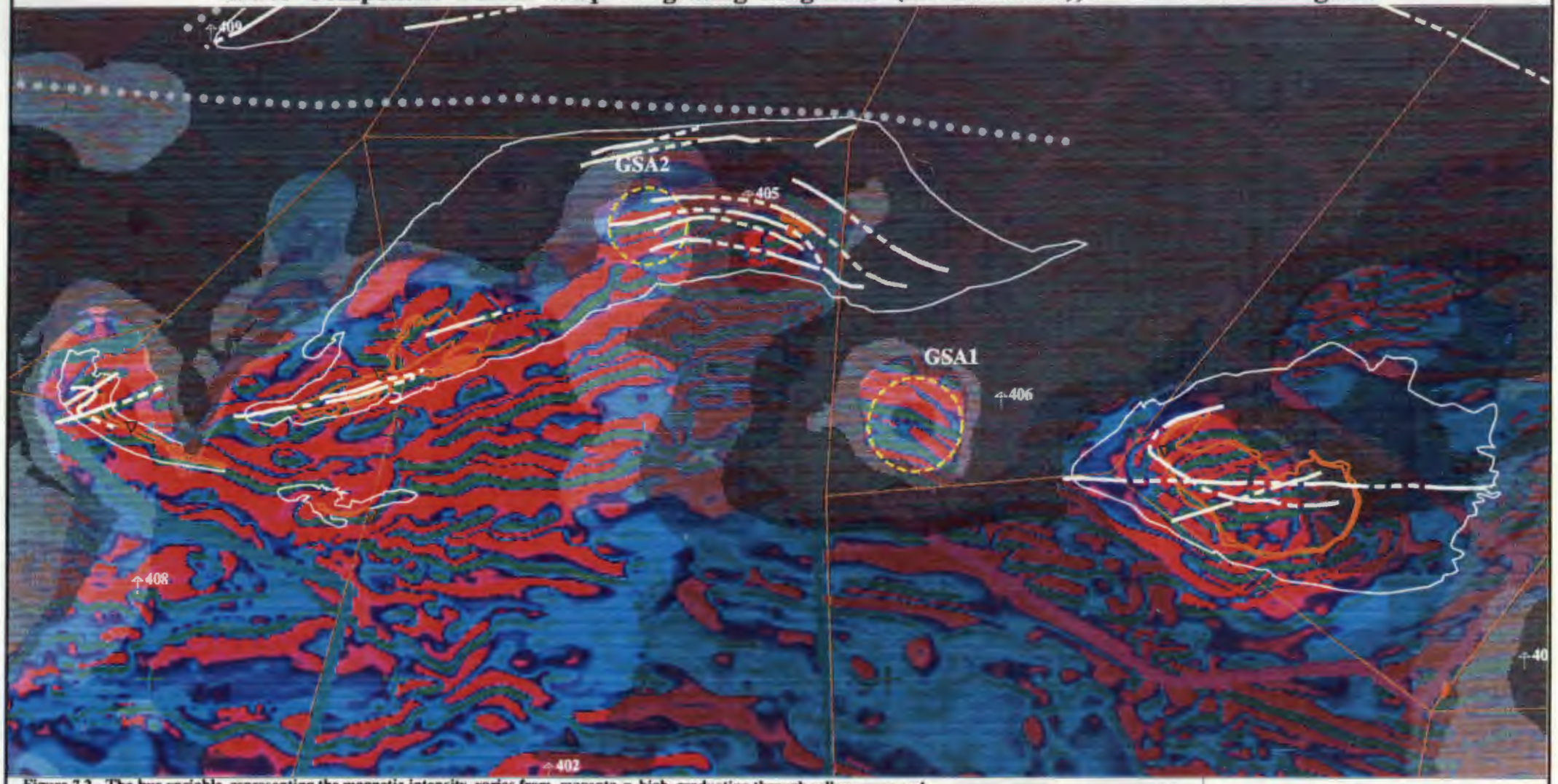

Figure 7.2 - The hue variable, representing the magnetic intensity, varies from magenta = high, graduating through yellow, green and blue to red = low. Saturation and value components represent interpolated Zn and Pb data, respectively. Increasing purity of colour (saturation) and brightness (value) delineates increasing Zn and Pb values. Hence bright areas in full colour represent areas where both Zn and Pb are anomalously concentrated. Areas saturated in black mark areas with low Zn and Pb. In some cases, high zinc in these areas may be masked. The areas in bright magenta represent areas were all three variable data sets have high intensity values, and correspond closely with location of the four known ore-deposits. Four new "geoscience anomalies" GSA 1-4 are circled in broken, orange, fold-axial traces = white.

example, magnetite in sand dunes. Processing of the data using the above method delineated 10 significant Upward Continued (UC) anomalies (Stevenson, 1983; 401 to 410 in Figure 7.2). The deposits at Gamsberg, Broken Hill, Big Syncline and Black Mountain were not considered although their magnetic signatures are clearly visible (Stevenson, 1983).

"Geoscience" anomaly (GSA1) on the Aroams farm is associated with UC anomaly 406 and magnetic anomaly 59. Stevenson describes anomaly UC 406 as being fault bounded on the eastern and western sides. Anomaly UC5 is associated with a "geo-science" anomaly occurring on the farm Aggeneys (GSA 2). This anomaly occurs on the strike extension of magnetic anomalies enclosing the Big Syncline deposit. Both these anomalies are contained in an area with strong mineralisation. If surface expression of mineralisation in this area is rich, the potential for subsurface mineralisation in this area needs to be examined further.

"Geoscience" anomalies GSA3 and GSA4 on farm Haramoep are associated with UC anomaly 7. The latter anomaly is remnantly magnetised, with probable strike extent of up to 9 km (Stevenson, 1983). The strike length "downgrades" this anomaly, making it less significant than anomalies GSA1 and GSA2.

7.2.3.3. Integrating Geochemical and Geological data

Band 7 of the TM image in the hue component is combined with lead and zinc in the saturation and value component, respectively (Figure 7.3). TM band 7 coincides with an absorption band caused by hydroxyl ions in minerals (Sabins, 1978 pp. 86); and absorption caused by alunite and clay minerals results in low reflectance in band 7. Areas to the north display high lead and zinc values, corresponding with red in the hue variable. This represents areas where hydroxyl ions concentrated on the surface, and do not correspond to alteration zones associated with mineralisation. These areas include scree slopes; slimes dumps (red square area in Figure 7.3); roads on which ore trucks have travelled and shed some of their cargo; in short, areas with a high concentration of clay minerals at surface. The ore lithologies (orange lines) are overlain on this image, and no correspondence exists between the ore-lithologies and red hue.

Three Component Colour Map integrating TM (Band 7), Zn and Pb data, Using the HSV Colour Model

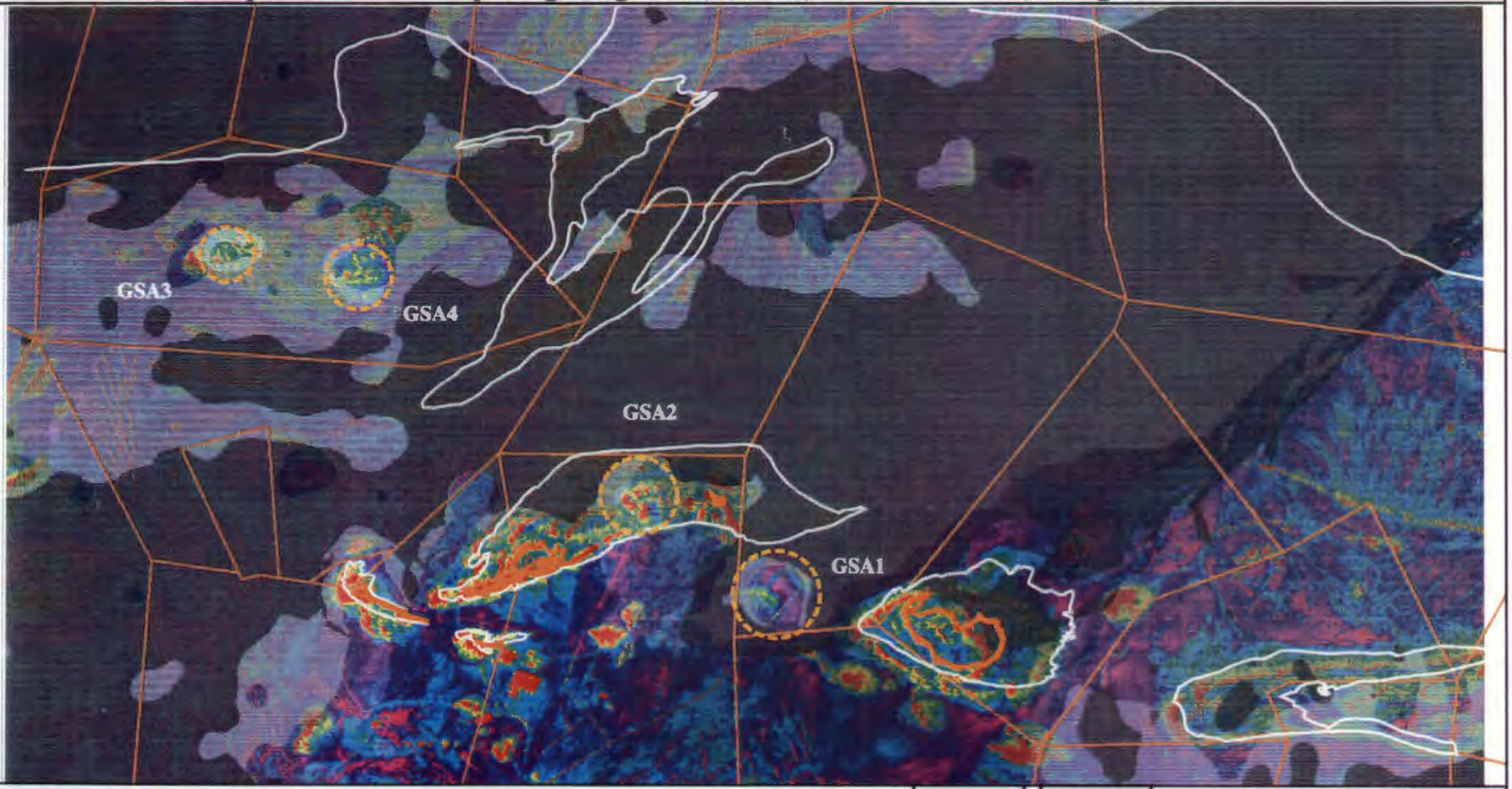

Figure 7.3 - The hue component delineates electromagnetic wavelength features captured in band 7 of TM image. Saturation and value variables represent interpolated Zn and Pb data, respectively. Areas in magenta have a high reflectance in TM band 7 and colour red low reflection. Areas defined by bright, saturated colours display anomalous Pb and Zn values. Red (low reflectance in band 7) highlights areas with high hydroxyl ion content, for example, clay minerals. Geoscience anomalies are circled and marked GSA 1 to 4.

Three Component Colour Map integrating TM (Band 7), Zn and Pb data, Using the HSV Colou

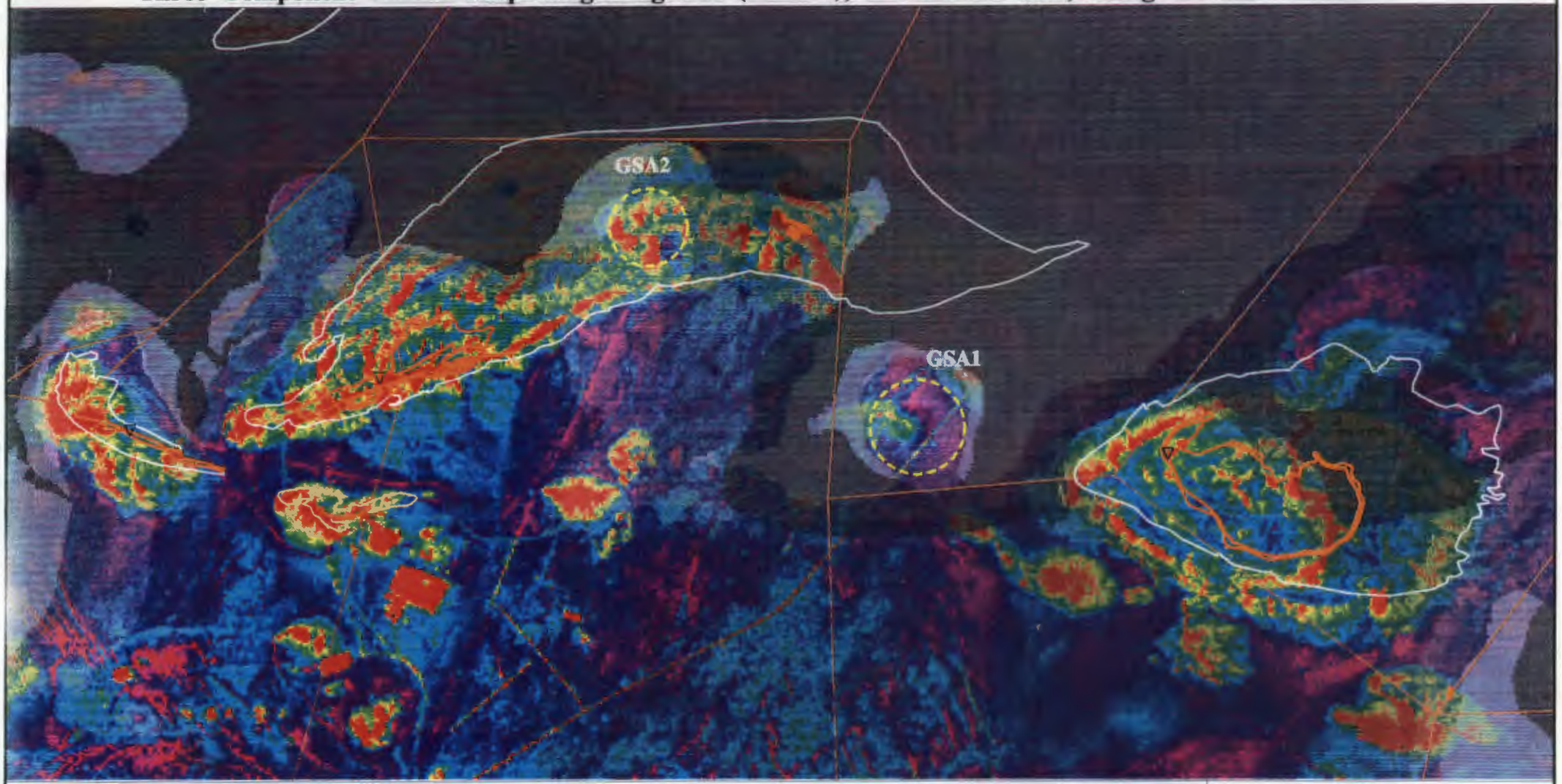

Figure 7.3 - The hue component delineates electromagnetic wavelength features captured in band 7 of TM image. Saturation and value variables represent interpolated Zn and Pb data, respectively. Areas in magenta have a high reflectance in TM band 7 and colour red low reflection. Areas defined by bright, saturated colours display anomalous Pb and Zn values. Red (low reflectance in band 7) highlights areas with high hydroxyl ion content, for example, clay minerals. Geoscience anomalies are circled and marked GSA 1 to 4.

Although "geoscience" anomalies GSA3 and GSA4, on the farm Haramoep are not as distinctive as GSA1 and GSA2 (Figure 7.3), overlaying the fold axial traces on this image shows a correlation of the Haramoep anomalies with an F2 and F3 fold structure. This makes them worthy of further investigation. The axial trace overlay also shows correspondence between the four known deposits and F2 and F3 structures, as would be expected from the geological model outlined in Table 3.3.

7.2.3.4 Integrating Geochemistry, Magnetics and Geology

Figure 7.4 combines three sets of data: magnetics (first derivative) in the hue component; lithology (TM band 7) in the saturation component; and combined lead and zinc data in value component. This image integrating a variable from each sub-discipline, highlights all the patterns described above. This image is studied more closely at a local scale of 1:1130, discussed below.

7.3. Local Analysis

The distinct patterns associated with the four known deposits and the new clear "geoscience" anomalies located on the farm Aroams and Aggeneys, stimulated a more focused analysis of this area (Figure 7.5).

7.3.1. Integrating Geology, Geophysics and Geochemistry

The image of lithology in the hue component is combined with magnetics in saturation, and with combined lead zinc data in the value component (Figure 7.5). Interpreting structural trends using magnetic information delineates a large open syncline (F3) which can be easily traced from the core of Black Mountain anomaly through the Big Syncline anomaly to join-up with the Gamsberg deposit, as previously recognised by Stevenson (1985).

Stevenson (1985) recognised three broad zones of magnetic characteristics associated with lithology.

Type (i)

areas of low magnetic magnitude associated with rocks of:

Basal Augen Gneiss

Haramoep Gneiss

Namies Schist

Three Component Colour Map integrating TM (Band 7), Magnetics (1st derivative) and combined Pb/Zn data grids

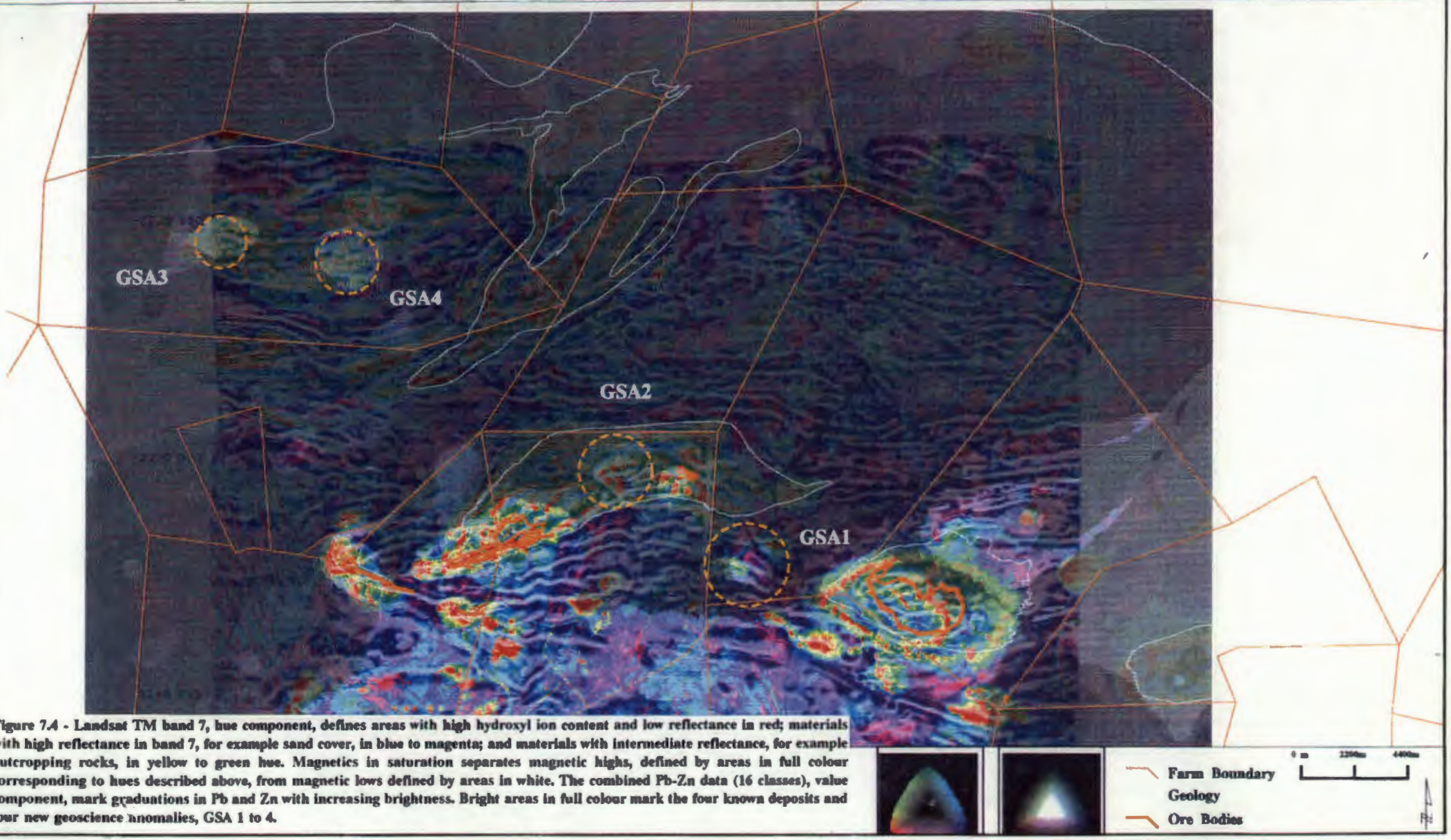

Figure 7.4 - Landsat TM band 7, hue component, defines areas with high hydroxyl ion content and low reflectance in red; materials with high reflectance in band 7, for example sand cover, in blue to magenta; and materials with intermediate reflectance, for example outcropping rocks, in yellow to green hue. Magnetics in saturation separates magnetic highs, defined by areas in full colour corresponding to hues described above, from magnetic lows defined by areas in white. The combined Pb-Zn data (16 classes), value component, mark graduations in Pb and Zn with increasing brightness. Bright areas in full colour mark the four known deposits and four new geoscience anomalies, GSA 1 to 4.

Three Component Colour Map integrating TM (Band 7), Magnetics (1st derivative) and combined Pb/Zn data grids

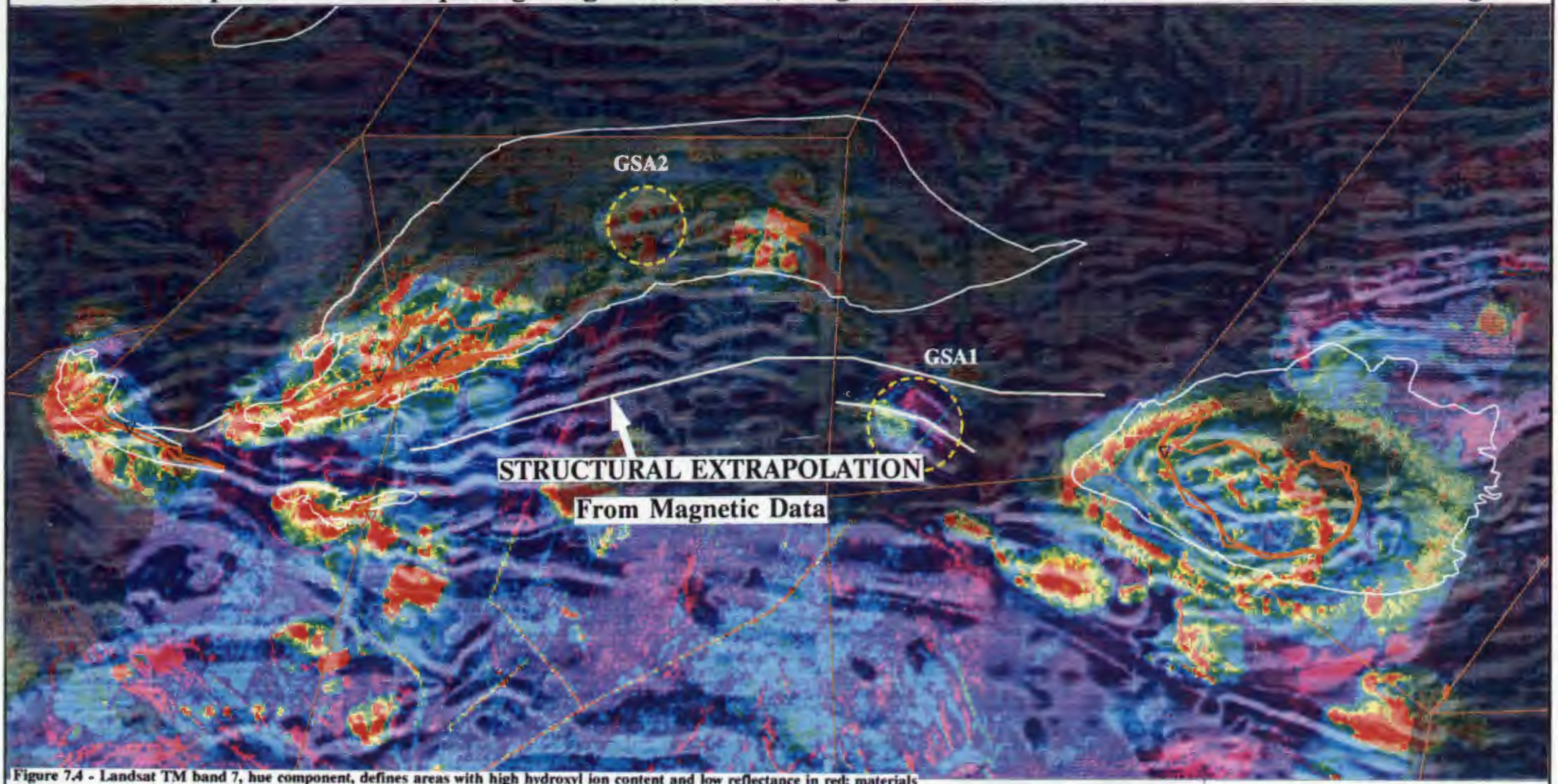

Figure 7.4 - Landsat TM band 7, hue component, defines areas with high hydroxyl ion content and low reflectance in red; materials with high reflectance in band 7, for example sand cover, in blue to magenta; and materials with intermediate reflectance, for example outcropping rocks, in yellow to green hue. Magnetics in saturation separates magnetic highs, defined by areas in full colour corresponding to hues described above, from magnetic lows defined by areas in white. The combined Pb-Zn data (16 classes), value component, mark graduations in Pb and Zn with increasing brightness. Bright areas in full colour mark the four known deposits and four new geoscience anomalies, GSA 1 to 4.

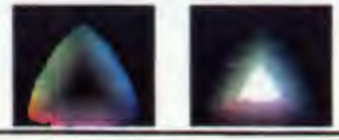

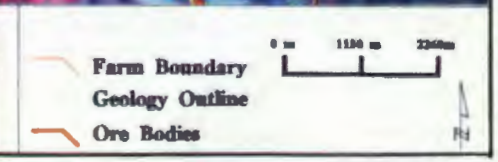

Three Component Colour Map integrating Lithology, Magnetics (1st derivative) and combined Zn and Pb data grids

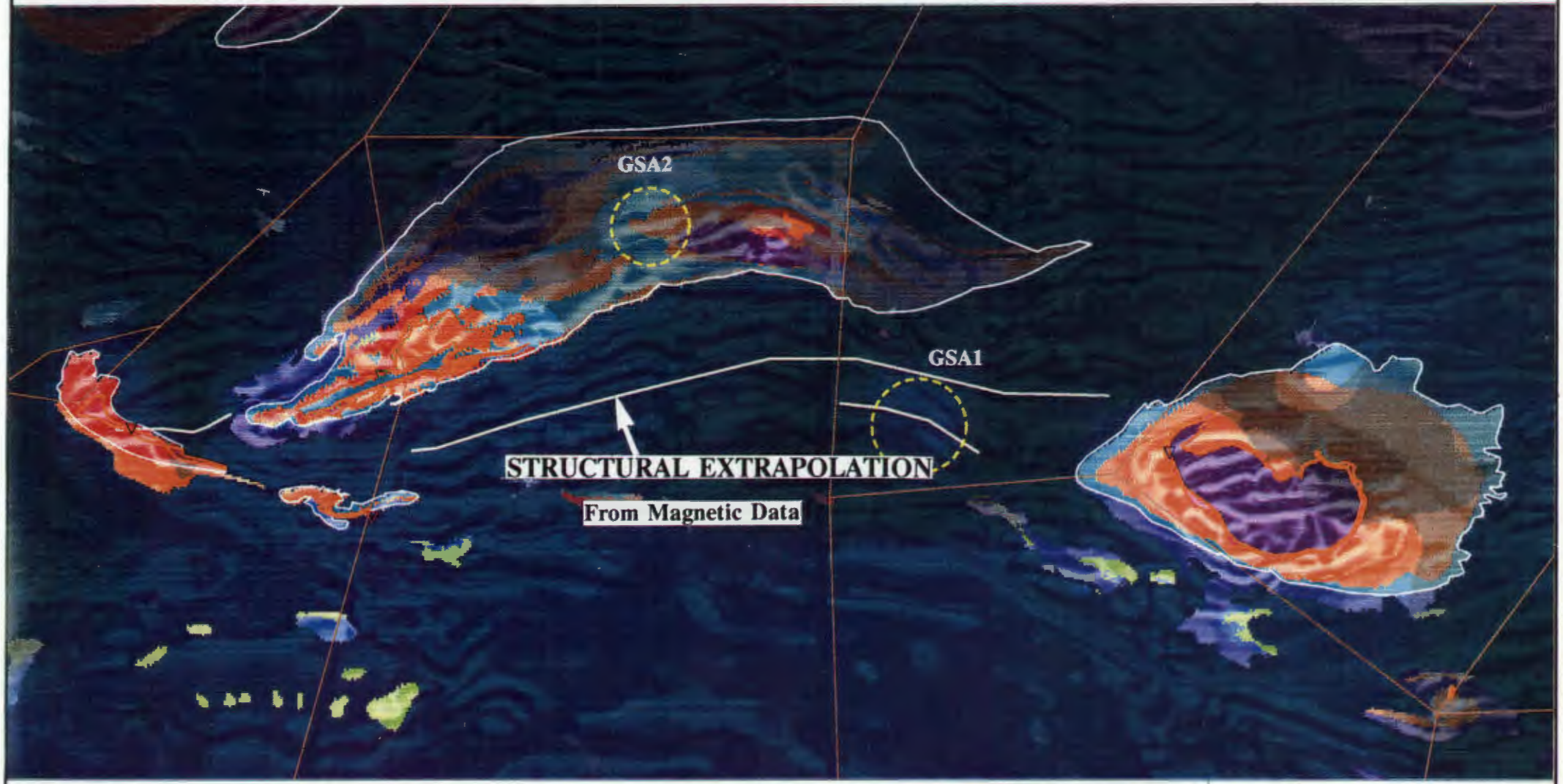

Figure 7.5 - Lithological map Figure 2.3, in hue component shows quarzites in orange, pink gneiss in purple, schist in sea green and quartz muscovite rock in red. Magnetics in saturation component marks magnetic highs in full colour and magnetic lows in white. The combined Pb-Zn data (16 classes) in value component, show graduations in Pb and Zn with increasing brightness. GSA1 does not show up well in this composite because no lithology is mapped in this area and therefore hue is very dark, masking the value component.

Pella Quartzite Formations

Stevenson inferred that this was because these rocks contain little or no magnetite

Type (ii)

moderate magnitude magnetic anomalies attributable to rocks of the

Nousees Mafic Gneiss

Thin bands of amphibolite within this formation are responsible for its distinct magnetic signature

Type (iii)

Very high magnitude magnetic anomalies correspond to the Gams Iron Formation; where the ore bodies are associated with magnetite rich rocks commonly well-preserved in the hinge zone of major folds.

Tracing the high magnitude magnetic anomalies directly from Big Syncline through to Gamsberg, the "geo-science" anomaly on the farm Aroams is traversed. This magnetic trace pattern appears to correspond to the F2 axial trace in the area (Figure 2.4). The area between Gamsberg and Aggeneysberge has not yet been structurally investigated, mainly because of lack of outcrop. The recognition of this probable continuation of an F2 axial trace in this area using the magnetic data, together with the known association on of F2 folds with mineralisation, is thought to be significant.

7.4. Discussion and Conclusions

The geological, geochemical and geophysical datasets can be successfully integrated using quantitative colour analysis. Lithological and structural descriptive data are stored in the spatial database as vector maps. Overlaying vector data sets on grid-composites of up to three data sets promoted information integration and analysis immensely. The ease of data manipulation and analysis in AGGED, and the results of analysis, is limited by the analytical (computational) tools available and the understanding of the principles inherent in the tools.

Data combination and modelling within GIS is versatile. Images processed in an image processing system were combined readily with other data types, viz. vector line or point data. Gridded data was processed from geochemical (point) and geological (line) datsets, resolving them to the same data structure as the geophysical data sets.

Quantitative compositing of spatially gridded geological, geochemical and geophysical datasets using colour representations, helped delineate four new "geoscience" Anomalies. These anomalies are summarised in Chapter 8.

Chapter 8

Summary and Conclusions

8.1. Digital Integration

Spatial integration and geological analysis focused on an area 60 by 30 km in extent. This area is characterised by four major known Pb-Zn deposits. By examining mineralisation patterns coincident with the four known mineral deposits, and comparing them with patterns visible in other areas, new areas with signatures comparable to the known mineralisation were delineated. The methodology employed is to examine all possible spatial combinations of the data in the AGGED database, using three component colour mapping. This constitutes a digital synthesis of previous manual integration of data in the area.

Digital integration and visual examination of data sets in AGGED clearly delineates significant correlations in some geographical areas (Figure 7.1 to 7.5). These new targets areas were recognised from re-examination and combination of geoscience exploration datasets, hence the term "geoscience" anomalies, available over the area. The graphical display of the data delineates these correlations unambiguously (Figures 7.1 to 7.5). However, in previous regional statistics performed on the data, these correlations were masked, and the circled areas (Figures 7.1 to 7.5) were thus overlooked as possible exploration targets. Bolivar (1983) describes similar results, where both obvious and subtle features and correlations were delineated from graphical integration of datasets stored in a spatial database. The more subtle features were probably also masked in previous manual data integration. A similar methodology, comparing the results of manual and digital exploration data integration, is described by Pratt (1983) in the Rollo Quadrangle, Missouri. United States.

All the data stored in the AGGED database were collected and evaluated during the past two decades of exploration in the Bushmanland area. The results of this study, therefore, testify to the effectiveness of spatial data analysis and integration, applied to large multidisciplinary data sets. It has been shown in this study that, in GIS the information potential of the data stored in AGGED can be more efficiently, and effectively extracted using statistical interpolation methods such as Kriging. The

information in the data sets was graphically displayed using 255 different tonal variation on a colour monitor. Up to three variable spatial data sets were spatially integrated using three component colour mapping, combining intensity, hue and saturation components of the red/green/blue (RGB) colour co-ordinate space. This approach delineated four areas, excluding the four known mineral deposits in the area, that may be targeted for future exploration.

8.2. Newly Identified Target Areas

"Geoscience" Anomalies 3 and 4, marked in the areas to the north of the study area (Figure 7.4) display a moderate intensity geochemical anomaly for Pb and Zn, and a moderate correlation between geoscience datasets. "Geoscience" Anomalies 1 and 2, located in the vicinity of the four known Pb-Zn deposits, in the south of the study area, display anomalous concentrations of Pb and Zn, which coincide with sub-surface magnetised lithologies.

The two southern anomalies were examined at a smaller scale, centred around the Aggeneysberge-Gamsberg area. The most intense anomalies are situated between the south eastern tip of Aggenysberge and Gamsberg, on the farm Aroams (Figure 7.5). The second anomaly occurs on the farm Aggeneys, and is of intermediate intensity between the anomaly on farm Aroams and the two anomalies to the north. Thus, in measure of intensity the "geoscience" anomalies would grade as follows:
"Geoscience" Anomaly 1 - on the farm Aroams, is the most intense anomaly. This anomaly was not recognised previously.
"Geoscience" Anomaly 2 - on the farm Aggeneys, has an intense signature and has been recognised before.
"Geoscience" Anomalies 3 and 4 - on the farm Haramoep occur in the northern part of study area. Association of these anomalies with F2, F3 fold structure mapped in the area is interesting. Associated intensity of geochemical anomalies in Pb and Zn are moderate compared with previously mentioned anomalies.

The stratiform base metal deposits in Bushmanland are stratabound and believed to be syngenetic. The sedimentary sequence containing the deposits subsequently experienced complex polyphase deformation and metamorphism. The sedimentary

sequence deposited in Bushmanland has, in places, been infolded into the basal augen gneisses and the mineralised formations are often preserved in the cores of F2 folds (Table 3.3). Hence the structure in the vicinity of the four known deposits was extrapolated from mapped axial planes through magnetised lithologies in the area, through the two delineated anomalies. This is presented in Figure 7.5 as overlay 1. It appears entirely feasible that the two anomalies GSA 1 and GSA2, identified in this study, could contain similar structurally controlled mineralisation known to exist in nearby deposits. The two anomalies on the farms Aggeneys and Aroams therefore warrant further investigation.

Digital synthesis of the data has probably exhausted delineation of ore-bodies using sub-surface exploration data. Exploration for deep seated ore bodies require alternative surveying practises eg. rock chip sampling as opposed to surface sediment sampling, as well as processing and downward continuation modelling of geophysical images, to enhance deeper seated magnetic bodies.

8.3. Concluding Remarks

8.3.1. Fractal Analysis in the further study of the distribution of ore Deposits in Bushmanland

Our present pace of discovery of mineral accumulation in the earths crust do not necessarily indicate that we are about to converge upon the spot where all the minerals lie buried. The process of discovery could continue indefinitely. This is either because the complexity of nature is truly bottomless or because we have chosen a particular way of describing nature which, while being as accurate as we desire, is none the less at best always but an asymptotic approximation to which an infinite number of refinements can be made to fit reality exactly (Barrow, 1991).

Fractal analysis has gained wide usage in the earth sciences. Turcotte (1991) suggests that fractals can bridge the gap between geostatistics and physical and chemical modelling of geological processes. The paragraph composed above is adapted from a quotation in John D. Barrow's book 'Theories of everything". The theory expounded above is very relevant to spatial distribution and discovery of minerals. We have currently chosen to describe the reality of nature in a particularly modular framework.

The data models used in GIS describe reality to a particular level of completeness Peuguet (1984), which Barrow notes is but "as accurate as we desire... and an asymptotic approximation". The models used by geologists and explorationist use similar "approximations". The theory of fractal analysis examines this theory of describing the "infinite number of refinement" that could possibly represent reality of nature more accurately.

Combining fractal analysis, spatial analysis and geology, the geological controls and spatial distribution of ore deposits in the Bushmanland sequence can be geostatistically examined. The scale invariance in fractals used in conjunction with the theory of chaos (exponential divergence from initial conditions) could facilitate such examinations. Carlson (1991) describes the apparent fractal characteristics of geologic controls on the location of hydrothermal deposits of precious metals in the Basin and Range, Western United States.

A similar type of examination in the Bushmanland area will probably provide an interesting new way of modelling and predicting geological controls on stratiform Pb-Zn mineralisation. The spatial distribution of the four deposits and two new targets delineated, all fall within 23 Km of each other. B.B. Mandelbrot (1962, 1983), the founder of fractal analysis, proposed that ore deposits are clustered at many different scales and that fractal distributions are appropriate for their study.

Clustering of ore deposits is significant at all scales between 1 and 1000 km, which reflects geologically significant controls on mineralization acting at all of these scales (Carlson, 1991, pp. 114). Geologic controls together with clustering on the scale of metallogenic provinces, tectono-stratigraphic terranes, or major zones of crustal weakness are credible, and should be investigated (Turcotte, 1991). The deposits in the Aggeneys area, provide a suitable test-case for such an investigation.

8.3.2. Limiting factors of GIS and proposed future developments

One of the glaring disadvantages of GIS, is that data must be converted to a specific unique format of the GIS system. Further, they are converted before all possible applications are known. In most cases, data conversion is a tedious time and labour

intensive exercise. The formats imposed by different software packages are also constraining. More recently, however, data conversion utilities within GIS systems do allow data exchange between selected supported system formats; but this is not yet universally done.

Most recently developed or updated GIS packages support both raster a vector data structures. However, software packages allowing full integration of raster and vector data processing, without the need for conversion to a common structure (either raster or vector), are not yet available. Development of a fully integrated GIS should, should be seamless in maintaining both raster and vector representations of field data. That means, it should allow simultaneous spatial query and analysis of raster and vector data, rather than restructuring (Maguire and Dangermond, 1991). This would promote statistical and deterministic modelling of earth processes in GIS (Ehlers et al., 1989).

Eventually users of spatial information systems, should be able to devote all of their time to analysing their data utilising a range of commercially available GIS software packages. They should not be unduly burdened with manipulating their data sets to get them into some prescribed format. This can be accomplished, firstly by providing transparent access to a diverse range of spatial data sets, via mechanisms such as a live link. Shepard (1991) describes the live link mechanism, which will enable items of information in separate application programs to be interconnected, without exporting them out of the "native" system. Secondly, GIS should allow processing of this separate data as if they where native to the GIS system (Piwowar et al., 1990).

The current data analytical capabilities of GIS are limited, particularly in the spatial analytical and three dimensional modelling domains. The time, expense and effort required to create a GIS (digital map) database should guarantee improved analytical capabilities in GIS. Notwithstanding, GIS is an emerging technology and new approaches for analysing spatial data in the computing environment are rapidly being developed (Peuguet and Marble, 1991). Current analytical capabilities of GIS, and developments in the foreseeable future that may influence exploration applications, are briefly reviewed below.

At present exploratory data analysis, involving pattern description is possible with available GIS tools. But the description of spatial variation patterns requires that the causes of these spatial patterns and relationships be explored. For example, if a pattern exists what causes it? Given the spatial pattern of a particular variable of interest, what are the principle spatial covariates? The present analytical tools of GIS cannot address these queries. The present generation of GIS lacks relevant *spatial analysis* procedures (Maguire, 1991, Goodchild, 1991; Openshaw, 1991; Maguire and Dangermond, 1991) which is a major drawback, particularly in exploration.

Spatial analysis is very relevant to GIS and mineral exploration, and has not yet been incorporated as part of the general GIS toolbox. However at the present rapid development rate of GIS technology, users may look forward to a standard toolbox of spatial analysis procedures and techniques in future GIS (Openshaw; 1991). Incorporation of spatial analysis tools within GIS, enables the explorationist to link the cartographic domain with the key areas of applied quantitative, statistical and mathematical analysis and modelling. Spatial analysis is a technique based on the application of statistical (quantitative) methods to spatial data (Berry and Marble , 1968). Quantitative description of patterns and pattern relationships could help to more clearly define the possible causes of patterns in spatial datasets.

Description could include probabilistic statements about the outcome of GIS operations (Openshaw, 1991). For example the probability of a selected variation pattern being due to mineralisation could be quantified by testing hypotheses. The hypotheses should relate to mineralisation of a similar genetic type but can not be generated from the data being tested. Standard statistical methods; factor analysis, regression analysis; could be used to analyse data for spatial associations and covariations.

In developing a research agenda for spatial analysis in future GIS's; six key spatial analytical research topics where defined by Openshaw, 1990a (see Table 8.1). Placing these topics in an exploratory geographical analysis framework, he identified a set of basic generic functions that reflect the need for relevant spatial technology within present GIS's (Table 8.2; Openshaw, 1990b). All of the spatial analytical research

topics and related basic generic spatial procedures, outlined in Table 8.1 and 8.2, should be applied in mineral exploration.

Table 8.1 - Key spatial analytical research topics that should be incorporated in future GIS after Openshaw (1990a).

1. Response modelling for large data sets with mixed scales and measurement levels
2. Practical methods for cross area estimation
3. Zone design and spatial configuration engineering
4. Exploratory geographical analysis technology
5. Application of Bayesian methods
6. Application of artificial neural nets to spatial pattern detection

Table 8.2 - Basic generic spatial analysis procedures after Openshaw (1990b).

1. Pattern spotters and testers
2. Relationship seekers and provers
3. Data simplifiers
4. Edge detectors
5. Automatic spatial response modellers
6. Fuzzy pattern analysis
7. Visualisation enhancers
8. Spatial Video Analysis

Concurrent with the development of powerful processing and memory technologies that will advance GIS technology, research and development into new visualisation, spatial analysis and integrating tools are progressing. Some of the more interesting and revolutionary topics are discussed below: *Multimedia-databases*, embracing audio, video and animated information in conventional GIS databases. *Interactive-hypermedia-systems* which interconnects all information and knowledge available for an area, from a multimedia type database. The user wanders through the universe of stored information, makes appropriate associations, and creates his/her own islands of meaning from the data. The user integrates data based on criteria s/he selects. Current GIS supports computer integration, rather than user integration. User integration is presently confined to choosing the data sets to integrate, prior to input to GIS.

Virtual-reality-systems which will allow integration of information, in a more comprehensive manner than currently available systems. The objective of virtual reality, is to simulate a fully three dimensional environment which is represented realistically; in which changes occur in real time; and where the user can modify the environment. This will encourage affective, together with cognitive, visual information processing. *Knowledge Based Systems (KBS)* that would facilitate complex computational model building of complex domains. KBS are being researched as an extension to the relational model, where knowledge of an expert in a particular field, for example geology, is represented in terms of logic. Through the logical specification of deductive rules, knowledge may be represented that is independent of a specific implementation.

The GEOscience Spatial Information System (GEOSIS) project are seeking to create data structures that represent knowledge in geoscience data. Hierarchical data structures are used to represent spatial objects and relationships between them, creating explicit links in the overall data structure, and hence allowing the user move through the data knowledgably (Figure 8.1; Currie and Ady, 1989). The overriding objective of the GEOSIS project is to create a GIS system "that can be used by geoscientists for sophisticated query and analysis without he geoscientist being aware of the GIS technology that makes this possible" (Currie and Ady, 1989).

Figure 8.1 - Example of the hierachical data structure for roch classification in GEOSIS (modified from Curry and Ady, 1989).

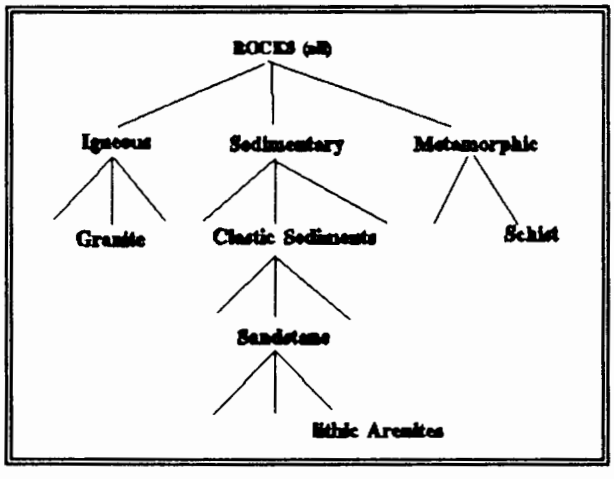

Presently, data is structured using either the raster or the vector data model. Much of the information richness of the world is ignored and information included is over-

emphasised (Shepard, 1991). In *geocomputing*, most decisions are based on graphical patterns. It is important that the information and knowledge produced when studying the data, is a correct representation of the process and patterns that occur in the environment from which the data was taken.

Probable future developments in GIS related technologies could create tools that allow the integration, visualisation and spatial analysis of the richness of real earth data. Computer graphic models can be created, that approximate closely to the phenomena being modelled. The Earth Scientist could move into realms that do not exist, through animation and virtual reality systems. Many of the earth processes we study, occurred millions of years ago, and in many cases, are not operational at present. Knowledge based modelling, multimedia databases, virtual reality systems, interactive hypermedia systems will enable the geoscientist to seek new insight and explore new frontiers in Earth Science phenomena, using GIS visualisation and analysis.

The success of the above tools depend on technological as well as conceptual development. Conceptual development includes data structures, data models, database design, and requires a clearer knowledge of the nature of both spatial and temporal data. The transient nature of data needs to be explored, and data structures should be developed to facilitate this sort of data.

References

Aangeenburg, R.T. (1991), A Critique of GIS, In: Geographic Information Systems: Principles and Applications, (edited by D.J. Maguire, M.F. Goodchild and D.W. Rhind), Longman, London, Vol. 1, pp. 101-107.

Albat, H.M (1984), The Proterozoic granulite facies terrane around Kliprand Namaqualand Metamorphic Complex, Bull. Precambrian Res. Unit, University of Cape Town, No. 33, pp. 386.

Armstrong, R.A., Reid, D.L., Watkeys M.K., Welke H.J., Lipson R.D. and Compston W. (1988), Zircon U-Pb ages from the Aggeneys area, central Bushmanland. Ext. Abs. 22nd Earth Sc. Congr. Geol. Soc. S.A., Univ. Natal Durban, p.493-496.

Barr, J.M. (1988), Isotope Character of Barite and Ore Genesis in Central Bushmanland, Unpublished M.Sc Thesis, Univ. Cape Town.

Barrow, J.D. (1991), Theories of everything: the quest for ultimate explanation, Cox and Wyman, Reading.

Barton, E.S. (1983), Reconnaissance isotopic investigations in the Namqua mobile belt and implications for Proterozoic crustal evolution - Namaqualand Geotraverse, Spec. Publ. Geol. Soc. S. Afr., Vol. 10, pp. 45-66.

Beeson, R., Brunke, E.G., and Dent, R.H. (1978), Preliminary Results from a Regional Geochemical Survey in the North-Western Cape Province, Mineralization in Metamorphic Terranes, Verwoerd, W.J., Spec. Publ. geol. Soc. S. Afr., Vol. 4, pp. 189-203.

Berry, J.L., and Marble, D.F. (1968), Spatial Analysis: a reader in statistical geography, Prentice Hall, Engelwood Cliffs New Jersey.

Betton, P.J. (1984), Nd and Sr isotopic evidence for the evolution of the Namaqualand mobile belt, Southern Africa, Abstr. Int. Conf. on Middle to Late Proterozoic Crustal Evolution, Precambrian Res. Unit, University of Cape Town.

Blignault, H.G., Van Aswegen, G., Van Der Merwe, S.W., and Colliston, W.P (1983), The Namaqualand geotraverse and environs: Part of the Proterozoic Namaqua mobile belt, In Namaqua Metamorphic Complex (edited by B.J.V. Botha), Spec. Publ. geol. Soc. S. Afr., Vol. 10, pp. 1-29.

BMM Company Reports (1983), The history of Aggeneys, Unpublished.

Bolivar, S.L., Freeman, S.B., and Weaver, T.A. (1983), Evaluation of integrated datasets - four examples,

Computers and Geosciences, Vol. 9, No. 1, pp. 7-15.

Bonham-Carter, G.F., Agterberg, F.P. and Wright, D.F. (1990), Integration of geological datasets for gold exploration in Nova Scotia, Introductory readings in Geographic Information Systems, (edited by Peuguet, D.J., and D.F. Marble), Taylor and Francis.

Botha, B.J.V. (editor; 1983), Namaqualand Metamorphic Complex. Geol. Soc. S. A. Spec. Publ., No. 10.

Burrough, P.A. (1986), Principles of Geographic Information Systems for land resources assessment, Clarendon Press: Oxford.

Carlson, C.A. (1991), Spatial Distribution of ore deposits, Geology, Vol. 9, pp. 111-114.

Colliston, W.P. and Praekelt, H. E. (1988), The recognition of overthrust terranes in the Namaqua Mobile belt., Ext. Absr. Geocongress 1988, Geol. S. Afr., Durban, pp. 113-116.

Colliston, W.P., Praekelt, H.E. and Schoch, A.E. (1989), A broad perspective (Haramoep) of geological relations established by sequence mapping in the Proterozoic Aggeneys terrane, Bushmanland, South Africa, S. Afr. J. Geol,. Vol. 92, pp. 42-48.

Coppock, J.T., and Rhind, D.W. (1991), The history of GIS, In: Geographic Information Systems: Principles and Applications, (edited by D.J. Maguire, M.F. Goodchild and D.W. Rhind), Longman, London, Vol. 1, pp. 21-43.

Currie, A. and Ady, B. (1989), GEOSIS project: knowledge representation and data structures for geoscience data, In: Statistical Applications in the Earth Sciences (edited by Agterberg, F.P. and Bonham-Carter. G.F.), Geological Survey of Canada, pp. 111-116.

Cutpill, S.C. (1991), Spatial data exchange and standardisation, In: Geographic Information Systems: Principles and Applications, (edited by D.J. Maguire, M.F. Goodchild and D.W. Rhind), Longman, London, Vol. 1, pp. 515-530.

Clifford, T.N., Gronow, J., Rex, D.C., and Burger, A.J. (1975), Geochronological and petrogenetic studies of high-grade Metamorphic rocks and intrusives in Namaqualand, South Africa. J. Petrol. Vol. 16, pp. 154-188.

Clifford T.N., Stumpfl E.F., Burger A.J., McCarthy T.S., and Rex D.C. (1981), Mineral-chemical and isotopic studies of Namaqualand granulites, South Africa., Contrib. Min. Petrol. Vol. 77, pp. 225-250.

Date, C.J. (1986), Relational Databases: Selected Readings, Addison Wesley Publishing Co.

Dangermond, J. (1990), A classification of software components used in GIS, In: Introductory readings in Geographic Information Systems, Peuguet, D.J., and Marble, D.F., Taylor and Francis, pp. 30-51.

Dangermond, J. (1991), The commercial setting of GIS, In: Geographic Information Systems: Principles and Applications, edited by D.J. Maguire, M.F. Goodchild and D.W. Rhind), Longman, London, Vol. 1, pp. 55-65.

Duane, M.J., and De Wit, M.J. (1988), Pb-Zn ore deposits of the northern Caledonides - products of continental scale fluid mixing and tectonic expulsion during continental collision, Geology, Vol. 16, pp. 999-1002.

DeBeer, J.H. and Meyer, R. (1983), Geoelectrical and gravitational characteristics of the Namaqua-Natal mobile belt and its boundaries, Spec.Publ.geol.Soc.S.Afr., No. 10, pp.91-101,

Dickinson, W.R. (1974), Plate tectonics and sedimentation, In: Tectonics and sedimentation, edited by Dickinson, W.R., Spec. Publ. Soc. Econ. Paleontologists and Mineralogists, No. 22, pp. 1-27.

Drury, S.A., and Walker, A.S.D (1991), The use of Geophysical images in Subsurface investigations of the Solway Basin, England, Surveys in Geophysics, Vol. 12, No. 6, pp. 565-581

Eglington, B.M., Harmer, R.E. and Kerr, A. (1989), Isotope and geochemical constraints on Proterozoic crustal evolution in south-eastern Africa, Precambrian Research., Vol. 45, pp. 159-174.

ESRI, (1991), ARC/INFO V. 6.01 Users Guide, ESRI Inc., Redlands, California.

Estes, J.E. (1981), Remote Sensing and Geographic Information Systems Coming of age in the Eighties, Proceedings, PECORA VII Symposium, pp. 23-40.

Ehlers, M., Edwards, G., and Bedard, Y. (1989), Integration of remote sensing with GIS : a necessary evolution. Photogrammetric Engineering and Remote Sensing, Vol. 55, No. 11, pp. 1619-1627.

Flowerdew, R. (1991), Spatial Data integration, In: Geographic Information Systems: Principles and Applications, (edited by D.J. Maguire, M.F. Goodchild and D.W. Rhind), Longman, London, Vol. 1, pp. 375-387.

Frimmel, H.E, Hoffman, D., and Moore, J.M. (1993), Preservation of syn-depositional geochemical

characteristics of the Broken Hill massive sulphide deposit, South Africa, during upper amphibolite metamorphism. Abstr. 2nd Biennial SGA Meet., Granada.

Garson, M.S., and Mitchell, A.H.G. (1991), Precambrian ore deposits and plate tectonics, In: Pecambrian Plate tectonics, (edited by Kroner. A), Elsevier, Amsterdam, pp.689-731.

Goodchild, M.F. (1991), The technological setting of GIS, In: Geographic Information Systems: Principles and Applications, (edited by D.J. Maguire, M.F. Goodchild and D.W. Rhind), Longman, London, Vol. 1, pp. 45-54.

Groenewald, P.B., Grantham, G. H., and Watkeys, M. K. (1991), Geological evidence for a Proterozoic to Mesozoic link between southeastern Africa and Drauning Maud Land, Antarctica., J. geol. Soc. Lond, Vol. 148, pp. 1115-1123.

Gustafson L.B. and Williams, N. (1981), Sediment-Hosted Stratiform Deposits of Copper, Lead and Zinc, Economic Geology, 75th Anniversary Volume, pp. 139-178.

Harris, R.W. (1992), A structural analysis of the Hartbees river thrust belt, with special emphasis on the nature and origin of the change in structural patterns across the boundary between the Bushmanland and Gordonia Subprovinces, Unpubl. Ph. D. Thesis, University of Cape Town.

Harris, R.W. (1990), Shear strain analysis along the southeastern segment of the Pofadder lineament, Abstracts, 23rd Earth Science Congress, Geol. Soc. S. Afr., pp. 214-217.

Hartnady C. J. H., Joubert P., and Stowe, C. (1985), Proterozoic Crustal Evolution in South Western Africa, Episodes, Vol. 8, No. 4, pp. 236-244.

Hess, R. W., and Hekommer, M. A. (1993), General principles and efficient approaches to computer contour mapping, Earth Observation Magazine, pp. 46-49.

Jacobs, J., Thomas, R.J. and Weber, K. (1993), Accretion and indentation tectonics at the southern edge of the Kaapvaal Craton during the Kibaran (Grenville) Orogeny, Geology, Vol. 21, pp. 203-206.

Joubert P. (1986a), The Namaqualand Metamorphic Complex - a summary, Mineral Deposits of Southern Africa, Vol.1&2, pp. 1395-1420.

Joubert, P. (1986b), Namaqualand - a model of Proterozoic accretion, Trans. Geol. Soc. S. Afr. Vol. 89, pp. 79-96.

Joubert P. (1971), The regional tectonism of part of Namaqualand. Bull. Precambrian Res. Unit, Univ. Cape Town 10, pp. 220.

Joubert, P. (1978), The fault pattern south of Kakamas - an example of convergent Wrench Tectonics, In: Mineralisation in metamorphic terranes (edited by Verwoed, W.J.), Spec. Publ. Geol. Soc. S. Afr., Vol. 4, pp. 215-222.

Joubert, P. (1974a), Wrench-fault tectonics in the Namaqualand Metamorphic Complex, Bull. Precambr. Res. Unit, University of Cape Town, No. 15, pp. 17-23.

Joubert, P. (1974b), The gneisses of Namaqualand and their deformation. Trans. Geol. Soc. S. Afr. No. 77, pp. 339-345.

Kay, G. (1993), Colour Analysis and the classification of fruit, Unpubl. M. Sc. Thesis, University of Cape Town.

Koeppel, V. (1980), Lead Isotope studies of stratiform ore deposits of the Namaqualand, N.W. Cape Province, South Africa, South Africa, and their implications on the age of the Bushmanland Sequence, Proc. 5th IAGOD Symp., Vol. 1, pp. 195-307.

Krige, D.G. (1976), A review of the development of geostatistics in South Africa, In: Advanced geostatistics in the Mining Industry, (edited by Guarascio, M., David, M., and Huijbregts C.), pp. 279-93. Dordrecht, Holland: Reidel.

Kroner, A. and Blignaut, H.G. (1976), Towards a definition of some tectonic and igneous provinces in the western South Africa and southern South-West Africa, Trans. Geol. S. Afr., Vol. 79, pp. 232-238.

Large, D.E. (1980), Geological parameters associated with sediment-hosted, submarine exhalative Pb-Zn deposits: an empirical model for mineral exploration. Geol Jahrb, 40:59-129.

Lam Nina Siu-Ngan (1983), Spatial Interpolation Methods: A Review, The American Cartographer, Vol. 10, No. 2, pp. 129-149.

Lipson, R.D. (1978), Some aspects of the geology of part of the Aggeneysberge and surrounding gneisses, Namaqualand, Unpubl. M. Sc. Thesis, University of Witwatersrand.

Lipson, R.D. (1990), Lithogeochemistry and origin of metasediments hosting the Broken Hill deposit, Aggeneys, South Africa, and implications for ore genesis. Unpubl. Ph. D. Thesis, University of Cape Town

pp-250.

Macleod, I.N. (1989), Computing in Canadian Exploration, Mining Magazine, November edition, pp. 460-464.

Maguire, D.J. (1991), An Overview and the definition of GIS, In: Geographic Information Systems: Principles and Applications, (edited by D.J. Maguire, M.F. Goodchild and D.W. Rhind), Longman, London, Vol. 1, pp. 9-19.

Maguire, D.J., and Dangermond, J. (1991), The functionality of GIS, In: Geographic Information Systems: Principles, Vol. 1 (edited by D.J. Maguire, M.F. Goodchild and D.W. Rhind), Longman, pp.319-334.

Marble, D.F., and Peuguet, D.J. (1983), Geographic Information Systems, In: Manual of Remote Sensing, 2nd Edn, American Society of Photogrammetry, (edited by Colwell R.N.), Falls Church, pp. 923- 958.

Marble, D. F., (1990), Geographic Information Systems: An overview, In: Introductory readings in Geographic Information Systems (edited by Peuguet, D.J., and Marble, D.F.), Taylor and Francis, pp. 8-17.

Matheron, G. 1971. The theory of regionalised variables and its application. Les Cahiers du Centre de Morphologie Mathematique de Fontainebleau, Vol. 5, pp. 221.

Mandelbrot, B.B. (1962), Statistics of natural resources and the law of Pareto, Watson Research Centre, New York, I.B.M. Research note NC-146, pp. 131.

Mandelbrot, B.B. (1983), The fractal geometry of nature, W.H. Freeman and Company, New York, pp. 468.

Mc Cammon, R.B. (1989), Prospector III: Towards a map-based expert system for regional mineral resource assessment, In: Statistical Applications in the Earth Sciences (edited by Agterberg, F.P. and Bonham-Carter. G.F.), Geological Survey of Canada, pp. 396-404.

Mc Stay J.H. (1992), Granulite faces metamorphism Fluid-buffering and partial melting in the Buffels River area of the Namaqualand Metamorphic Complex, South Africa., Upubl Phd, Cape Town, pp. 401.

Meyer C. (1981), Ore-Forming Processes in Geologic History, Economic Geology, 75th Anniversary Volume, pp. 6-41.

Moore J.M. (1977), The geology of Namiesberg, northern Cape. Precambr. Res. Unit, Univ. Cape Town Bull. No. 20, pp. 69.

Moore, J.M. (1989), A comparative study of metamorphosed supracrustal rocks from the western Namaqualand Metamorphic Complex, Bull. Precambr. Res. Unit, Univ. Cape Town, Bull. No. 37.

Moore, J.M., Reid, D.L. and Watkeys, M.K. (1990), The regional setting of the Aggeneys/Gamsberg base metal deposits, Namaqualand, South Africa, In: Regional metamorphism of ore deposits (edited by Spry, P.G. and Bryndzia, L.T.), pp. 77-95.

O'Callaghan, J.F. and O'Sullivan, J.F. (1982), Image-based Geographic Information Systems for mineral exploration: the Broken Hill project, Australia, papers presented at the International symposium on Remote Sensing on Environment, Second Thematic Conference, Remote Sensing for Exploration Geology, Forth Worth, Texas, pp. 133- 135.

Odling, N.E. (1983), The structure of Gamsberg, Namaqualand, N.W. Cape - an intermediate report, 18-20th Precamb. Res. Unit. Ann. Report., University of Cape Town, pp. 76-104.

Odling, N.E. (1987), Structural analysis and three dimensional modelling at Gamsberg, N.W. Cape, Bull. Precambr. Res. Unit, University of Cape Town, No. 34.

Oliver , J. (1986), Fluids expelled tectonically from orogenic belts: Their role in hydrocarbon migration and other geologic phenomena, Geology, Vol. 14, pp. 99-102.

Openshaw, S. (1991), Developing appropriate Spatial Analysis methods for GIS, In: Geographic Information Systems: Principles and Applications, (edited by D.J. Maguire, M.F. Goodchild and D.W. Rhind), Longman, London, Vol. 1, pp. 389-402.

Openshaw, S. (1990a), Towards a spatial analysis research strategy for the Regional Research Laboratory initiative, In: Geographical Information Management: methodology and applications, (edited by Masser, J. and Blakemore, M.J.), Longman, London.

Openshaw, S. (1990b), Spatial analysis and GIS : a review of progress and possibilities, In: Geographical Information Systems for urban and regional planning, (edited by Scholten, H.J. and Stilwell, J.C.H.), Kluwer, Dordrecht, pp. 156-163.

Ortega, E., Artieda, J., Haydn, R., and Volk, P. (1990), Remote Sensing in mineral exploration - really a practical tool?: image processing and GIS application in exploration projects, paper presented at

conference - Remote Sensing: an operational technology for the mining and petroleum industries, Institute of Mining and Technology, pp. 259-262.

O'Sullivan, K.N. (1986), Computer enhancement of Landstat, magnetic, and other regional data, In: Geology and Exploration, Berkman, D.A., Publication of 13th CMMI Congress, pp.1-10.

Peuguet, D.J. (1984), A conceptual framework and comparison of spatial data models, Cartographica, Vol. 21, No. 4, pp. 66-113.

Peuguet, D. J. (1990), A conceptual framework and comparison of spatial data models, In: Introductory readings in Geographic Information Systems, edited by Peuguet, D.J., and Marble, D.F., Taylor and Francis, pp. 250-285.

Peuguet, D.J., and Marble, D.F. (1990), What is a Geographic Information System? In: Introductory Readings in Geographic Information Systems, edited by Peuguet, D.J., and Marble, D.F., Taylor and Francis: London, pp. 1.

Peuguet, D.J., and Marble, D.F. (1991)

Pearson, R.C., Hanna, W.F., James, H.L., Loen, J.S., Moll, S.H., Ruppel, E.T., and Trautwein, C.M. (1991), Map showing mineral resource assessment for silver cobalt, and base metals in Proterozoic sedimentary rocks; and for iron, chromium, nickel, talc, chlorite, gold and graphite in Archaean crystalline rocks, Dillon 1° by 2° quadrangle, Idaho and Montana, Department of Interior, United States Geological Survey, Miscellaneous Investigations Series.

Plimer, I.R.(1987), Sediment Hosted Exhalative Pb-Zn Deposits - Products Of Contrasting Ensialic Rifting, Trans. geol. Soc. S. Afr., Vol. 89, pp. 57-73.

Piwowar, J.M., and LeDrew, E.F. (1990), Integrating spatial data: A users perspective, Photogrammetric Engineering and Remote Sensing, Vol. 56, No. 11, pp. 1479-1502.

Pratt, W.P (1983), Mineral Resource appraisal of the Rolla 1^0 * 2^0 Quadrangle, Missouri; Manual versus digital (computer-assisted) synthesis, proceedings volume of the International Conference on Mississippi Valley Type Lead-Zinc deposits, (edited by Kisvarsanyi, G, Grant, S.K, Pratt, W.P., and Koenig, J.W.), pp. 584-595.

Praekelt H.E., Colliston, W.P., and Schoch, A.E. (1983), The stratigraphic interpretation of a highly deformed Proterozoic region in central Bushmanland, South Africa; first correlation of structurally

separated metasediments of the Aggeneys Subgroup, Precambr. Res., Vol. 23, pp. 177-185.

Reedman, J.H. (1979), Techniques in mineral exploration, Applied Science Publishers Ltd.

Reid D.L. (1982), Age relationships within the Vioolsdrif batholith, lower Orange River region. II: A two stage emplacement history and the extent of Kibaran overprinting. Trans. Geol. Soc. S.A. No. 85, pp. 105-110.

Reid, D.L. and Barton, E.S. (1983), Geochemical Characterization of granitoids in the Namaqualand geotraverse. Spec. Publ. Geol. Soc. S. A., No. 10, pp. 67-82.

Reid D.L., H.J. Welke, A.J. Erlank, and P. J. Betton (1987), Composition, age and tectonic setting of amphibolites in the central Bushmanland Group, western Namaqua Province, southern Africa. Precambr. Res., No. 36, pp. 99-126.

Robinson, A.H., Sale, R.D., Morrison, J.L., and Muehrcke, P.C. (1984), Elements of Cartography, 5th edition, Wiley, New York.

Rozendaal, A. (1975), The geology of Gamsberg, Namaqualand, South Africa, M. Sc. Thesis (Unpubl.), University of Stellenbosch.

Rozendaal, A. (1977), Geological structure of the Gamsberg zinc deposit, Namaqualand, South Africa, Ann. Univ. Stellenbosch, Ser. Al, Vol. 2, pp. 1-32.

Rozendaal A. (1982), The petrology of the Gamsberg zinc deposit and the Bushmanland iron formation with special reference to their relationships and genesis, Ph.D. Thesis (Unpubl.), University of Stellenbosch, pp. 363.

Rozendaal, A. (1986), The Gamsberg Zinc Deposit, Namaqualand District, In: Mineral Deposits of South Africa, (edited by Anhaeusser C.R. and Maske S.), Vols.I&2, Geol. Soc. S. Afr., pp. 1477-1488.

Ryan P.J., A.L. Lawrence, R.D. Lipson, J.M. Moore, A. Patterson, D.P. Stedman and D. Van Zyl (1986), The Aggeneys base metal sulphide deposits, Namaqualand District. In: Mineral Deposits of South Africa, (edited by Anhaeusser C.R. and Maske S.), Vols.I&2, Geol. Soc. S. Afr., pp. 1447-1473.

Sabins, F.F. (1978), Remote Sensing Principles and Interpretation., W.H. Freeman and Co., New York.

Sawkins, F.J. (1990), Metal Deposits in relation to plate Tectonics, Springer-Verlag, Berlin: Heidelberg,

second edition.

Shepard, I.D.H. (1991), Information integration and GIS, In: Geographic Information Systems: Principles and Applications, (edited by D.J. Maguire, M.F. Goodchild and D.W. Rhind, Longman, London, Vol. 1, pp. 337-360.

South African Committee for Stratigraphy (SACS) (1980) Stratigraphy of South Africa, Part 1. Handb. 8 Geol. Surv. S. Afr., Pretoria.

Star J.L., J.E. Estes and F. Davis (1991), Improved integration of Remote Sensing and Geographic Information Systems: A Background to NCGIA Initiative 12. Photogrammetric Engineering and Remote Sensing, Vol. LVII, No.6.

Stevens, S.S. (1946), On the theory of scales of measurements, Science, Vol. 103, pp. 677-680.

Stevenson, F. (1985), Response of the Black Mountain, South Africa, sulphide deposit to various geophysical techniques and implications for exploration of similar deposits, M.Sc. Thesis, Dept. Geosciences, University of Arizona.

Stevenson, F. (1983), Reassessment of Scintrex Helicopter borne Magnetometer Survey in the Area of Non Competition, Unpubl. BMM Report.

Stowe C.W. (1984), The Lower-Middle Proterozoic tectonic framework of Southern Africa. Abs. Int. Conf. Mid-Late Protero. Evol. pp. 30-32, Precambr. Res. Unit, Univ. Cape Town.

Tanaka, S.M., and Segal, D.B. (1989), Integrated Remote Sensing\Vector based GIS technology for gold exploration, Round Mountain District, Nevada, USA, paper presented at the Seventh Conference on Remote Sensing for Exploration Geology, Alberta, Canada, pp. 1269-1283.

Tankard, A.J., Jackson, M.P.A., Eriksson, K.A., Hobday, D.K., Hunter, D.R., and Minter, W.E.L. (1982), Crustal Evolution of Southern Africa. 3.8 Billion Years of History. Springer-Verlag, New York. pp. 523.

Taylor, S.R., and McLennan, S.M. (1985), The continental Crust: its Composition and evolution, Blackwell: Oxford, pp.67.

Thomas, R.J., von Veh, M.W., and McCourt, S. (1993), The tectonic evolution of Southern Africa: an Overview, Journal of African Earth Sciences, Vol. 16, No. 1/2, pp. 5-24.

Thomas, R. J., Du Plessis, A., Fitch, F., Marshall, C. G. A., Miller, J.A., von Brunn, V., and Watkeys, M.K. (1992), Geological studies in the southern Natal and Transkei: Implication for the Cape Orogen, In: Inversion tectonics of the Cape Fold Belt, Karoo and Cretaceous basins of southern Africa, (edited by De Wit, M. J. and Ransome, I.G.D.), Balkema, Rotterdam, pp. 229-236.

Thorpe, L. and Hobbs, J.B.M. (1984), Report on the 1983 mapping Program on the Farms Haramoep, Koeris, Rozynbosch and Wortel in the Aggeneys area of Non Competition, Unpublished BMM. Report.

Thorpe, L. (1986), Final Report documenting exploration activity within the Aggeneys area of non-competition for the period 1983-1986, Unpublished BMM Report.

Tomlin, C.D. (1991), Geographic Information Systems and Cartographic Modelling, In: Geographic Information Systems: Principles and Applications, (edited by D.J. Maguire, M.F. Goodchild and D.W. Rhind, Longman, London, Vol. 1, pp. 361-374.

Tomlinson, R.F. (1990), Current and potential uses of geographic information systems: the North American experience, Introductory readings in Geographic Information System, (edited by Peuguet, D.F., and Marble, D.F.), Taylor and Francis.

Turcotte, D.L. (1991), Fractals in Geology: What are they and what are they good for?, GSA Today, Vol. 1, No. 1., pp. 2-4.

Unwin, D.J. (1981), Introductory Spatial Analysis, Methuen, London.

Understanding GIS, The ARC/INFO method ESRI, 1991.

Van Aswegan, G., Strydom, D., Colliston, W.P., Praekelt, H.E., Schoch, A.E., Blignout, H.J., Botha, B.J.V., and Van Der Merwe, S.W. (1987), The structural-stratigraphic development of part of the Namaqua Metamorphic Complex, South Africa - an example of Proterozoic major thrust tectonics. In Proterozoic Lithospheric Evolution (edited by Kroner, A.), Geodynamics Series, Vol. 17, pp. 207-216.

Wadge, G. (1993), Computers and Geological Information: The depth and Width of it, Geoscientist, Vol. 3, No. 2, pp. 10-13.

Waters D.J. (1986), Metamorphic zonation and thermal history of pelitic gneisses from western namaqualand, south africa. Trans. Geol. Soc. S.A., Vol. 89, Pp. 97-102.

Waters D.J. (1988), Partial melting and the formation of granulite facies assemblages in Namaqualand,

South Africa. J. Met. Geol. Vol. 6, pp. 387-404.

Watkeys M.K. (1986), The Achab Gneiss: a "floor" in Bushmanland or a flaw in Namaqualand? Trans. Geol. Soc. S. Afr. Vol. 89, Pp. 103-116.

Watkeys M.K., J.M. Moore and A. R. Duncan (1988), The pink gneiss of Bushmanland: Mid-Proterozoic felsic pyroclastics. Ext. Abs. 22nd Earth Sc. Congr. Geol. Soc. S.A., Univ. Natal Durban, pp.717-720.

Welke H.J. and C.B. Smith (1984), Lead isotope characterization of the Aggeneys-Gamsberg ore bodies in relation to possible source rocks, with implications for Bushmanland metallogenesis. Int. Conf. Mid-late Protero. Evol., Pecambr. Res. Unit, Univ. Cape Town. pp. 8-9.

Wheatley, C.J.V. (1978), Aspects of Geochemical Exploration in the Bushmanland Region, North-West Cape, In: Mineralization in Metamorphic Terranes, (edited by Verwoerd), W.J., Spec. Publ. Geol. Soc. S. Afr., Vol. 4, pp.205-215.

Willner, A.P., Schreyer, W., and Moore, J.M. (1990), Peraluminous metamorphic rocks from the Namaqualand Metamorphic Complex, South Africa: Geochemical evidence for an exhalation-related, sedimentary origin in a Mid-Proterozoic rift system, Chem. Geol., Vol. 81, pp. 221-240.

Wilsher, W., Herbert, R., Wullschleger, N., Naicker, I., Vitali, E., and M. de Wit (1993a), Towards intelligent spatial computing for the Earth sciences in South Africa, South African Journal of Sciences, Vol. 89, pp. 315-323.

Wilsher, W. (1994), The distribution of selected elements within mineral deposits across Gondwana: Geodynamic Implications, PhD thesis in preparation.

Windley, B.F., (1993), Uniformitarianism today: plate tectonics is the key to the past, J. geol. Soc. Lond., Vol. 150, pp. 7-19.

Appendices

Appendix 1

The Functionality of GIS

The tasks carried out in building a functional GIS database are outlined here, following the functional classification illustrated in Figure 4.1.

A. Capture

The data captured was compiled from information stored in maps, tabular/text and image formats.

Cartographic map data

Analog map data was captured using secondary geographical data collection devices. These included vector table digitisers and raster scanners. Digitising was done using PC ARC/INFO, and this data was transferred to the SUN workstation where validation, editing was done.

All map data was digitized, except for the geology map which was scanned. The high density of information in the geology map would have led to inaccurate and very long hours of digitising. Scanning saved time, but cost money (R800 for the geology map Figure 2.2). Long hours still had to be spent editing, cleaning and validating this map. Scanning produces an image of the data, and vectorisation of the scanned map adds alphanumeric identifiers to each line feature.

Primary map data captured include:

1) an interpretative geologic map showing 29 different rock units, 9 stratigraphic groupings, (Figure 2.2)

2) 2 structural maps including a generalised structural map (Figure 2.4 overlay 1) complied by BMM mining and an UOFS interpretative structural map (Figure 2.4 overlay 2).

3) Interpretative geophysical maps: derived from the image of the Phelps Dodge Survey (AGRES.LAN, AGDRV1.LAN, AGTOT.LAN).

magnetic bodies (amibody)

magnetic boundaries (amibound)
dykes or sills (amidyke)
fractures or faults (amifault)

Black Mountain area of Non-Competition prospecting data compilation maps of:
electromagnetic test line (NCEM)
gravity survey (NCGRAV)
induced polarization survey (NCIP)
magnetic survey (NCMAG)
"TEM" survey (NCTEM)
and induced polarization and magnetic grids of 1:50 000 maps
4) geochemical data maps showing geochemical sample and mineral occurrence localities, and contours of element concentration data
5) streams maps delineating drainage
6) maps showing cadastral information: roads (RDS main, secondary, footpaths, other), telephone and power lines (TLPL), point localities of other mines, prospects, dwellings (PT).

Tabular and Text data:
Stream sediment geochemical data was in variable format spreadsheet files. The tabular data, comprising x, y co-ordinate locations (latitude-longitude) with attribute data for each sample, was manipulated within QUATTRO-PRO, a spreadsheet programme. For processing and generation in ARC-INFO, files have to be in a standard format
X1, Y1, A1, B1, C1
X2, Y2, A2, B2, C2
X3, Y3, A3, B3, C3
.
.
.
Xn, Yn, AN, BN, CN
END
Where X1 to Yn and Y1 to Yn give the co-ordinate of each point. And A, B and C

give the attribute data for each co-ordinate location. Data files in the principal system independent format ASCII (American Standard Code Information Interchange) were, with data records in the order specified above.

The sample co-ordinates were in spherical co-ordinates, and were projected from spherical (latitude, longitude) to planar co-ordinate system (x,y). The co-ordinate data was then processed using a point generation function to produce vector point feature maps.

Analytical results for Pb, Zn, Cu, Mn and Ni in ppm, contained in each sample, was imported into the relational attribute database. Unique codes for each sample location within the vector point sample map, are duplicated in the RDBMS to relate the spatial map and attribute data. Other attribute data (text and numeric) was input via the keyboard. The x, y co-ordinate data were used to generate vector point maps. The attribute data was input into the INFO relational database. First, tables were defined in INFO that would store this attribute data. The names, type of data (character, numeric), and length of data stored in each column had to be specified.

Image Data

Image data was supplied in ERDAS format, a standard format that the ARC-INFO system can read directly. Image data included a data captured using airborne magnetic methods and satellite scanners (LANDSAT Thematic Mapper). The original Landsat TM data and magnetic data were processed, manipulated and enhanced by P.G. Schutte and Paul Versnel at the Remote sensing Unit, Gold Fields of South Africa Ltd. The procedure followed is summarised below.

Aeromagnetic Data

The magnetic force field data was digitised from contour maps and re-expressed as images. This was done by interpolating the digitised data and assigning values of a particular force field to each cell within a rasterised grid (cell dimension 50 for local surveys and 250 for regional survey). The range of interpolated values, generally covering negative and positive values for total magnetic field intensity, were then re-scaled to the range of 0 to 255, the 8 bit range of digital numbers that is commonly

employed in digital image display and processing.

The data was analysed using I^2S image processing system to fit polynomial surfaces to the raw data and to generate the corresponding trend surface grids. The wavelength in an aeromagnetic image relate to the depth to their source. The long wavelength effects of deep sources, which give rise to the regional field, are removed. This isolates the shorter wavelength features. This technique is used to enhance the distribution and nature of shallower sources. Subtraction of trend surface or regional field grids from the original gridded raw data produces residual anomaly image (viz. AGRES and BRES in AGGED). This method is a rapid, qualitative means of generating models of sub-surface structure (Drury and Walker,1991).

Landsat TM Data

From the 7 band raw Landsat Thematic Mapper data supplied by EOSTAT, a 3 band false colour composite was produced. In the composite image band 7 is displayed as red, band 4 as green and band 1 is displayed as blue on a colour monitor. The image was processed and enhanced on an I^2S image processing system.

With ARC-INFO GIS the image data could not be processed as images, and were available only for display. Converting the image data to gridded format using the IMAGEGRID function, the data could be manipulated and analysed using GRID functions.

B. Transfer

Cartographic map data

Map data was captured (digitised) in the PC environment and transferred to the workstation environment. DOS and UNIX are the operating systems used by the workstation and PC, respectively. The digital map data was exported out of ARC-INFO on the PC and converted using the DOS2UNIX command. This converts data from a DOS to UNIX compatible format. The data was then transferred from the PC to the workstation, using the File Transfer Process (FTP), which is an electronic network that allows transfer between the PC to the workstation. The data was imported into Arc-Info version 6, and was ready for manipulation. The import and

export, and DOS2UNIX functions are local to Arc-Info.

Attribute Data

ASCII text files were transferred from the PC to workstation environment using FTP. Data from ASCII files were loaded into these pre-defined tables in the relational database.

Image Data

The processed images from Gold Fields were on magnetic dual cartridges. All the images were converted to ERDAS format (pre. 7.4. version) at Gold Fields. This is an Arc-Info system dependant format and was loaded directly in ARC-INFO, from the magnetic dual-cartridge tapes.

C. Validate and edit

The graphical map database was edited and validated to produce maps that were, as far as possible, error free and ready for manipulation. The digitised and scanned vector maps had to be rigorously edited and validated, to remove errors and inconsistencies. This was done by cross checking the digital data against the original analog maps and looking for unusual and unspecified values. Corrections, additions, deletions and changes to the digital map were made where necessary. Arc-Info stores vector data in a fully topologic structure. After editing and validation the topological structure of all the vector maps were topologically constructed using the CLEAN function for polygon, and BUILD function for line and point data, in ARC-INFO.

D. Storage and Structure

In Arc-Info locational data are represented using the topological spatial data model ARC. Thematic data are stored in the tables of the relational database INFO. The software components (ARC and INFO) can be addressed separately using either the ARC macro language and INFO commands respectively. Tight coupling between ARC and INFO ensures integrity of relationships between spatial entities and their attributes is maintained.

Storage and structure of the geographical and attribute data was performed while

digitising. Each geographical feature (point, line, area) was uniquely identified by a numeric code. The unique identifier is used as the primary key in the relational attribute table. When the geology map was scanned no structure was defined. This scanned data required intensive editing at the keyboard to create a topological polygon structure from a mass of line data. This entailed creating closed polygons of lines for homogenous areas. A point identifier for each polygon was added.

Chapter 4 gives details of conceptual and physical storage and structure of data in GIS.

E. Restructuring

The georelational (vector) model forces a reductionist view of the data and focuses on the differences rather than the similarities between individual elements (Maguire and Goodchild, 1991). This problem can be addressed by restructuring the data within a module of the Arc-Info system called GRID. This is a composite map (raster) model within GIS system. Raster (GRID) data structures effectively represent continuous spatial data. Location is not defined as an attribute but is inherent in the data. Points, lines, polygons, surfaces are all treated as cells in a grid, reducing them to the same data structures providing a means of creating consistency between disparate data sets allowing:

a) one semantical language to be used

b) data types can be integrated with no prior separation of data structures. The grid function allows analysis of grid data via grid algebra which includes mathematical operators, commands for data input and management, specialised cell based spatial value manipulations, and statements for conditional and processing control of map algebra.

The information content of geophysical and geochemical data in the database differs. The magnetic image data represents points on continuous potential fields which relate to sub-surface magnetisation distributions. Stream sediment geochemical data are collected at discrete sampling points on a topographic surface. They do not represent a sample of a continuous field but are affected by the geology within the distinct drainage catchment areas. To be integrated successfully these differences in information content needed to be transformed. This was done by restructuring the

geology and geochemical data sets.

Within GIS the vector and point data can be gridded to a cell dimension. A cell dimension is chosen to preserve maximum information potential when continuous surface is created. A cell dimension of 50m was chosen (see discussion on map scale for reasons).

The ERDAS image data was converted to a grid with resolution equal to the pixel size of the image (50 and 250 metres) using the grid function. Each pixel is mapped to the range 0-255 of values and the frequency of each value is recorded as the count item in the value attribute table (VAT) associated with the creation of gridded data. The objective of doing this was to add intelligence to the image data in this rasterised grid format which is lacking in the merely pictorial raster image data format. Image data can be manipulated using a image processing system eg. I^2S or Intergraphs Imager software. Within ARC-INFO no image enhancement and manipulation tools exist, but there is a image integrator (for basic overlaying of data) and the GRID function explained above.

F. Generalise

Generalisation includes functions of that smooth and aggregate data in GIS. The CLEAN function, while building topology, weeds coordinates from lines and get rid of dangling arcs. The BUILD function was used to update changes made after certain edits.

G.Transformation of attribute data

Surfaces can be stored as integer or floating point grids. Within the GRID subsystem in Arc-Info floating-point surface grids can be created by interpolating attribute data. The attribute data are linked to geographical point locations.

Three functions are offered to generate surface grids from point attribute data: Trend, IDW and Kriging. Each function provides a different approach to interpolation. The function chosen should be dictated by the distribution of sample points to be interpolated and the phenomenon being studied. Appendix 5 discusses this further.

H Query

Interrogation and searching of the data stored in a GIS database is possible by either querying the spatial data on the screen or attributes of the data stored in the database. The IDENTIFY function in ARCPLOT and GRIDQUERY function in GRID, are two examples of the querying facility related to data displayed on screen. Using the IDENTIFY function, the cursor is used to query a geographic features on the display screen. The attribute information stored for the selected feature is returned on the command line. The GRIDQUERY function only features selected from the chosen grid is displayed on the screen, for example GRIDQUERY lithology = quartzite, will display on screen only grid cells from grid named lithology, that represent quartzite. Vector and raster data were queried, integrated, overlayed and modelled in the GIS environment.

I. Analyse

A subset of the analysis functions available in GIS were used in this project, and is discussed in Chapter 6.

J. Presentation of data

Hardcopy maps, graphs, tables, reports were generated to present the results of analysis functions. Maps were composed using editing, display and presentation tools in ARCPLOT. In ARCPLOT the line, point and shade symbols are chosen for the graphical display of data. The information content and contrast is effectively represented using these display tools. Scale markers, north arrows, figure captions, legends, etcetera, that help explain the data maps, are added to map compositions in ARCPLOT. When a map was ready for hardcopy output, a graphics or postscript file of the map data was generated. These graphics files were plotted using a LASERJET 11 printer for black and white prints, a INKJET plotter for colour prints.

Appendix 2

Co-ordinate systems and Map projections

Transformation of geographical data involved affine transformation of scale, rotation, translation and inversion. Affine transformations employs ground control points of known positions to determine the transformation parameters (Maling, 1991). Map projection functions are used to relate the cartesian (x,y) co-ordinates of points digitised on a source map to their geographical co-ordinates on the earths surface (sphere or spheroid).

Cartesian Co-ordinate System (Planar)

The cartesian coordinate system is used to introduce locations in planar geometry. In the Northern Hemisphere co-ordinate pairs are expressed as X representing the horizontal position, Y representing the vertical position with reference to 0,0 origin (Figure A2.1). Horizontal lines above the origin and vertical lines to the right of the origin are assigned positive value; those below or to the left are negative. Four quadrants are created representing four possible combinations of positive and negative x and y co-ordinates.

However coordinate geometry in the Northern hemisphere differs from the South African survey practice. In the South African cartesian system, Y is represents the horizontal position and X the vertical position with reference to a 0,0 origin.

To tailor South African surveys and maps to Arch-Info GIS, which is designed to suit Northern hemisphere co-ordinate geometry, the y,x co-ordinate pair(South African survey) has to be switched to x,y and both the x and y must be multiplied by -1 because we fall within the third quadrant $y<0$, $x<0$.

Spherical Co-Ordinate System (Geographic)

Spherical coordinates are measured in latitude and longitude. Treating the earth as sphere, latitude and longitude are angles measured from the Earths centre to a point on the Earths surface (Figure A2.1). Latitude and longitude are measured in degrees, minutes and seconds(DMS). In the spherical system vertical lines are called lines of longitude or meridians; horizontal lines are lines of latitudes or parallels. Origin of the

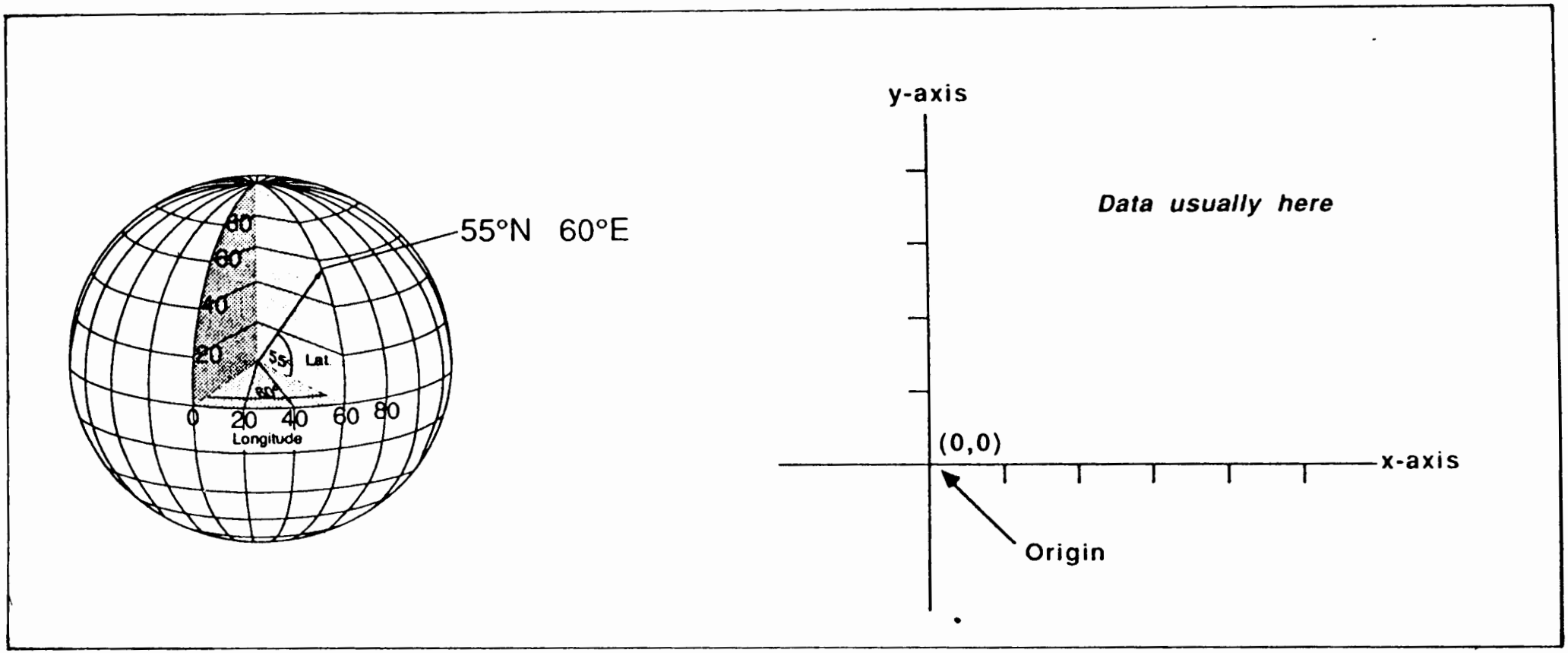

■ Spherical coordinate system

■ Cartesian coordinate system

Figure A 2.1 - Illustration of the geographic and planar co-ordinate system.

spherical system is at the intersection of the equator with Greenwich Prime Meridian (0,0). The Y co-ordinate increases west and the X-co-ordinate increases south.

This geographic system can serve as a reference position on the earths surface for all available map projections. Hence it is called a Global Reference System. Because geographic reference systems measures angles from the centre of the earth, rather than distances on the Earths surface, it is not a two dimensional planar co-ordinate system.

Map Transformation

Projection formula are used to convert data from a geographical location (lat,long) on a sphere or spheroid to a representative location on a flat surface (map sheets).
A map projection is selected to eliminate or reduce some, but not all, distortions on a paper map created by this conversion process.

The Transverse Mercator or Gauss Conform projection is based on a conformal projection, which preserves local shape by retaining angles and bearings on the ellipsoid. The Transverse Mercator projection uses meridians which run north south as lines of tangency and scale is true along them. The central meridian is centred on the region to be highlighted.
Distortion increases with distance from the central meridian.

South African surveyors use a cartesian co-ordinate system based on the Transverse Mercator or Gauss Conform Projection and Clarke 1880 (modified) ellipsoid, called the Lo system. In this system the odd numbered meridians eg. 17, 19, 21 are taken as the central meridians, with limits one degree on either side of these central meridians. These are referred to as zones. The entire country is covered by a number of these zones. Maps and surveys of the Cape Town area are referred to by the 19°East central meridian.

The narrow width of the zones in the lo-system limits the distortion of scale. The central meridian has a scale factor 1:1 and near the edge of the zone the scale enlargement is about 1:5600. This means that a distance measured as 5600m on the ground would be 5601m on the map. Since the study area is situated next to lo 19, the

scale distortion should be small. When digitising the random mean squared (RMS) error was small when areas were located close to the central meridian and increased further away from the central meridian.

Ellipsoid

The earth is an oblate ellipsoid ie. its diameter is larger at the equator than at the poles. The geoid represents the gravitational surface of the earth. The geoid is an irregular surface due to variations in gravity which affects the orbits of satellites from which positions on earth are determined. To offset this, geodesists chooses the ellipsoid which matches as well as possible the geoid in the region s/he works.

The Clarke 1880(modified) ellipsoid with a flattening factor (1/f) of 293.47 is chosen by surveys and mapping in South Africa as being the ellipsoid which matches as well as possible with the geoid in this region. The datums for the maps in that area will be based on the chosen ellipsoid. In ARC/INFO the earth is treated as a sphere/ellipsoid having a radius valued at 6,370,997 metres. This assumption that the earth is a sphere can be used for maps with scales less than 1:5,000,000.

Map Scale

Referenced from Fisher(1991).

Scale determines the smallest area that can be drawn and recognised on a paper map. The map scale for source maps input to the geographical database for this project is 1: 50000. That is 1 centimetre on the map represents 500 meters on the ground. This a an intermediate scale map as far as informational content and size of area is concerned. At this scale it is not possible to represent accurately any object of dimensions less than 25m across. Different mapscale are characterised by different mapping units. This reflects different levels of mapping purity. That is lithological class in an area is based on dominant lithology and there may be significant inclusion of other lithologies present.

At this mapscale detection of geographical features and patterns are discernable at 50m. Hence this was the resolution at which data was restructured. The mapscale determines the size of the minimum mapping area.

However once the data is in the database it may be portrayed at any scale. This makes the digital map database seem independent of scale. It is important to remember that the map series of source maps for this project was 1:50 000. The accuracy of the database as a representation of the map is for, this study, taken at 50m resolution.

Appendix 3

Geochemical Data Listing

The geochemical data used in this study constituted analyses for 3745 different sample points. Some samples were analysed for some elements and not others. For interpolation using kriging, only samples points that were analysed for the element being interpolated was selected. For the element Pb, Zn, Cu, Mn and Ni used in this study, 1374 of the 3745 were analysed. Data for other element analyses are also stored in the database but was not used in this study. The following table is partial listing of the geochemical data, with co-ordinates and sample identifiers. A comprehensive data listing takes up over 100 pages. The data is available on floppy disk in QUATRRO-PRO spreadsheet format.

Areas with rock outcrop were rock chip sampled and in areas of soil cover, soil was sampled. Hence the analytical data reflect a combination of these two sampling methods. This data was analysed using Atomic Absorption Spectrometry. Since most of the area is covered in soil, the majority of samples are soil samples.

Table A 3.1 - Partial listing of geochemical data stored in AGGED.

$RECN	X-COORD	Y-COORD	TREG-	PB-PPM	ZN-PPM	CU-PP	MN-PP	NI-PPM
1	-1,461.378	-3210941.000	1,290	49	51	38	69	13
2	-7,469.266	-3210943.000	1,122	57	40	3	82	15
3	-13,801.910	-3210949.000	954	-9999	-9,999	-9999	-9999	-9999
4	-14,451.410	-3210950.000	926	-9999	-9,999	-9999	-9999	-9999
5	-36,209.830	-3210998.000	310	-9999	-9,999	-9999	-9999	-9999
6	-39,619.750	-3211009.000	226	-9999	-9,999	-9999	-9999	-9999
7	-2,597.922	-3211310.000	1,263	46	60	144	83	31
8	-15,262.800	-3211320.000	899	42	103	43	75	38
9	-16,561.760	-3211322.000	871	-9999	-9,999	-9999	-9999	-9999
10	-27,440.610	-3211343.000	563	31	81	30	83	59
11	-36,533.410	-3211368.000	311	-9999	-9,999	-9999	-9999	-9999
12	-38,157.130	-3211373.000	255	-9999	-9,999	-9999	-9999	-9999
13	-39,131.360	-3211377.000	227	38	90	31	75	45
14	-1,623.675	-3211495.000	1,291	45	97	29	71	36
15	-3,409.717	-3211495.000	1,235	-9999	-9,999	-9999	-9999	-9999
16	-11,690.460	-3211501.000	1,011	-9999	-9,999	-9999	-9999	-9999
17	-13,476.510	-3211503.000	955	39	76	22	63	69
18	-14,450.710	-3211504.000	927	41	77	27	73	25
19	-17,698.070	-3211508.000	843	42	84	64	93	59
20	-18,185.180	-3211509.000	815	-9999	-9,999	-9999	-9999	-9999
21	-19,321.750	-3211511.000	787	-9999	-9,999	-9999	-9999	-9999
22	-22,569.110	-3211517.000	703	45	62	47	81	308
23	-29,388.590	-3211532.000	507	24	55	20	63	41
24	-32,473.600	-3211541.000	423	30	64	22	74	32
25	-33,610.180	-3211544.000	395	27	82	30	75	38
26	-34,422.020	-3211546.000	367	36	30	3	57	32
27	-37,182.300	-3211555.000	283	-9999	-9,999	-9999	-9999	-9999
28	-40,429.700	-3211566.000	199	38	47	15	71	24
29	-487.095	-3211680.000	1,319	-9999	-9,999	-9999	-9999	-9999
30	-4,546.217	-3211680.000	1,207	46	54	15	71	39
31	-5,520.407	-3211681.000	1,179	46	67	20	59	36
32	-6,332.231	-3211681.000	1,151	-9999	-9,999	-9999	-9999	-9999
33	-7,468.786	-3211682.000	1,123	-9999	-9,999	-9999	-9999	-9999
34	-8,442.976	-3211683.000	1,095	50	54	14	76	37
35	-9,904.261	-3211684.000	1,067	39	86	24	67	33
36	-12,502.100	-3211686.000	983	57	40	5	59	18
37	-20,458.000	-3211698.000	759	47	67	42	82	85
38	-24,517.140	-3211706.000	647	25	47	11	74	28
39	-25,491.330	-3211708.000	619	29	75	24	86	36
40	-26,303.160	-3211710.000	591	29	51	15	71	29
41	-28,576.290	-3211715.000	535	29	60	19	76	19
42	-10,553.550	-3211869.000	1,039	58	57	16	66	34
43	-21,269.490	-3211884.000	731	41	67	23	66	67

Appendix 4

Registration problems with the aeromagnetic data

A regional aeromagnetic, surveyed by the Government (1973), over the study area was available as an image. The image contained geographic co-ordinates tick markers to for geo-referencing purposes. The image was transformed from geographic co-ordinates based on a spherical map projection to cartesian co-ordinate based on a planar system. The geology map was overlain on the image to check or correspondence of known features. The distinctive feature of the Gamsberg basin and Aggeneysberge could be seen on the magnetic image, but did not correspond with the same vector features in the geology overlay. The data was re-projected, to discover if the projection and registration of the data was the cause of the problem. However, the same misalignment was observed. This can be seen clearly in Figure A 4.1. The geographic co-ordinates for each tick marker were checked for possible inconsistencies, but none were found. I concluded that the original tick co-ordinates are incorrectly recorded. The co-ordinates recorded on the geology map are correct, and no problem was encountered when overlaying the geological map on other projected image data. This registration problem demonstrates how geo-referencing errors can influence data integration, and the danger of integrating and analysing data with no prior knowledge of the data or the area being studied. Similarly integration of the data sets is useful for delineating errors in georeferencing of data sets. If the geology was not overlain on the image this problem would have not been noticed.

Registration problems with Government Aeromagnetic Data

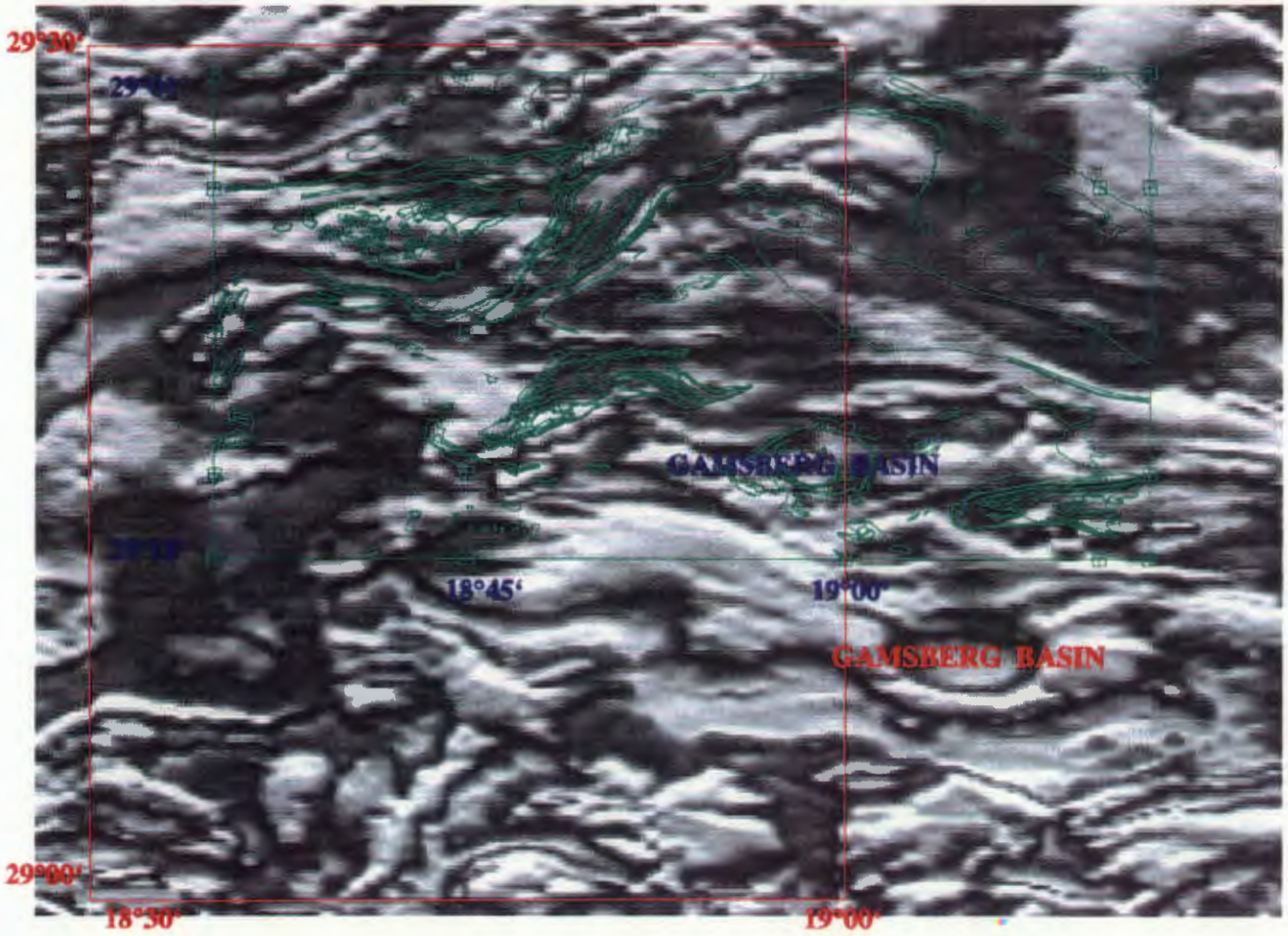

Figure A2 - Geology vector map overlain on Government aeromagnetic image. Misalignment of geographic markers on the magnetic image (red text) occurs relative to the markers on the geology map (green text). The Gamsberg Basin is clearly observed and annotated in red on the magnetic image, and does not overlay with the geology map, Gamsberg basin annotated in green.

Appendix 5

Explanation for not using the Digital Elevation Model produced by the Regional Department of Surveys and Mapping.

Elevation data over Southern Africa, in digital format, is available from the National Department of Surveys and Mapping. The data was obtained by scanning orthophotos from N to S, at a scale 1:50 000. The average height in each 400m by 400m block is then recorded as a single value to create the Digital Elevation Model. In more mountainous terrain data is recorded in 200m grid cells. This data was acquired for the project, and converted to a Triangulated Irregular Network (TIN) to produce a 3-dimensional view of the relief in the area. The resolution at which the data was collected (400m) was to small at the given map scale. Variations in relief were not adequate and difficult to recognise; it was, therefore, decided not to use data set. Contoured relief maps were digitised seperately for this project, and a DEM was created from this new data set.

Appendix 6

Principles of Interpolation using Kriging

Interpolation of the geochemical data requires a model that will represent continuous spatial change. Continuous spatial change is best described using a smooth mathematically defined surface (Burrough, 1986).

Inverse Distance Weighting (IDW) and Kriging are local fitting techniques, and estimate values based on a localised window of neighbourhood points. Geochemically anomalous areas, associated with localised variation in values, are accommodated in IDW and Kriging. In local fitting techniques IDW and Kriging, estimations at unsampled points are based on variances associated with neighbourhood points only. Interpolation of values at points outside the chosen neighbourhood are not affected by localised variance in value. This is important in geochemical analysis of the element data in mineralised districts, where localised variation in patterns associated with mineralisation is expected to occur, and are sought. Trend surface analysis is a global fitting technique which does not accommodate local variation, unlike IDW and Kriging. Trend surface analysis (TSA) was investigated and did not fit the requirements of this investigation.

Discounting TSA, the choice of interpolation technique was between IDW and kriging. The theory fundamental to kriging is that spatial patterns of surface phenomenon are too irregular to be modelled by a smooth mathematical function and are better represented by a stochastic (statistically derived) surface (Burrough, 1986). IDW surfaces are modelled using smooth mathematical functions, see Burroughs (1986) pp. 153-154.

Results of a test case, interpolating lead data using both IDW and Kriging techniques are presented in Figure A 6.1. The kriging function produces a smoother surface, with much less error associated with variance of the data.

Kriging requires user evaluation to choose the appropriate search parameters and modelling parameters that best represents the characteristics of the data being interpolated. Semivariograms modelling the surface variation are tested on each data

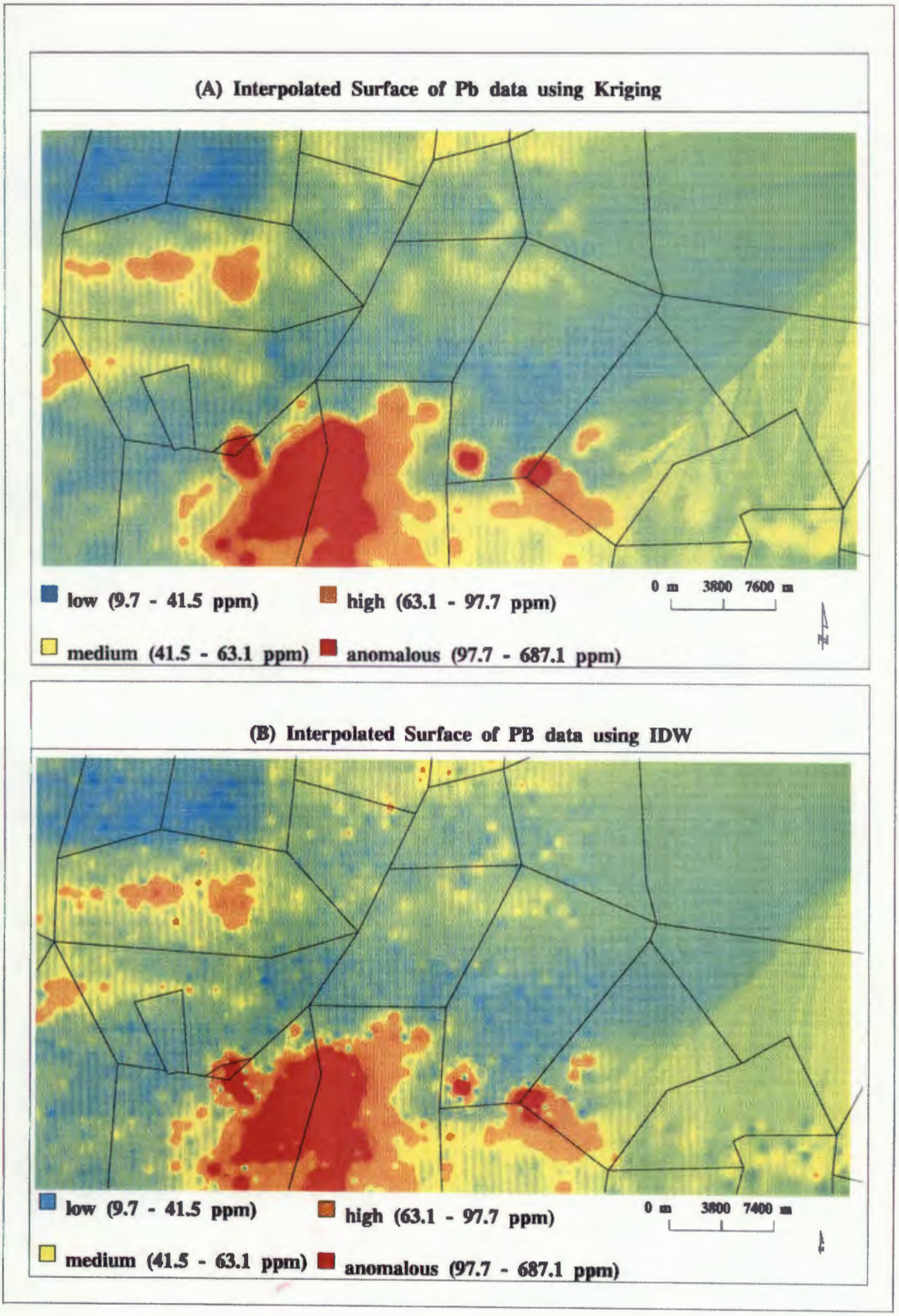

Figure A 6.1 (A-B) - Comparison of Pb point data interpolated using Kriging (A) and Inverse Distance Weighting (IDW; B) function. The Kriging produces raster grid which displays smoother variation in values compared to IDW. IDW produces a patchy distribution of interpolated data values.

set to determine the appropriate size of the search window and functional form (spherical, gaussian, exponential, circular, linear) that will optimise interpolation using the Kriging function.

The functional form models local variation effects by choosing the optimal weights (λ) for interpolation. These optimal weights provide the Best Linear Unbiased Estimate (BLUE) of the variable being estimated at a given point eg, ppm Cu, ppm Zn. Spatial variation in sample points, is measured using semivariance

$$g(h) = \frac{1}{2n} \sum_{i=1}^{n} (Z(x_i) - Z(x_i + h))^2$$

For all point pairs (n) the difference in z value between Xi and Xi+h is measured. The summation of these squared differences divided by 2n (to eliminate double measurement), determines the semivariance at that point. This calculation derives an estimate of population variation assuming that variance is constant over the surface (regionalised variable theory).

Evaluating different functional forms and search window sizes, the exponential method with search window (sample size) of twelve displays the best fit between actual and fitted curves. The semivariograms graphed for Pb, Zn, Cu, Mn and Ni data is presented in Figure A 6.2. The relationship between influence (weights) and distance, termed semivariance, graphically represented in the semivariograms (Figure A4), is input to the Kriging function in the term e'(x).

The formula for kriging is

$$Z(x) = m(x) + e'(x) + e''$$

m(x) models an underling global trend

e'(x) model the overlying spatially correlated local trend

e" is a random error term

In the geochemical data sets, local variation effects are of interest. The estimation of z values (element concentration in ppm) is determined by weighting the distance each unknown point is from a known sample points, using the term e'(x). The assumption of simple Kriging is that no global trend exists in the data and if it exists it is does not

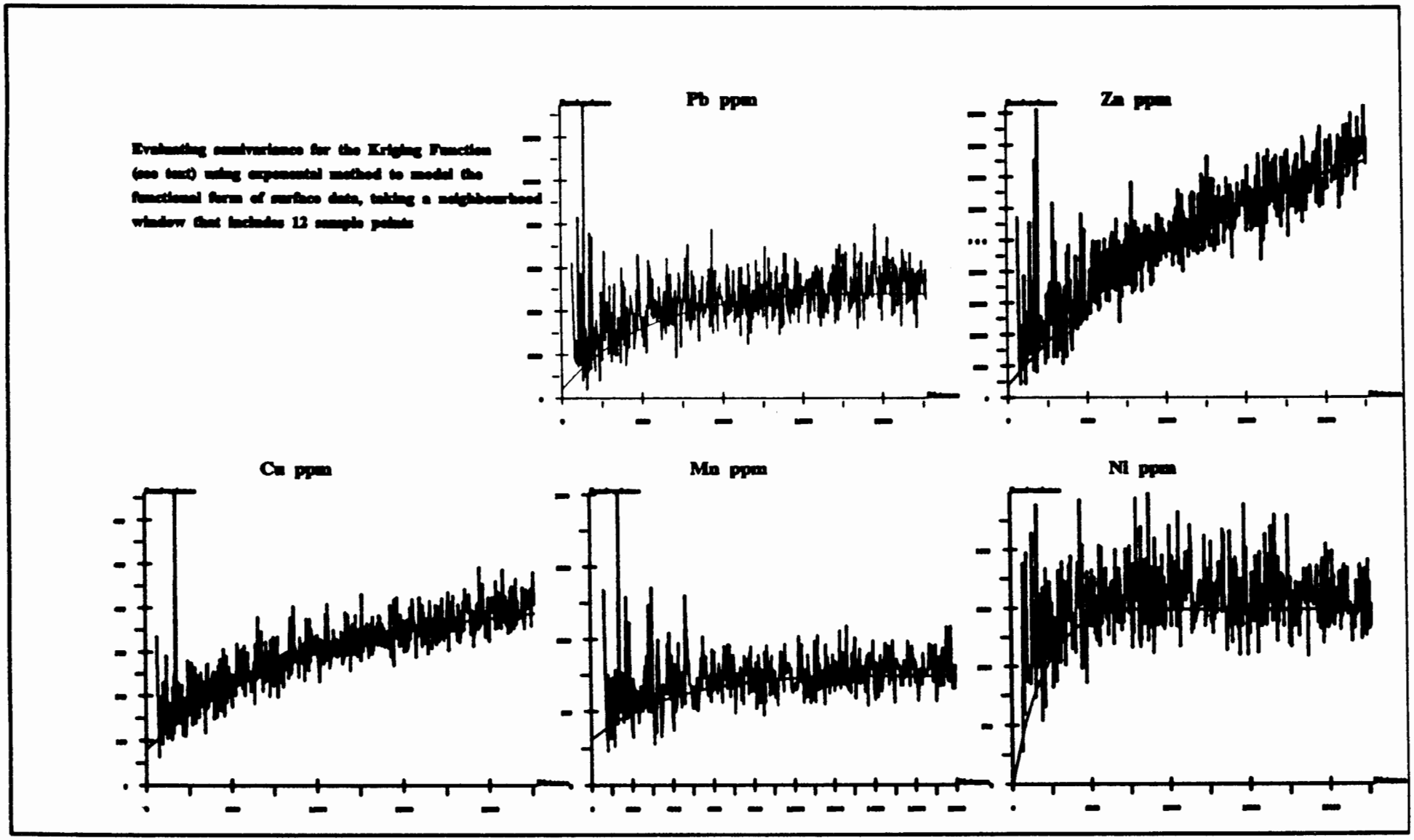

Figure A 6.2 - Semivariograms modelling Lead (Pb), Zinc (Zn), Copper (Cu), Manganese (Mn) and Nickel (Ni) traverse geochemical data. The graphs describe the relationship of sample distance between points (x-axis) and variance between points (y-axis). The extent of the x-axis equals the distance between the most widely separated pair of points defined by the sample neighbourhood for interpolation (12 points here). The actual semivariance is described by the wavy line. The smooth black line model the term e'(x) (see text) and is the function used to model the local effect. This smooth line shows the predicted variance. The exponential function with sample size 12 models the local effect in the graphs above. These model choices set the optimal weights for interpolation based on the influence of distance.

affect local trends ie. there is a certain amount of stationarity over space. This is known as the regionalised variable theory of kriging, where the statistical surface to be interpolated is regarded as a regionalised variable that has a certain degree of continuity over space. Hence global variation (structural component) is not modelled, and the term m(x) is assumed to be zero. Z(x) is the interpolated output cell value calculated using the best linear unbiased estimate from sampled points.

The fundamental problem underlying all interpolation models is that each is a sort of hypotheses about the surface, and that hypotheses may or may not be true (Lam, 1983). The assumption that regionalised variables are stationary is often untrue; an alternative hypothesis is contained within Universal kriging which describes the trend or drift (global variation) using a polynomial function (Lam, 1983). Universal kriging is not used because although the assumptions of simple kriging are restrictive, fewer computational problems are associated with it. Universal kriging has more general assumptions but computations are difficult and computer intensive.

Figure A 6.3 (A-B) show the interpolated surface grid and output variance grid, respectively, of kriged Zn data. In Figure A2B the output variance grid represents a surface that provides an estimate of the error and confidence interval for each of the points interpolated in Figure A 6.3 A. The error information in figure A 6.3 B reflects the density and distribution of control points and the degree of spatial autocorrelation within the surface. This variance surface is very useful in analysing the reliability of each feature in the kriged map (Lam, 1983). Green in Figure A 6.3 B represents areas were variability in surface values is low and hence confidence in corresponding interpolated surface values is high. Those areas with high estimated variability (red) indicate that corresponding interpolated values should be regarded with caution (viz. significant uncertainty in value). In these areas additional sampling would improve the results of kriging operation.

The points overlayed on Figure A 6.3 A and A 6.3 B show sampled points from which output cell values were interpolated. In the area outlined with the solid box (west sector of image) lack of sampled data clearly indicates high variability in values (red). The confidence in interpolated cell values in this area are associated with a high

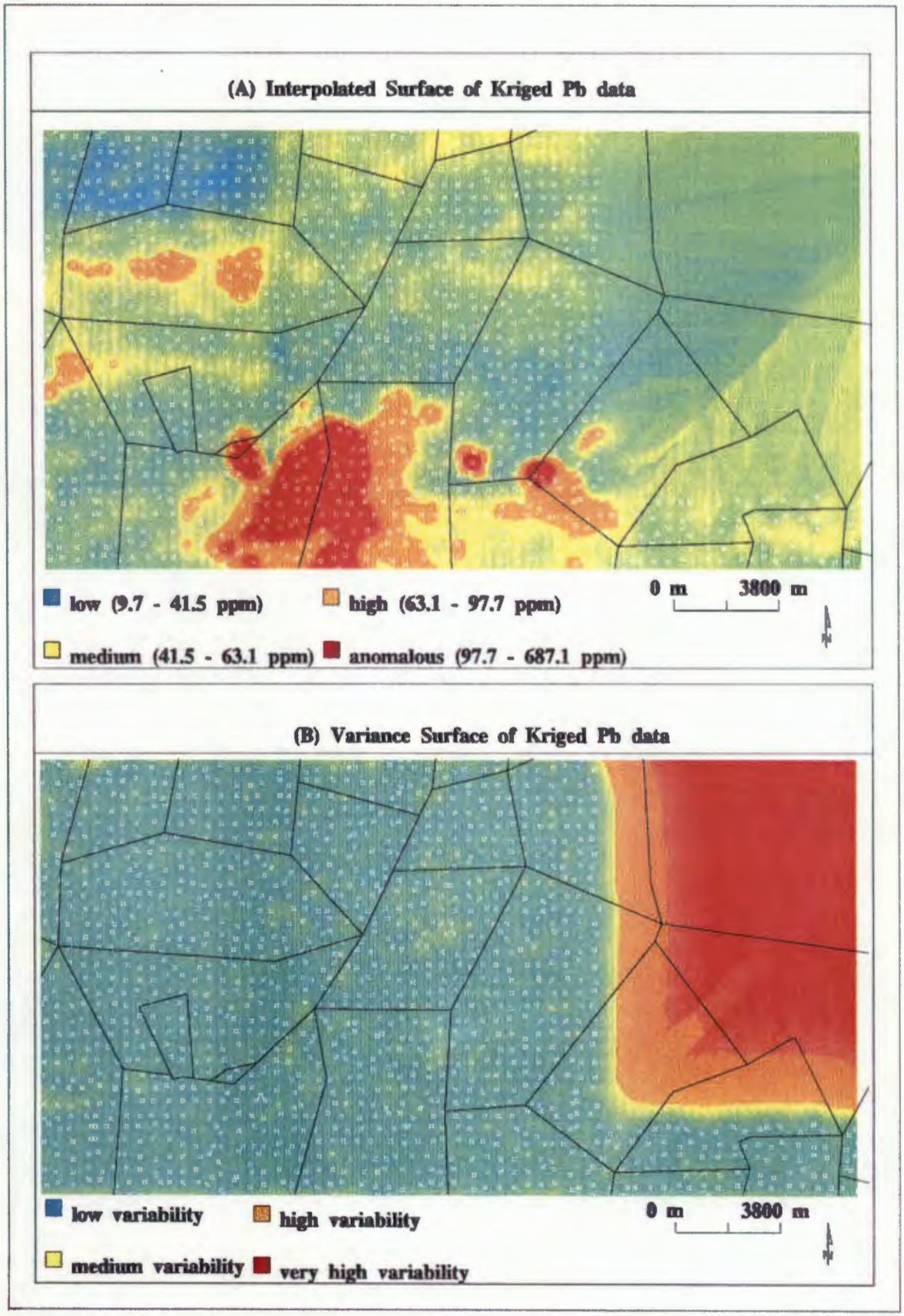

Figure A 6.3 (A-B) - Comparison of PB data interpolated surface (A), and semivariance associated with the interpolated surface (B). Sample data points from which elements were analysed and surfaces interpolated are overlaid on A and B. The interpolated surface (A) was generated using the Kriging function (see text). The variance surface (B) shows the estimated variance associated with each interpolated cell in (A). Areas coloured red display high estimated variability and indicates areas where additional samples would help to improve the results of interpolation, presented in surface (A). Areas coloured green represent areas where estimated variability is low and data interpolation in these areas have a high confidence level. Areas coloured yellow to gold display intermediate estimated variability. Interpolated Pb data values range from low (turquoise) concentrations in north to intermediate (yellow to gold) and high (red) values in the south.

degree of uncertainty. All other areas show low variability and hence high confidence in interpolated cell values. The modelled spatial variation in element values in these areas are highly reliable and have an associated high confidence level.

Appendix 7

Colour display of raster data using spectral remapping on the computer graphics screen

The continuous data contained in spatial surface files, as represented on the computer display screen, are controlled by the frame buffer. The frame buffer is a large matrix in which each cell may take the value 0 or 1 to control whether the electron beam is off or on over a particular part of the screen (Burrough, 1986). Colour or grey tones are generated by adding bit planes to the frame buffer of the display screen. The display screen of the computer system used records data in 8 bit planes, giving 256 possibilities (2^8) for display. The integer range 0-255 the 8-bit range (byte format) of digital values is employed in digital image display and processing (Drury and Walker, 1991). The range of floating point and integer values represented in surface raster files are rescaled to the integer range 0-255. The information from these bit planes control the red blue and green electron guns of the monitor tube look up tables, and displays this rescaled range as a combination of colours.

BINARY CODE	256	128	64	32	16	8	4	2

The look up tables are programmed to use standard Munsell Colours (Hue-Saturation -Value and Red-Green-Blue) allowing the colour graduations on the map, representing the range of values in the surface file, to be continuously displayed.

Appendix 8

Remapping of data values in the Hue-Saturation-Value Colour Model.

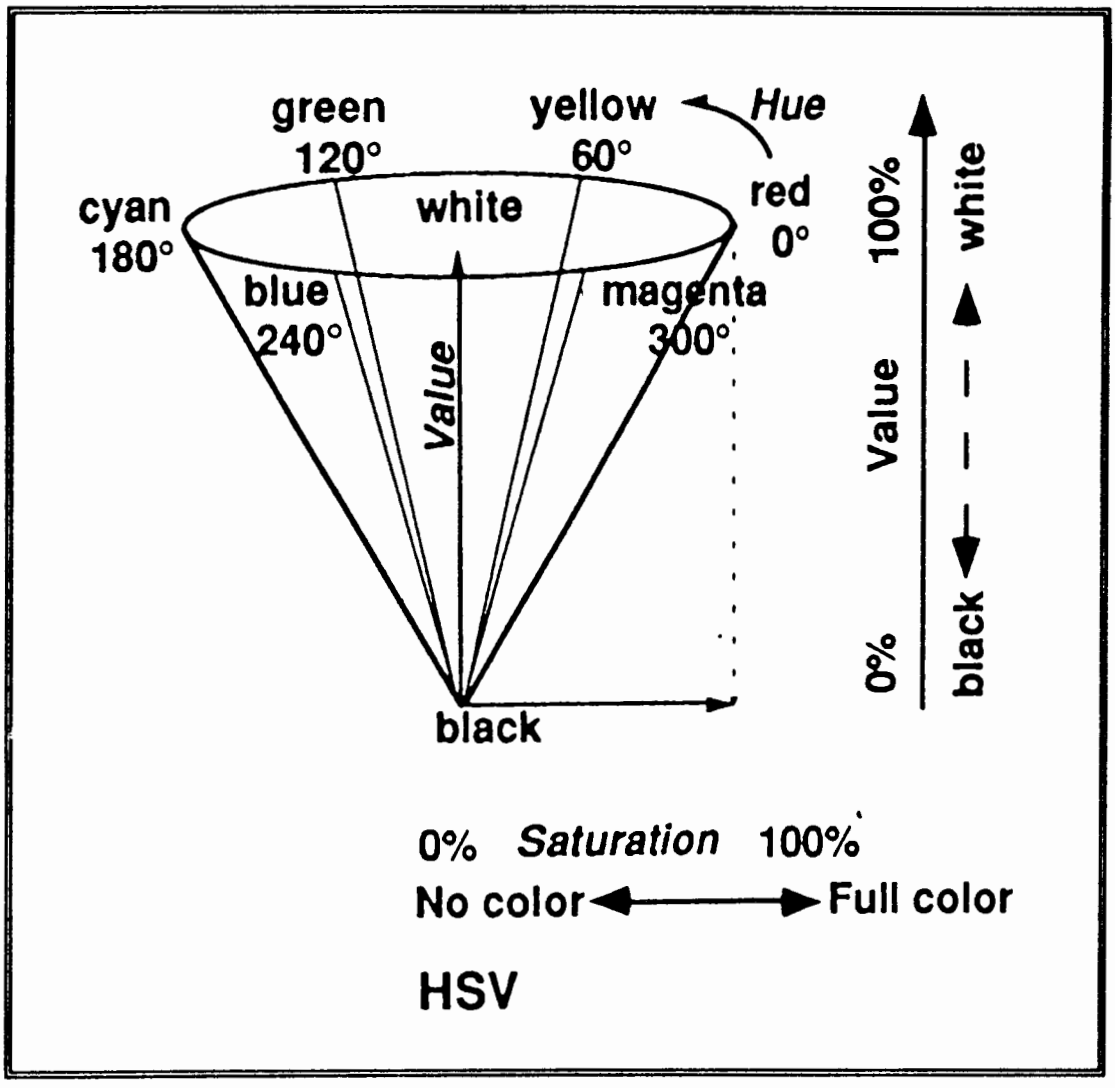

Figure A 8.1 - Conical representation of the Hue-Saturation-Value (HSV) model.

The RGB colour or hue colours originates at the apex of the cone in Figure A 8.1 and around the edges of the triangle in Figure 6.7. In the HSV model, hue defines the specific colour to be set eg. red, blue and yellow and is given as integer between 0 to 360. This represents the angle increasing anti-clockwise around the top of the colour cone (Figure A 8.1). Saturation defines the intensity or purity of this colour and is set an integer value between 1 to 100. Value or brightness specifies the amount of grey mixed in the colour, also defined as an integer between 1 to 100. Looking at the colour cone in Figure A 8.1, saturation increases horizontally from the centre of the cone to the edges. Value increases vertically from the bottom to top of the cone. Hue changes

anti-clockwise around the disc of the cone.

At the top of the HSV colour cone value is set to 100 representing mixture with white. At value set to 100 hue is saturated increasingly with white depending on the estimate of saturation (1-100), becoming saturated with white at the centre. Hence hue at the edges of the cone (at the top) are purest with saturation value of 100. Moving down the cone to the apex value decreases from 100 to 0. Hue which is pure at the cone edges becomes increasingly mixed towards the centre.